

Search for bottom-type, vectorlike quark pair production in a fully hadronic final state in proton-proton collisions at $\sqrt{s} = 13$ TeV

A. M. Sirunyan *et al.**
(CMS Collaboration)

 (Received 22 August 2020; accepted 9 October 2020; published 7 December 2020)

A search is described for the production of a pair of bottom-type vectorlike quarks (VLQs), each decaying into a b or \bar{b} quark and either a Higgs or a Z boson, with a mass greater than 1000 GeV. The analysis is based on data from proton-proton collisions at a 13 TeV center-of-mass energy recorded at the CERN LHC, corresponding to a total integrated luminosity of 137 fb^{-1} . As the predominant decay modes of the Higgs and Z bosons are to a pair of quarks, the analysis focuses on final states consisting of jets resulting from the six quarks produced in the events. Since the two jets produced in the decay of a highly Lorentz-boosted Higgs or Z boson can merge to form a single jet, nine independent analyses are performed, categorized by the number of observed jets and the reconstructed event mode. No signal in excess of the expected background is observed. Lower limits are set on the VLQ mass at 95% confidence level equal to 1570 GeV in the case where the VLQ decays exclusively to a b quark and a Higgs boson, 1390 GeV for when it decays exclusively to a b quark and a Z boson, and 1450 GeV for when it decays equally in these two modes. These limits represent significant improvements over the previously published VLQ limits.

DOI: [10.1103/PhysRevD.102.112004](https://doi.org/10.1103/PhysRevD.102.112004)

I. INTRODUCTION

One of the biggest puzzles in elementary particle physics concerns the large difference between the electroweak scale and the Planck scale, and the related problem of the unexpectedly low value of the Higgs boson mass [1]. In the standard model (SM), the Higgs boson H is assumed to be a fundamental scalar (spin-0) particle. Unlike the fundamental fermions (leptons and quarks) and the vector gauge bosons, the corrections to the Higgs boson mass due to vacuum energy fluctuations are quadratic, driving the Higgs boson mass to the cutoff value of the vacuum energy fluctuations. In the absence of any new physics below the Planck scale, this cutoff is about 10^{19} GeV. In that case, the Higgs boson mass would naturally be expected to be seventeen orders of magnitude greater than its measured mass of 125 GeV.

Although supersymmetry provides an elegant solution to this problem [2,3], the lack of evidence for the production of supersymmetric particles at the CERN LHC indicates that, if supersymmetry is realized in nature, it is broken at an energy scale greater than a few TeV and, therefore, does not solve the fine tuning of the 125 GeV Higgs boson mass.

Several alternative theories have been proposed for solving this fine tuning problem. These theories include composite Higgs models [4–6], in which the Higgs boson is not a fundamental particle, but rather contains constituents bound by a new type of gauge interaction, and little Higgs models [7,8], in which the Higgs boson is a pseudo-Nambu–Goldstone boson that arises from spontaneous breaking of a global symmetry at the TeV energy scale. Both of these types of models predict a new class of vectorlike fermions [9] with the same charges as the SM fermions, but with purely vector current couplings to the weak gauge bosons. In composite Higgs models, the vectorlike quarks (VLQs) are excited bound-state resonances, while in little Higgs models they are fundamental particles that cancel loop divergences.

Since the VLQs are nonchiral, Lagrangian mass terms not arising from Yukawa couplings to the Higgs field are allowed, thereby avoiding the constraints on heavy, sequential fourth-generation quarks set by the measured cross section for Higgs boson production at the LHC [10,11]. Requiring VLQs to have renormalizable couplings to the SM quarks permits only four types of VLQs, defined by their charge q : $q = -1/3$ (B), $q = +2/3$ (T), $q = -4/3$ (X), and $q = +5/3$ (Y) [12]. These are arranged into seven multiplets: two singlets (T and B), three doublets (TB , XT , and YB), and two triplets (XTB and TBY) [13]. This analysis focuses on the $q = -1/3$ (B) type of VLQ.

The branching fractions \mathcal{B} of the T and B are model specific and depend upon the VLQ multiplet configuration, the mass of the VLQ, and the coupling of the VLQ to chiral

*Full author list given at the end of the article.

Published by the American Physical Society under the terms of the [Creative Commons Attribution 4.0 International license](https://creativecommons.org/licenses/by/4.0/). Further distribution of this work must maintain attribution to the author(s) and the published article's title, journal citation, and DOI. Funded by SCOAP³.

quarks [14]. In general, up-type quark mass eigenstates will be mixtures of the chiral up-type quarks with the T VLQ, while down-type quark mass eigenstates will be mixtures of the chiral down-type quarks and the B VLQ. Precision measurements of the couplings of the first and second generation SM quarks constrain their mixings with VLQs and indicate that the only sizable couplings of the T and B VLQs allowed are to SM quarks of the third generation, although couplings to other quarks are not excluded [13,15,16]. In this analysis, we assume the B VLQ has three decay modes: $B \rightarrow bZ$, $B \rightarrow bH$, and $B \rightarrow tW$. In most models, for a B VLQ mass greater than the current limit of approximately 1000 GeV, there is a small difference between $\mathcal{B}(B \rightarrow bZ)$ and $\mathcal{B}(B \rightarrow bH)$, depending on the VLQ mass, but the difference is essentially zero for masses greater than 2000 GeV. The expected values of $\mathcal{B}(B \rightarrow bZ)$ and $\mathcal{B}(B \rightarrow bH)$ also depend upon the multiplet configuration. They are 50% for both the XTB triplet and the BY doublet, and 25% for the TBY triplet and the B singlet. The branching fractions for the TB doublet depend upon the mixing of the T and B VLQs with chiral quarks. If the Tt mixing is zero, the $B \rightarrow bH$ and $B \rightarrow bZ$ branching fractions are 50%. If the Tt and Bb mixing are equal, these branching fractions are 25%. If the Bb mixing is zero, these branching fractions are zero [12].

Results from both the ATLAS and CMS Collaborations using events with fully hadronic final states, based on data

from proton-proton (pp) collisions at $\sqrt{s} = 13$ TeV with an integrated luminosity of 36 fb^{-1} , have excluded a pair-produced B with mass up to approximately 1100 GeV. The ATLAS analysis [17] was based on a classification of event signatures using neural networks, while the CMS analysis [18] used event shapes to identify Lorentz-boosted objects. The ATLAS (CMS) results exclude masses, at 95% confidence level (C.L.), up to 1010 (980), 710 (1070), and 950 (1025) GeV for the 100% $B \rightarrow bH$, 100% $B \rightarrow bZ$, and the BY doublet cases, respectively. In addition, an ATLAS analysis [19] combining both fully hadronic and leptonic channels excludes values of the B mass up to 1140 GeV for the BY doublet case. The analysis presented here improves on these results by using the full 137 fb^{-1} dataset collected by CMS in 2016–2018, and by fully reconstructing the event kinematics, thereby allowing the mass of the B to be reconstructed.

II. ANALYSIS OVERVIEW

This analysis involves a search for the production of a pair of bottom-type VLQs with mass greater than 1000 GeV, using data from pp collisions at $\sqrt{s} = 13$ TeV at the LHC collected by the CMS detector during 2016–2018, corresponding to an integrated luminosity of 137 fb^{-1} . The analysis is focused on events in which each of the VLQs decays to a b or \bar{b} quark and to either a Higgs

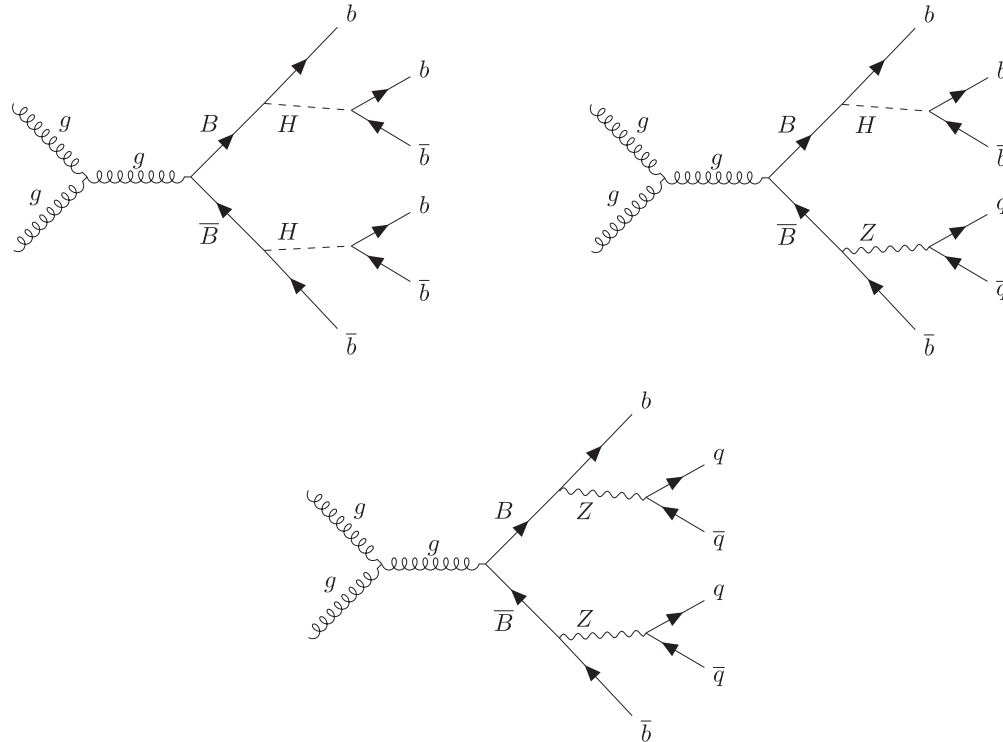


FIG. 1. Dominant diagrams of the pair production of bottom-type VLQs (B) that subsequently decay to a b or \bar{b} quark and either a Higgs or Z boson. In events targeted by this analysis, the Z boson then decays to a pair of quarks, where q denotes any quark other than a top quark, while the Higgs boson decays to b quarks. Upper left: $hhbH$ mode, upper right: $hbHbZ$ mode, lower: $bZbZ$ mode.

or Z boson. Since the dominant decay modes of the Higgs and Z bosons are to a quark and antiquark pair, we select final states consisting of jets resulting from the quarks and antiquarks produced in the decays of the VLQs and subsequent decays of the two bosons. The events are categorized into three modes, depending on the daughter bosons: $bHbH$, $bHbZ$, and $bZbZ$. Figure 1 shows the dominant Feynman diagrams for these three modes.

Background from SM processes (predominantly “multijet” events, consisting solely of jets produced through the strong interaction) is reduced by requiring that the jets are consistent with the production of a pair of bosons (either Higgs or Z), that the reconstructed VLQs have equal masses, and that some of the jets are tagged as originating from b quarks. For a highly boosted Higgs or Z boson, the two jets resulting from its daughter quarks might merge into a single reconstructed jet. In order to include these events, three orthogonal, fully independent analyses are carried out using exclusive sets of events categorized by the observed jet multiplicity: 4, 5, or 6 jets. The final result is obtained by combining these three independent analyses. In this paper, we use “jet tagging requirements” to refer to both single jets tagged as being from a b quark, and merged jets tagged as containing a $b\bar{b}$ pair.

To select the correct assignment of reconstructed jets to parent particles, a modified χ^2 metric, χ_{mod}^2 , is used. The χ_{mod}^2 value is determined by the differences between the masses of the two reconstructed bosons and the mass of the Higgs or Z boson, normalized by their resolutions, and by the reconstructed fractional mass difference of the two VLQs. The event mode is assigned as $bHbH$, $bHbZ$, or $bZbZ$, depending on which gives the smallest value of χ_{mod}^2 . An upper cutoff on the value of χ_{mod}^2 is applied to remove background.

The expected background is first determined by fitting the distribution of the number of events as a function of the reconstructed VLQ mass, before jet tagging requirements are applied, so this sample is overwhelmingly background dominated. The fraction of background expected to remain after jet tagging requirements are applied, called the background jet-tagged fraction, is measured using events with VLQ candidate masses in the range 500–800 GeV, in which a VLQ signal has already been excluded, and then corrected for a possible dependence on the VLQ mass by using a control region with a higher χ_{mod}^2 value. Both the χ_{mod}^2 selection and jet tagging requirements are simultaneously optimized for maximal sensitivity to a potential signal. This optimization is done separately for each event mode and jet multiplicity. For the final result, all event mode and jet multiplicity analyses are combined using the procedure in Ref. [20] to obtain VLQ mass limits as a function of $\mathcal{B}(B \rightarrow bH)$ and $\mathcal{B}(B \rightarrow bZ)$, as described further in Sec. X.

III. THE CMS DETECTOR

The central feature of the CMS apparatus is a superconducting solenoid of 6 m internal diameter, providing a magnetic field of 3.8 T. Within the solenoid volume are a silicon pixel and strip tracker, a lead tungstate crystal electromagnetic calorimeter (ECAL), and a brass and scintillator hadron calorimeter (HCAL), each composed of a barrel and two endcap sections. Forward calorimeters extend the pseudorapidity (η) coverage provided by the barrel and endcap detectors. Muons are detected in gas-ionization chambers embedded in the steel flux-return yoke outside the solenoid.

The electromagnetic calorimeter consists of 75 848 lead tungstate crystals, which provide coverage in $|\eta| < 1.48$ in a barrel region and $1.48 < |\eta| < 3.0$ in two endcap regions. In the region $|\eta| < 1.74$, the HCAL cells have widths of 0.087 in pseudorapidity and 0.087 in azimuth (ϕ). In the $\eta - \phi$ plane, and for $|\eta| < 1.48$, the HCAL cells map on to 5×5 arrays of ECAL crystals to form calorimeter towers projecting radially outwards from close to the nominal interaction point. For $|\eta| > 1.74$, the coverage of the towers increases progressively to a maximum of 0.174 in $\Delta\eta$ and $\Delta\phi$. Within each tower, the energy deposits in ECAL and HCAL cells are summed to define the calorimeter tower energies, which are subsequently used to provide the energies and directions of hadronic jets. When combining information from the entire detector, the jet energy resolution amounts typically to 15%–20% at 30 GeV, 10% at 100 GeV, and 5% at 1 TeV [21].

Events of interest are selected using a two-tiered trigger system [22]. The first level, composed of custom hardware processors, uses information from the calorimeters and muon detectors to select events at a rate of around 100 kHz within a fixed time interval of about 4 μs . The second level, known as the high-level trigger (HLT), consists of a farm of processors running a version of the full event reconstruction software optimized for fast processing, and reduces the event rate to around 1 kHz before data storage.

A more detailed description of the CMS detector, together with a definition of the coordinate system used and the relevant kinematic variables, can be found in Ref. [23].

IV. DATA AND SIMULATED EVENTS

The data used in this analysis were collected during the 2016–2018 LHC running periods and correspond to an integrated luminosity of 137 fb^{-1} [24–26].

Signal events with pair production of VLQs were simulated using the Monte Carlo generator MadGraph5_aMC@NLO [27], version v2.3.3 (v2.4.2) for samples corresponding to 2016 (2017–2018) data, at leading order with the NNPDF3.0 parton distribution functions (PDFs) [28]. The generated VLQ masses m_B cover the range 1000–1800 GeV in steps of 100 GeV. Hadronization

of the underlying partons was simulated using PYTHIA v8.212 [29] with the CUETP8M1 tune [30] for samples corresponding to 2016 data, and with the CP5 tune [31] for samples corresponding to 2017 and 2018 data. Corrections of the cross sections to next-to-next-to-leading order and next-to-next-to-leading logarithmic soft-gluon resummation were obtained using TOP++ 2.0 [32] with the MSTW2008NNLO68CL parton distribution set from the LHAPDF 5.9.0 library [33,34]. To simulate the effect of additional pp interactions within the same or nearby bunch crossings (“pileup”), PYTHIA v8.226 with a total inelastic pp cross section of 69.2 mb [35] was used. Following event generation, the GEANT4 package [36,37] was used to simulate the CMS detector response. Scale factors corresponding to jet energy corrections, jet energy resolutions [21], pileup, and jet tagging [38,39] are applied to the simulated signal events so that the corresponding distributions agree with those in data.

V. JET RECONSTRUCTION AND TAGGING

The global event reconstruction, also called the particle-flow event reconstruction [40], aims to reconstruct and identify each individual particle in an event, with an optimized combination of all subdetector information. In this process, the identification of the particle type (photon, electron, muon, charged hadron, or neutral hadron) plays an important role in the determination of the particle direction and energy. First, photons, electrons, and muons are identified using ECAL energy clusters, tracks in the tracker, and hits in the muon system. Then, charged hadrons are identified as charged particle tracks neither identified as electrons, nor as muons. Finally, neutral hadrons are identified as HCAL energy clusters not linked to any charged hadron trajectory, or as a combined ECAL and HCAL energy excess with respect to the expected charged hadron energy deposit. The energy of charged hadrons is determined from a combination of the track momentum and the corresponding ECAL and HCAL energies, corrected for the response function of the calorimeters to hadronic showers, and the energy of neutral hadrons is obtained from the corresponding corrected ECAL and HCAL energies.

For this analysis, two types of hadronic jets are clustered from these reconstructed particles, using the infrared and collinear safe anti- k_T algorithm [41,42]. The first type, “AK4 jets,” uses a distance parameter $\Delta R = \sqrt{(\Delta\eta)^2 + (\Delta\phi)^2}$ of 0.4. However, since merged jets from a boosted Higgs or Z boson decay may be wider, a second set, using a distance parameter of 0.8 (“AK8 jets”) is also reconstructed from the same set of input particles. Jet momentum is determined as the vectorial sum of all particle momenta in the jet, and is found from simulation to be, on average, within 5% to 10% of the true momentum over the whole transverse momentum (p_T) spectrum and detector

acceptance. Pileup can contribute additional tracks and calorimetric energy depositions to the jet momentum. The pileup per particle identification algorithm (PUPPI) [43] is used to mitigate the effect of pileup at the reconstructed particle level, making use of local shape information, event pileup properties, and tracking information. A local shape variable is defined, which distinguishes between collinear and soft diffuse distributions of other particles surrounding the particle under consideration. The former is attributed to particles originating from the hard scatter and the latter to particles originating from pileup interactions. Charged particles identified as originating from pileup vertices are discarded. For each neutral particle, a local shape variable is computed using the surrounding charged particles compatible with the primary vertex within the tracker acceptance ($|\eta| < 2.5$), and using both charged and neutral particles in the region outside of the tracker coverage. The momenta of the neutral particles are then rescaled according to their probability to originate from the primary interaction vertex deduced from the local shape variable, superseding the need for jet-based pileup corrections [44]. Jet energy corrections are derived from simulation to bring the measured response of jets to that of particle level jets on average. In situ measurements of the momentum balance in dijet, photon + jet, Z + jet, and multijet events are used to account for any residual differences in the jet energy scale between data and simulation [21]. Additional selection criteria are applied to each jet to remove jets potentially dominated by anomalous contributions from various subdetector components or reconstruction failures.

This analysis only uses AK4 jets with $p_T > 50$ GeV and AK8 jets with $p_T > 200$ GeV, both within $|\eta| < 2.4$. For AK8 jets, the constituents are reclustered using the Cambridge–Aachen algorithm [45,46]. The “modified mass drop tagger” algorithm [47,48], also known as the “soft drop” algorithm, with angular exponent $\beta = 0$, soft cutoff threshold $z_{\text{cut}} < 0.1$, and characteristic radius $R_0 = 0.8$ [49], is applied to remove soft, wide-angle radiation from the jet. This results in a jet mass that, in the case of large mass, more accurately corresponds to the mass of the mother particle from which the jet originated. For events with boosted Higgs and Z bosons, the AK8 soft-drop mass is used to obtain the mass of the merged jet.

The event jet multiplicity is determined by the number of AK4 jets passing the requirements above. In signal events, decays of the VLQ pair and subsequent decays of the Higgs and Z boson daughters yield a total of six quarks. In all three event modes, at least two of these are b quarks. Considering the predominant $H \rightarrow bb$ decay, for the $bHbH$ event mode, all six are b quarks; for the $bHbZ$ event mode, four or six are b quarks; while for the $bZbZ$ event mode, two, four or six are b quarks. We note that of the hadronic Z boson decays, 15% are to a $b\bar{b}$ pair; however, $Z \rightarrow c\bar{c}$ decays also have a significant chance of passing the tagging requirements, as discussed in Sec. VI, and are also included

(along with other possible Z boson decay modes) in the signal efficiency. If all six quark jets are individually reconstructed, a 6-jet event is produced; if two jets merge into a single reconstructed jet, this produces a 5-jet event; and if two merged jets are produced, then a 4-jet event results. Note that the VLQ reconstruction does not consider the possibility of additional jets produced by initial state or final state radiation.

Because of the large number of b jets in signal events, b tagging is a powerful tool to significantly reduce the background from SM processes. Individual jets are tagged using the DeepJet b discriminant [38] applied to AK4 jets, while merged jets from $b\bar{b}$ pairs are double b tagged using the algorithm in Ref. [39], developed in the context of $H \rightarrow b\bar{b}$ searches, applied to AK8 jets.

VI. EVENT SELECTION

The events used in the analysis are first selected online by the CMS trigger system. The HLT trigger used requires the total p_T measured in the calorimeters to be at least 900 (1050) GeV for the 2016 (2017–2018) dataset. Offline, events with $H_T > 1350$ GeV are selected, where H_T is defined as the scalar sum of the jet p_T for all AK4 jets with $p_T > 50$ GeV and $|\eta| < 2.4$. The requirement is set higher than the trigger threshold to avoid effects due to trigger turn on. In order to minimize bias when measuring the efficiency of the HLT triggers, the efficiencies are measured in a dataset collected by an orthogonal trigger, which requires the event to have a single muon. For all years, the measured trigger efficiency for events with $H_T > 1350$ GeV is at least 99.6%. Table I shows the efficiency for simulated VLQ signal events after the H_T requirement for each of the three jet multiplicity channels and for each of three VLQ masses (1000, 1200, and 1400 GeV).

The number of tagged jets required to select an event, as well as the working points for the taggers used, are optimized separately for each of the three jet multiplicities and event modes, in order to maximize the expected signal sensitivity. For the working points selected, the single b tagger has an efficiency of 82% for b jets in simulated $t\bar{t}$ events with $p_T > 30$ GeV and a mistag rate of 1% for light quarks (u , d , or s) and approximately 17% for charm quarks

TABLE I. Signal efficiencies of the offline H_T selection, in %, for each of the jet multiplicity channels, for three VLQ masses (1000, 1200, and 1400 GeV). The efficiency is the fraction of events in each jet multiplicity category satisfying the $H_T > 1350$ GeV selection. Statistical uncertainties are negligible and therefore omitted.

VLQ mass [GeV]	4 jets	5 jets	6 jets
1000	95.1	89.4	81.4
1200	98.5	96.2	91.3
1400	99.5	98.4	95.0

TABLE II. Summary of the minimum number of single and double b tags required for each jet multiplicity and event mode.

Jet multiplicity	Tag	$bHbH$	$bHbZ$	$bZbZ$
4 jets	Single b	2	2	2
	Double b	1	1	0
5 jets	Single b	3	3	3
	Double b	0	0	0
6 jets	Single b	4	4	3

[38]. The double b tagger has an efficiency of 75% in simulated $H \rightarrow b\bar{b}$ events, and a mistag rate of 10% in simulated inclusive multijet events and 33% in simulated $H \rightarrow c\bar{c}$ events [39], where a mistag in the double b tag case means that at least one non- b quark subjet is present in the tagged jet. The number of tags required depends on the jet multiplicity as follows: in the 6-jet case, four AK4 jets are required to have a b tag, except in the $bZbZ$ event mode, for which three tags are required. In the 5-jet case, three of the AK4 jets not associated with the merged decay products are required to be b tagged; no double b tag requirement is applied to the AK8 jet associated with the merged decay. In the 4-jet case, two of the nonmerged AK4 jets are required to have a b tag, and one of the merged jets is required to have a double b tag, except in the $bZbZ$ event mode, for which no double b tag is required. These requirements are summarized in Table II.

VII. EVENT RECONSTRUCTION

In the case when the two jets produced from a H/Z boson decay are individually resolved, the mass of the parent boson can be estimated from the invariant mass of the two jets. In the case where the two jets are merged, the parent boson mass is instead estimated using the soft-drop mass of the AK8 jet. Only those AK8 jets that are within $\Delta R < 0.3$ of an AK4 jet are used. However, if a second AK4 jet is within $\Delta R < 0.6$ of the AK8 jet, this overlap could cause the AK8 jet mass to be misreconstructed, so in this case the AK8 jet is discarded and the two AK4 jets are treated as a resolved dijet boson candidate.

A central feature in the analysis is the selection of the correct way of combining jets in order to reconstruct the parent particles; this is a difficult task because of the large number of jets in the event. In 6-jet events, there are two pairs of jets originating from H/Z boson decay; and three jets (including two from the H/Z decay) associated with each VLQ decay. In 5-jet events, there is a pair of jets associated with one H/Z boson and a merged jet associated with the other H/Z boson; each of these is associated with one of the remaining two jets to form a VLQ candidate. In 4-jet events, there is a merged jet associated with each H/Z boson, each of which is paired to one of the remaining two jets to form a VLQ candidate. The final reconstructed VLQ

mass, m_{VLQ} , is defined as the average mass of the two individual reconstructed VLQs in the event.

The number of possible ways to combine the jets to reconstruct the two H/Z bosons and then to combine these with the two remaining jets to form the VLQ candidates is 720, 120, and 24 for the 6-, 5-, and 4-jet multiplicities, respectively. However, many of these different combinations simply involve different permutations among the jets that constitute the individual VLQs, and these permutations do not affect the reconstructed VLQ mass. The numbers of combinations that give distinct VLQ masses are only 10, 10, and 3 for the 6-, 5-, and 4-jet multiplicities, respectively. For the 5- and 4-jet multiplicities, however, the jet associated with the merged H/Z boson decay products distinguishes different combinations, since this jet is treated differently from the others by having a double b tag, rather than a single b tagging requirement. This doubles the

number of distinct 5-jet combinations and quadruples the number of distinct 4-jet combinations. The final number of distinct combinations is then 10, 20, and 12 for the 6-, 5-, and 4-jet multiplicities, respectively.

For each jet combination, χ^2_{mod} is determined using Eqs. (1)–(3) below, which depend on the measured mass of a dijet Higgs or Z boson candidate (m_{dijet}), the measured soft-drop mass of a merged-jet Higgs or Z boson candidate (m_{merged}), and the fractional mass difference of the two VLQ candidates (Δm_{VLQ}), where Δm_{VLQ} is the difference of the masses of the two VLQ candidates divided by the average mass of the two. The only use of AK8 jets in this calculation is to determine the mass of the merged H/Z candidates using the soft-drop mass of the matched AK8 jet. All other quantities are determined using AK4 jet kinematics.

$$\text{6-jet events: } \chi^2_{\text{mod}} = \frac{(m_{\text{dijet}_1} - \bar{m}_{\text{dijet}})^2}{\sigma_{m_{\text{dijet}}}^2} + \frac{(m_{\text{dijet}_2} - \bar{m}_{\text{dijet}})^2}{\sigma_{m_{\text{dijet}}}^2} + \frac{(\Delta m_{\text{VLQ}} - \overline{\Delta m_{\text{VLQ}}})^2}{\sigma_{\Delta m_{\text{VLQ}}}^2}, \quad (1)$$

$$\text{5-jet events: } \chi^2_{\text{mod}} = \frac{(m_{\text{dijet}} - \bar{m}_{\text{dijet}})^2}{\sigma_{m_{\text{dijet}}}^2} + \frac{(m_{\text{merged}} - \bar{m}_{\text{merged}})^2}{\sigma_{m_{\text{merged}}}^2} + \frac{(\Delta m_{\text{VLQ}} - \overline{\Delta m_{\text{VLQ}}})^2}{\sigma_{\Delta m_{\text{VLQ}}}^2}, \quad (2)$$

$$\text{4-jet events: } \chi^2_{\text{mod}} = \frac{(m_{\text{merged}_1} - \bar{m}_{\text{merged}})^2}{\sigma_{m_{\text{merged}}}^2} + \frac{(m_{\text{merged}_2} - \bar{m}_{\text{merged}})^2}{\sigma_{m_{\text{merged}}}^2} + \frac{(\Delta m_{\text{VLQ}} - \overline{\Delta m_{\text{VLQ}}})^2}{\sigma_{\Delta m_{\text{VLQ}}}^2}. \quad (3)$$

The means (\bar{m} and $\overline{\Delta m_{\text{VLQ}}}$) and standard deviations (σ_m and $\sigma_{\Delta m_{\text{VLQ}}}$) of the parameters used in these expressions are determined from simulated signal events in which the jets are matched to the generator-level quarks and H/Z bosons. These quantities are derived separately for each jet multiplicity, but do not depend on the simulated signal mass. For each parameter, the central core of the distribution is fit with a Gaussian function, whose mean and standard deviation are then used as the parameters in the expressions for χ^2_{mod} . As the distribution of the merged Higgs boson mass is asymmetrical, two Gaussian functions are separately fit above and below the peak of the distribution. Since the underlying distributions used in these expressions have non-Gaussian tails and are in some cases asymmetric, the values of χ^2_{mod} are not exactly distributed as a χ^2 variable. However, the difference is small, and χ^2_{mod} is only used to select events, so these deviations do not affect the analysis. Choosing the jet combination that has the lowest value of χ^2_{mod} gives a high probability of identifying the correct jet combination, and allows m_{VLQ} to be reconstructed. In simulation, this can then be compared with the generated B mass m_B . This is indicated in Fig. 2, which shows the average

value of the reconstructed VLQ mass for the jet combination with the lowest χ^2_{mod} for simulated signal events with $m_B = 1200$ GeV. In most cases, the VLQ mass is correctly reconstructed. We observe that the reconstructed mass distribution is consistently peaked at a value about 5% lower than the generated mass, for all generated signal mass values. The low-side tail is due to the presence of incorrectly reconstructed events.

Figure 3 shows the distributions of $\chi^2_{\text{mod}}/\text{ndf}$, where ndf is the number of degrees of freedom, for the best jet combination (i.e., the combination with the lowest χ^2_{mod}), from simulated 1200 GeV VLQ signal events, at each jet multiplicity. Each χ^2_{mod} expression has three degrees of freedom, one for each term. The distributions for the data are also shown for comparison. In these plots, the simulated signal and data distributions are normalized to the same integral value within the displayed χ^2_{mod} range. This figure demonstrates that requiring a small χ^2_{mod} value for the best jet combination provides an effective method for removing background.

The χ^2_{mod} value is also used to select the event mode. There are three possible decays of the bottom-type VLQ: $B \rightarrow bH$, $B \rightarrow bZ$, and $B \rightarrow tW$. This results in six

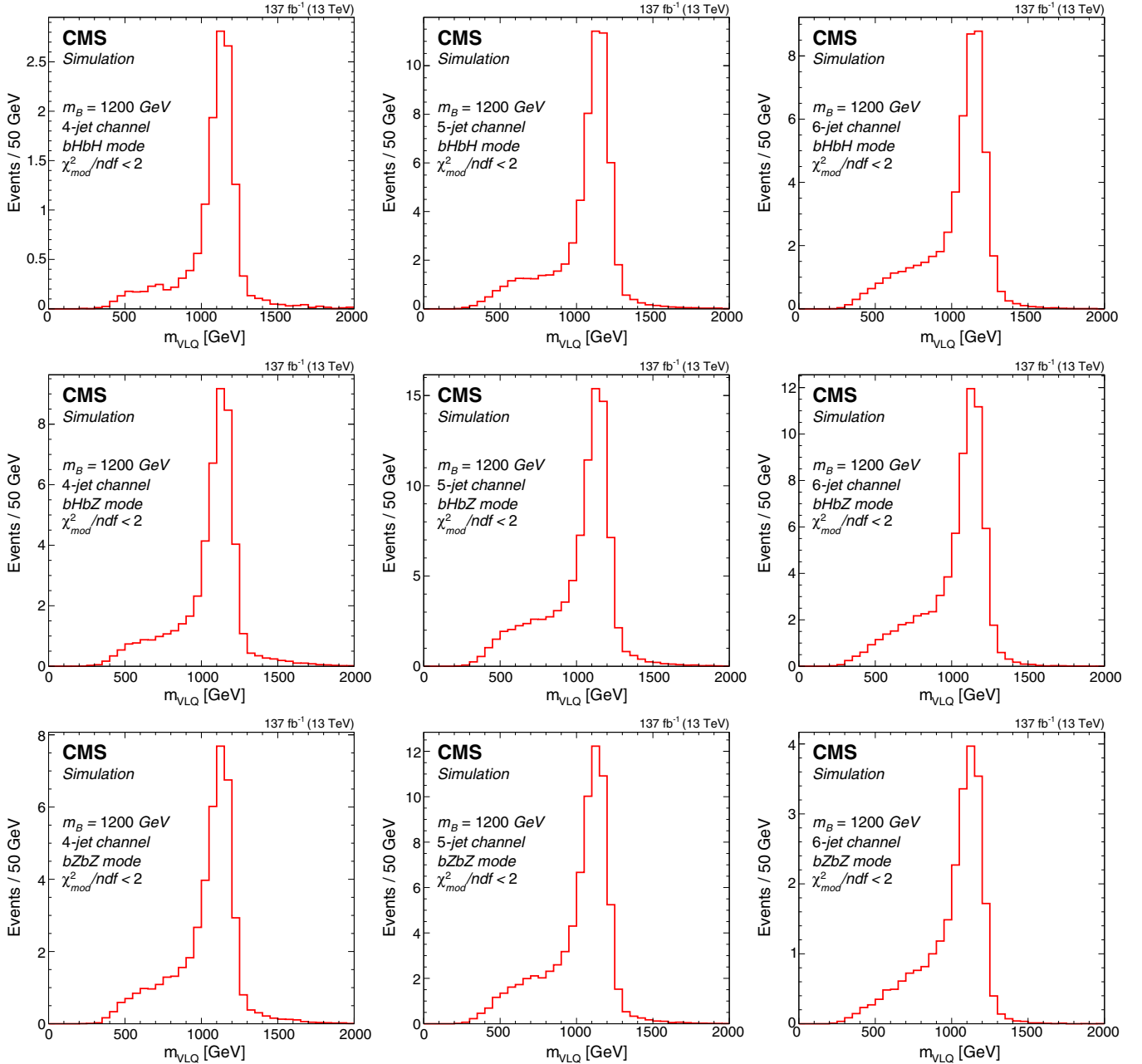


FIG. 2. Distributions of m_{VLQ} for simulated signal events with a generated VLQ mass $m_B = 1200$ GeV. A requirement of $\chi^2_{\text{mod}}/\text{ndf} < 2$ is applied to the events. Mass distributions for 4-jet (left), 5-jet (center), and 6-jet (right) events are shown for the three event modes: $bHbH$ (upper row), $bHbZ$ (middle row), and $bZbZ$ (lower row).

possible modes for the $B\bar{B}$ pair production events: $bHbH$, $bHbZ$, $bZbZ$, $tWbH$, $tWbZ$, and $tWtW$. The latter three modes involve one or two decays of a VLQ to a t quark and a W boson. These events either have a jet multiplicity greater than six, or contain leptons and missing transverse energy from the W decays. Although this analysis is not optimized for sensitivity to these events, events with $B \rightarrow tW$, if present, have some probability to be selected as one of the other three event modes and can affect the sensitivity of the analysis. These events are included

in the signal simulation and are added according to their reconstruction efficiency. For events that satisfy the H_T requirement and that are categorized as either 4-, 5-, or 6-jet multiplicity events, the χ^2_{mod} described above is calculated for each of the three event modes: $bHbH$, $bHbZ$, or $bZbZ$, and the mode of the event is selected as the one that has the best χ^2_{mod} value. Events are categorized by their jet multiplicity and their reconstructed mode, regardless of the underlying decay mode for simulated signal events.

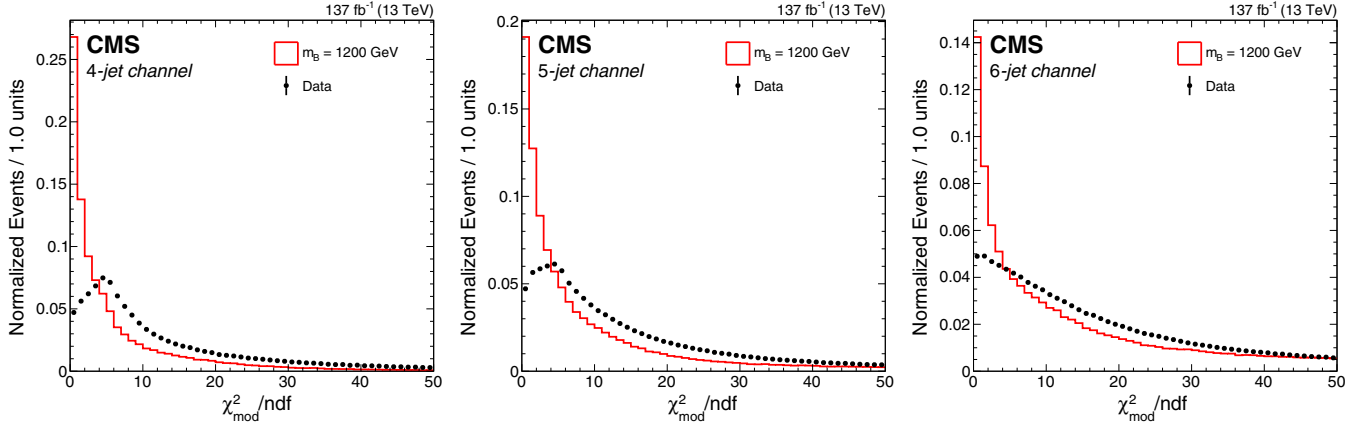


FIG. 3. Distribution of $\chi^2_{\text{mod}}/\text{ndf}$ for the best jet combination for simulated 1200 GeV VLQ events (red histogram) and data (black points), for 4-jet (left), 5-jet (center), and 6-jet events (right). The simulated signal events and data events are normalized to the same integral value within the displayed χ^2_{mod} range.

TABLE III. Optimized values of the $\chi^2_{\text{mod}}/\text{ndf}$ selection as a function of jet multiplicity and event mode.

Event mode	Jet multiplicity		
	4	5	6
$bHbH$	5.5	2	2.75
$bHbZ$	2.75	2.5	2.5
$bZbZ$	2	2	2.25

TABLE IV. Values of the BJTF for data events with m_{VLQ} in the range 500–800 GeV for each of the three event modes and three jet multiplicities.

	$bHbH$	$bHbZ$	$bZbZ$
4 jets	0.0042 ± 0.0014	0.0019 ± 0.0004	0.0025 ± 0.0004
5 jets	0.0041 ± 0.0003	0.0036 ± 0.0002	0.0048 ± 0.0009
6 jets	0.0019 ± 0.0002	0.0019 ± 0.0002	0.0020 ± 0.0005

Before examining the data in the potential signal region, the event selection parameters (the jet tagging parameters and χ^2_{mod}) are optimized. This optimization is performed by varying the parameters and selecting the values that maximize the sensitivity to a 1600 GeV VLQ signal. The mass of 1600 GeV is chosen because it is the point with maximum sensitivity of the analysis; however, the optimized parameters are largely independent of the point chosen. The optimized jet tagging parameters are described in Section VI, and the optimized $\chi^2_{\text{mod}}/\text{ndf}$ values are shown below in Table III. With the optimized selection, the overall signal efficiency measured in simulation for a generated VLQ mass of 1600 GeV is approximately 5% in the $\mathcal{B}(B \rightarrow bZ) = 100\%$ scenario, increasing to 10% for $\mathcal{B}(B \rightarrow bH) = 100\%$.

VIII. BACKGROUND ESTIMATION

The expected background is estimated in a low-mass sideband region in data, using the ratio of the number of

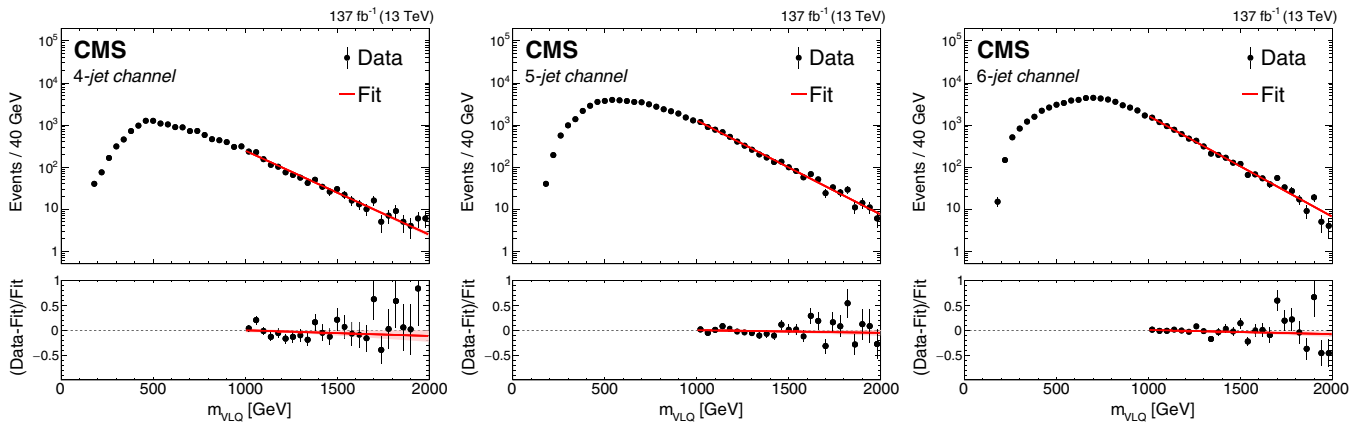


FIG. 4. Distributions of m_{VLQ} for the jet combination with the lowest χ^2_{mod} in 4-jet (left), 5-jet (center), and 6-jet (right) multiplicity events. The red lines show the exponential fit in the range 1000–2000 GeV. The lower panels show the fractional difference, (data – fit)/fit.

events passing the tag requirements to the number before these requirements are applied. The estimation is done separately for each of the three event modes, jet multiplicities, and three data-taking years, for a total of 27 cases.

Figure 4 shows the distribution of m_{VLQ} for the jet combination with the lowest χ^2_{mod} for each of the three jet multiplicities. All events shown in this plot are required to pass a selection of $\chi^2_{\text{mod}}/\text{ndf} < 4$. The falloff in the distribution at lower masses is due to the $H_T >$

1350 GeV requirement. The distributions are then fit with an exponential function for VLQ candidate masses greater than 1000 GeV; in all three cases, the function (shown by the red line) agrees with the data. An F -test [50] shows that a more complex model, namely an exponential plus constant background, offers no significant improvement over the exponential distribution. The lower plots show the fractional difference between the data and the fit. At this stage, since there is no requirement made on jet tagging, the

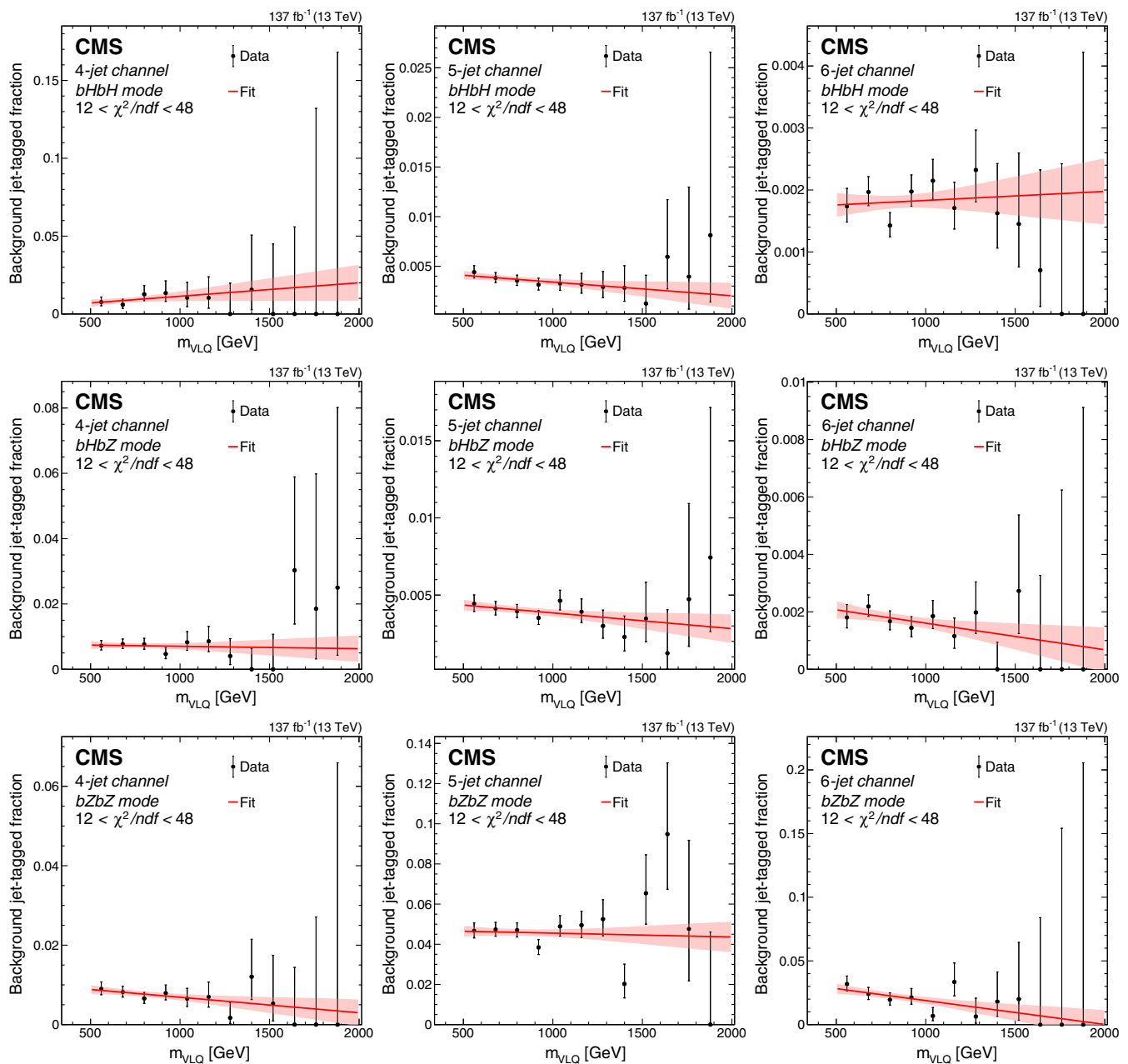


FIG. 5. Dependence of the BJTF on m_{VLQ} in the control region $12 < \chi^2_{\text{mod}}/\text{ndf} < 48$, for 4-jet (left column), 5-jet (center column), and 6-jet (right column) multiplicities, and for the $bHbH$ (upper row), $bHbZ$ (middle row), and $bZbZ$ (lower row) event modes. The data are shown as black points with vertical error bars, and the linear fit and associated uncertainty are shown as a solid red line and the shaded red band.

ratio of background to signal event acceptance is more than two orders of magnitude larger than after jet tagging, so the fits are insensitive to any possible signal events in the data.

The background jet-tagged fraction (BJTF) is the fraction of background events that remain after the jet tagging requirements, as described in Sec. V, are applied. Since the BJTF for events with $m_{\text{VLQ}} > 1000$ GeV could be biased due to signal events that might be in the data, the BJTF is initially determined only for events in which m_{VLQ} is

between 500 and 800 GeV, which is below the current lower exclusion limit on the VLQ mass [17,18]. Table IV shows the BJTF for data events with m_{VLQ} in the range 500–800 GeV for each of the three event modes and three jet multiplicities.

Because the jet tagging efficiency depends on the p_T of the jet, the BJTF might depend on the mass of the VLQ candidate, since events with greater VLQ mass generally have higher p_T jets. A control region is therefore used to

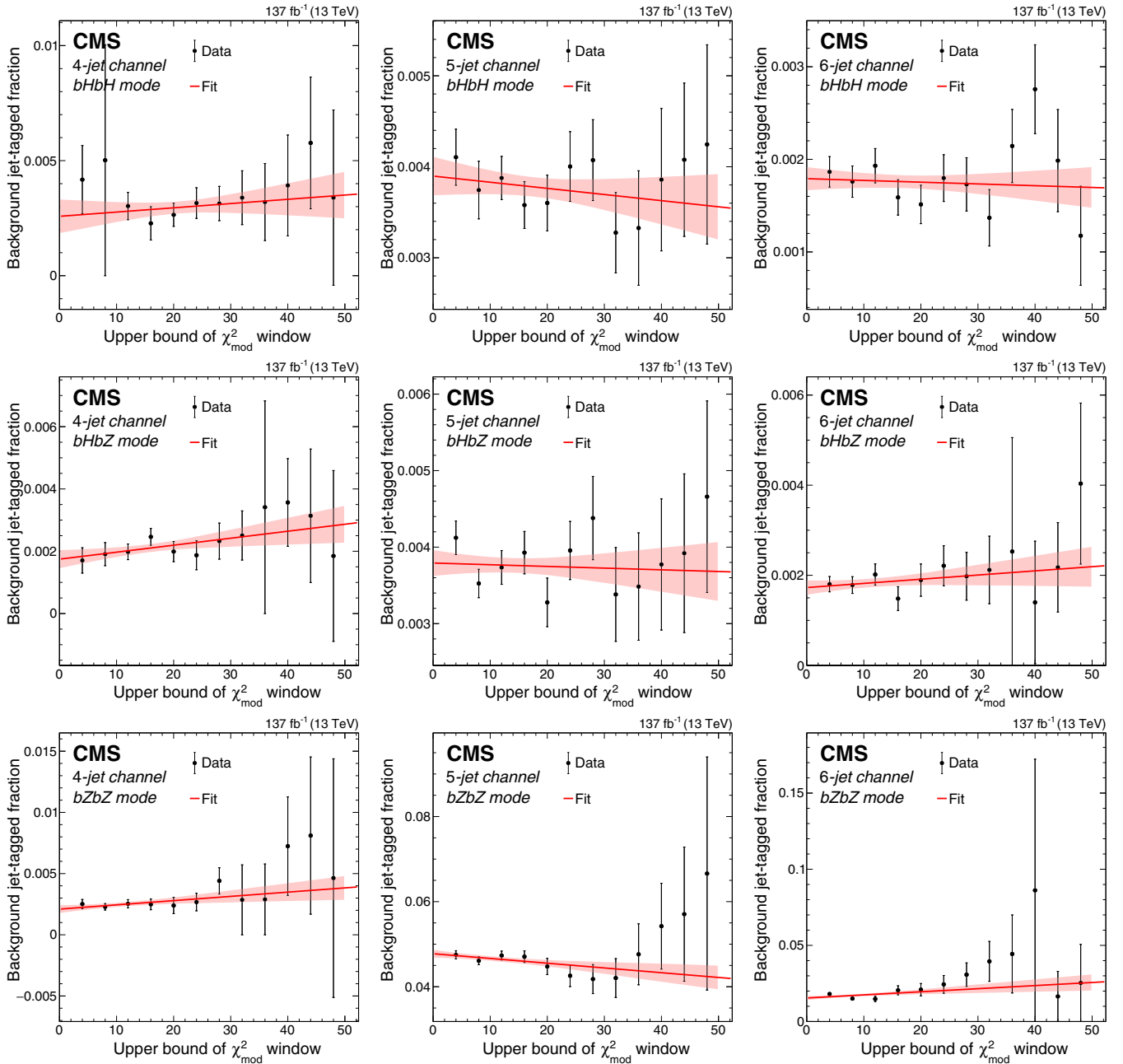


FIG. 6. Dependence of the BJTF on $\chi^2_{\text{mod}}/\text{ndf}$ in the low-mass (500–800 GeV) VLQ region, for 4-jet (left column), 5-jet (center column), and 6-jet (right column) multiplicities, and for the $bHbH$ (upper row), $bHbZ$ (middle row), and $bZbZ$ (lower row) event modes. The data are shown as black points with vertical error bars, and the linear fit and associated uncertainty are shown as a solid red line and the shaded red band.

determine the VLQ mass dependence of the BJTF by offsetting the window of the χ^2_{mod} selection. The signal χ^2_{mod} region depends on the event mode and multiplicity, as determined by the optimization procedure described in Sec. VII, but in all cases is at most $\chi^2_{\text{mod}}/\text{ndf} < 5.5$. A control region is defined by using a region of $12 < \chi^2_{\text{mod}}/\text{ndf} < 48$. Figure 5 shows the mass dependence of the BJTF for data events in the χ^2_{mod} control region. A first-order polynomial fit is used to determine the BJTF mass dependence. Another F -test shows that there is no improvement for a second-order polynomial fit compared to a first-order one, and also that the first-order polynomial fit performs better than a constant fit. A systematic uncertainty is assigned by comparing the first-order polynomial fit to an exponential fit, and using the average difference of these two fits over the mass range as the

uncertainty. This covers the uncertainty due to the choice of the BJTF shape.

In order to validate that the control region used has the same BJTF behavior as the signal region, we perform a test where the BJTF in the low VLQ mass range (500–800 GeV) is plotted as a function of $\chi^2_{\text{mod}}/\text{ndf}$, in twelve equally spaced regions for $\chi^2_{\text{mod}}/\text{ndf}$ from 0 to 48. This is shown in Fig. 6. The slope of this plot is consistent with zero, indicating no statistically significant dependence on $\chi^2_{\text{mod}}/\text{ndf}$.

Figure 7 shows the two-dimensional dependence of the BJTF in data on m_{VLQ} and $\chi^2_{\text{mod}}/\text{ndf}$, and Fig. 8 shows the corresponding distributions for simulated VLQ signal events with a generated VLQ mass of 1200 GeV. The signal region is indicated in these plots by the red rectangle, and is excluded from the data plots.

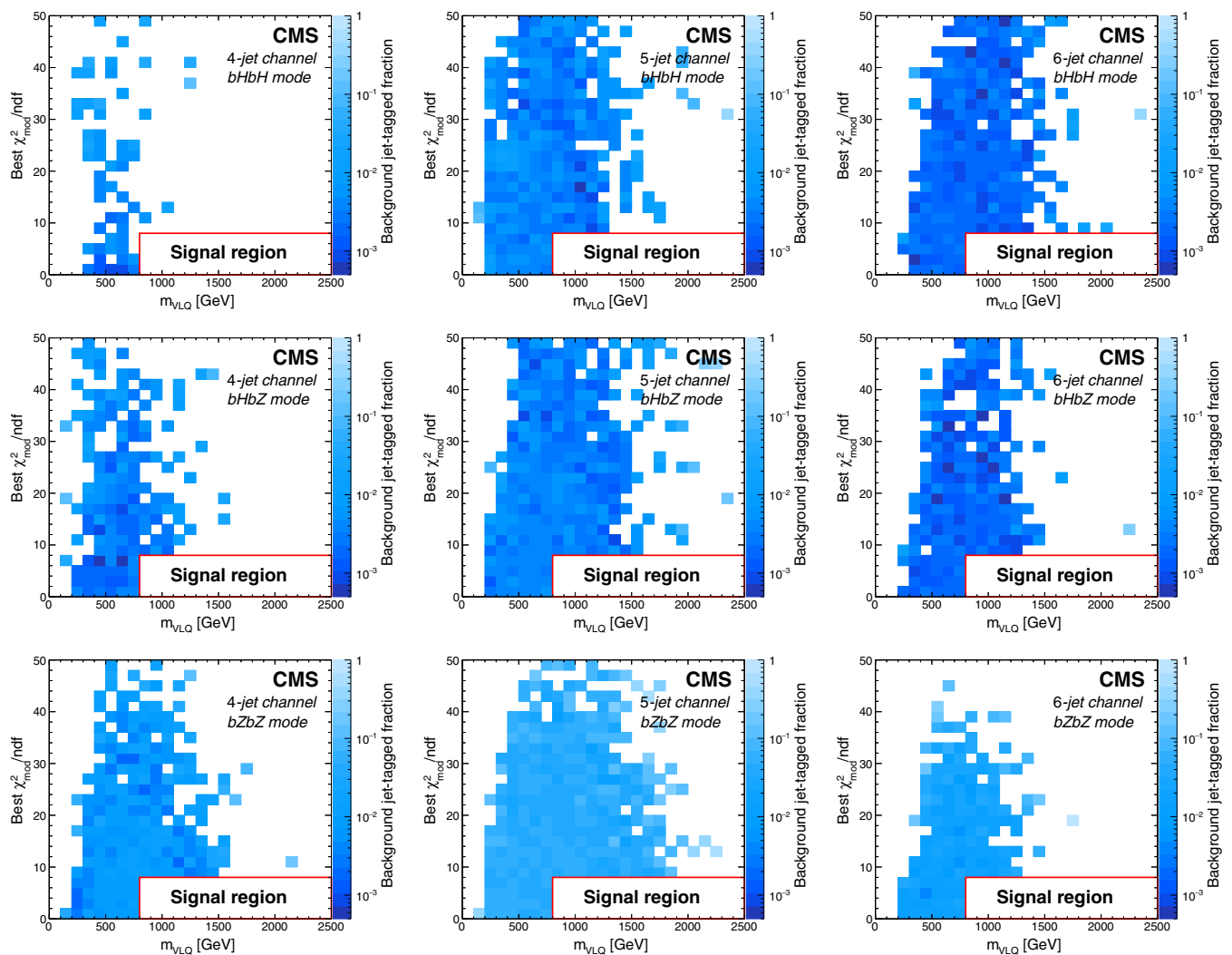


FIG. 7. Dependence of the BJTF on m_{VLQ} and the best $\chi^2_{\text{mod}}/\text{ndf}$ in data events, for 4-jet (left column), 5-jet (center column), and 6-jet (right column) multiplicities, and for the $bHbH$ (upper row), $bHbZ$ (middle row), and $bZbZ$ (lower row) event modes. The red box indicates the signal region, which is excluded from these plots.

The final estimate of the number of background events n_b as a function of VLQ mass m is given by the following expression:

$$n_b(m) = n(m)\epsilon_0 \frac{\epsilon(m)}{\left(\int_{500 \text{ GeV}}^{800 \text{ GeV}} \epsilon(m') dm'\right)/(300 \text{ GeV})}, \quad (4)$$

where $n(m)$ is the number of candidates as a function of m_{VLQ} before jet tagging for candidates passing the χ^2_{mod} selection shown in Fig. 4, ϵ_0 is the BJTF at low VLQ mass as shown in Table IV, and the last factor accounts for the potential mass dependence of the BJTF, with $\epsilon(m)$ the distribution of the BJTF as a function of mass, as shown in Fig. 5; the factor of 300 GeV is to normalize over the range considered. The final estimate is also validated by comparison with the region $8 < \chi^2_{\text{mod}}/\text{ndf} < 12$ and with simulated events.

IX. SYSTEMATIC UNCERTAINTIES

We consider two types of systematic uncertainties, those that are common to all event modes and jet multiplicities, and those that depend on the particular channel. The uncertainties in the first category are listed in Table V; these are the integrated luminosity, trigger efficiency, and the choice of fit function for the dependence of the BJTF on VLQ mass. The integrated luminosities of the 2016, 2017, and 2018 data-taking periods are individually known with uncertainties in the range 2.3%–2.5% [24–26], while the total 2016–2018 integrated luminosity has an uncertainty of 1.8%, the improvement in precision reflecting the (uncorrelated) time evolution of some systematic effects. The uncertainty associated with the choice of fit function for the m_{VLQ} dependence of the BJTF is determined by finding

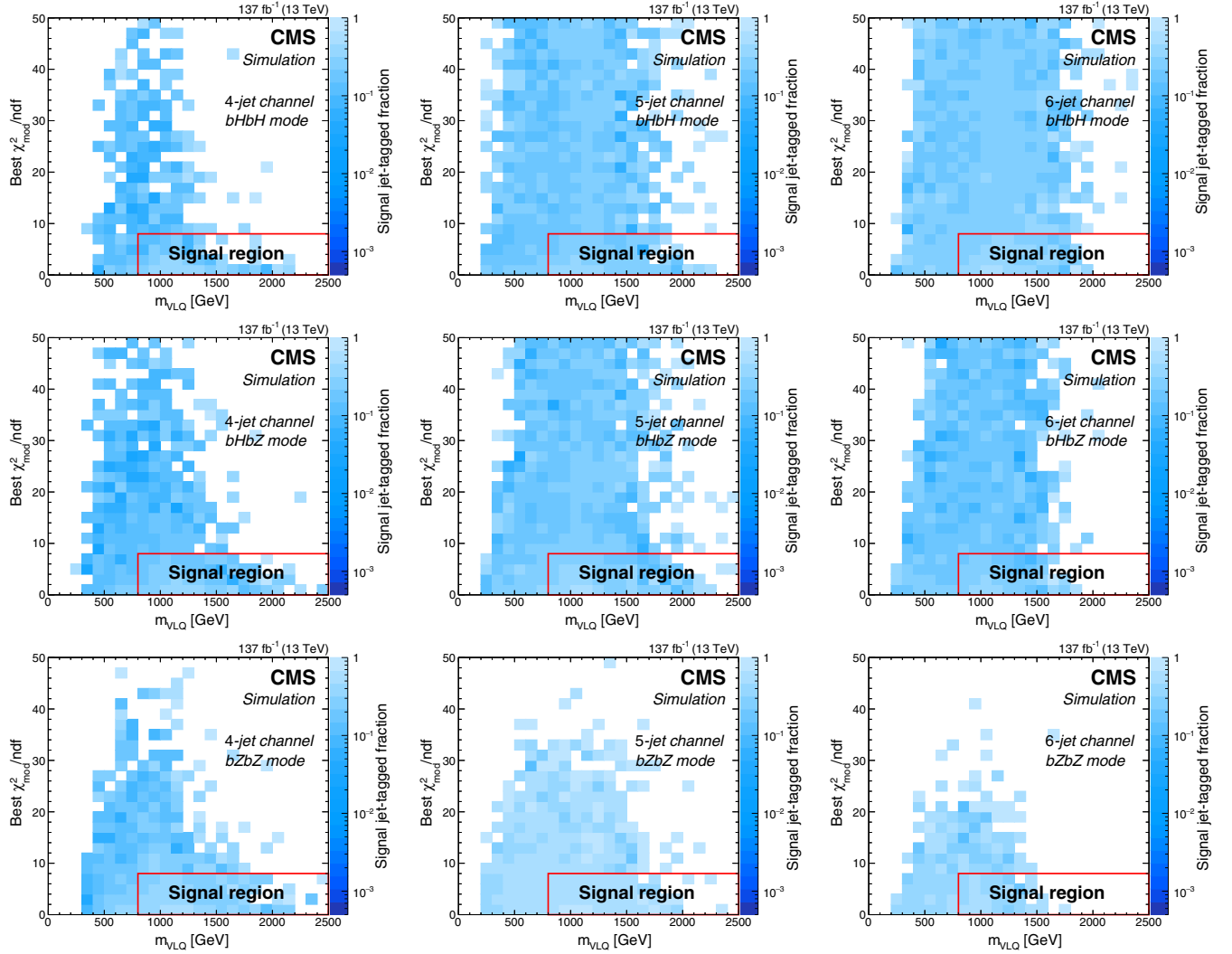


FIG. 8. Dependence of the BJTF on m_{VLQ} and the best $\chi^2_{\text{mod}}/\text{ndf}$ in simulated VLQ signal events with $m_B = 1200$ GeV, for 4-jet (left column), 5-jet (center column), and 6-jet (right column) multiplicities, and for the $bHbH$ (upper row), $bHbZ$ (middle row), and $bZbZ$ (lower row) event modes. The red box indicates the signal region.

TABLE V. Systematic uncertainties common to all three event modes and all three jet multiplicities. All uncertainties listed here are rate uncertainties, meaning they affect only the normalization.

Type	Signal/Background	Uncertainty
Integrated luminosity	Signal	1.8%
Trigger efficiency	Signal	0.02%
Choice of fit function	Background	4.9%

the average difference between the fit functions used for each mode and multiplicity combination, and using the maximum one as the common uncertainty for all modes and multiplicities. Table V also indicates whether an uncertainty affects the signal efficiency or the background estimate.

The uncertainties that depend on event mode and jet multiplicity are those due to the background estimation, jet tag scale factors, jet energy resolution and scale, choice of PDF, and pileup.

There are several sources of uncertainty in the background estimation, corresponding to the three terms in Eq. (4). The first uncertainty arises from the exponential fit to the distribution $n(m)$, the number of events as a function of mass before jet tagging is applied. The uncertainties in the fit parameters p_0 and p_1 are used to determine the uncertainty in the fit value for a given mass. The second is the uncertainty in the BJTF determined for low-mass VLQ candidates, ϵ_0 , as shown in Table IV. Finally, the third uncertainty arises from the third term, to account for a potential mass dependence of the BJTF, and is obtained from the uncertainties in the fit parameters, as in the first case.

The efficiencies for jet tagging are measured in simulated events and then corrected to data events using a data-to-simulation scale factor. The uncertainty in this scale factor is propagated to the signal reconstruction efficiency by varying the scale factors within their uncertainties [39]. The uncertainties due to the scale factors for jet energy scale and

TABLE VI. Table of systematic uncertainties for each event mode and jet multiplicity. The reported values indicate the uncertainty in the event yield in a ± 75 GeV window about the signal peak for a generated signal mass $m_B = 1600$ GeV.

Type	Signal/Background	Rate/Shape	4 jets	5 jets	6 jets
<i>bHbH event mode</i>					
Background fit p_0	Background	Shape	59%	14%	13%
Background fit p_1	Background	Shape	78%	18%	16%
BJTF m dependence p_0	Background	Shape	1.3%	5.9%	4.5%
BJTF m dependence p_1	Background	Shape	19%	25%	17%
Low-mass BJTF	Background	Rate	34%	9.7%	11%
Jet tag scale factors	Signal	Shape	16%	15%	17%
Jet energy scale	Signal	Shape	4.0%	5.3%	6.4%
Jet energy resolution	Signal	Shape	2.4%	1.5%	1.6%
Pileup	Signal	Shape	28%	28%	27%
PDF	Signal	Rate	1.5%	1.5%	1.5%
<i>bHbZ event mode</i>					
Background fit p_0	Background	Shape	21%	12%	10%
Background fit p_1	Background	Shape	21%	14%	12%
BJTF m dependence p_0	Background	Shape	2.1%	7.7%	3.5%
BJTF m dependence p_1	Background	Shape	21%	30%	27%
Low-mass BJTF	Background	Rate	22%	7.7%	11%
Jet tag scale factors	Signal	Shape	15%	13%	17%
Jet energy scale	Signal	Shape	4.9%	5.7%	5.1%
Jet energy resolution	Signal	Shape	1.8%	2.7%	3.2%
Pileup	Signal	Shape	33%	28%	21%
PDF	Signal	Rate	1.6%	1.5%	1.5%
<i>bZbZ event mode</i>					
Background fit p_0	Background	Shape	26%	17%	24%
Background fit p_1	Background	Shape	28%	21%	32%
BJTF m dependence p_0	Background	Shape	3.7%	0.6%	11%
BJTF m dependence p_1	Background	Shape	15%	7.8%	21%
Low-mass BJTF	Background	Rate	16%	19%	25%
Jet tag scale factors	Signal	Shape	8.9%	8.0%	11%
Jet energy scale	Signal	Shape	4.0%	2.9%	1.6%
Jet energy resolution	Signal	Shape	2.5%	2.5%	3.2%
Pileup	Signal	Shape	28%	28%	10%
PDF	Signal	Rate	1.5%	1.5%	1.5%

resolution [21] are determined similarly. The uncertainty due to the choice of PDF weighting is calculated from a set of 100 weights selected from the NNPDF3.0 distribution, following the prescription in Ref. [51]. The pileup uncertainties are due to a 4.6% systematic uncertainty in the pp inelastic cross section.

Table VI summarizes these uncertainties, and indicates whether they affect the signal efficiency or the background estimate, and whether the uncertainty affects the overall rate or the shape of the mass distribution. For the PDF systematic uncertainties, the values refer only to the event acceptance rate. There is in addition an uncertainty in the

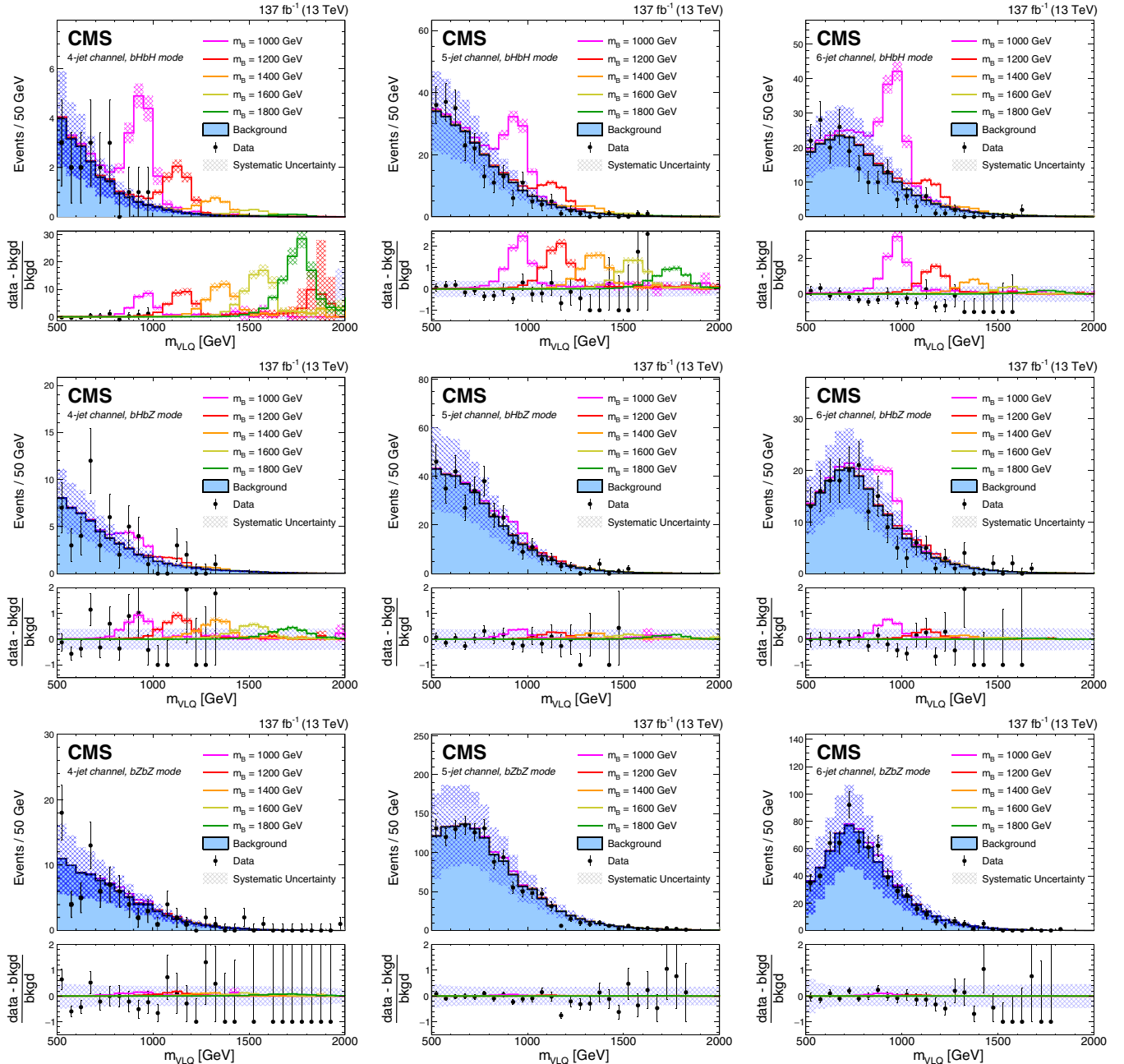


FIG. 9. Data (black points), expected background (solid blue histogram), and expected background plus a VLQ signal for different VLQ masses (colored lines), for 4-jet (left column), 5-jet (center column), and 6-jet (right column) multiplicities and for $bHbH$ (upper row), $bHbZ$ (middle row), and $bZbZ$ (lower row) event modes. For the signal, $\mathcal{B}(B \rightarrow bH) = 100\%$ is assumed. The hatched regions for the background and background plus signal distributions indicate the systematic uncertainties. All three data-taking years are combined.

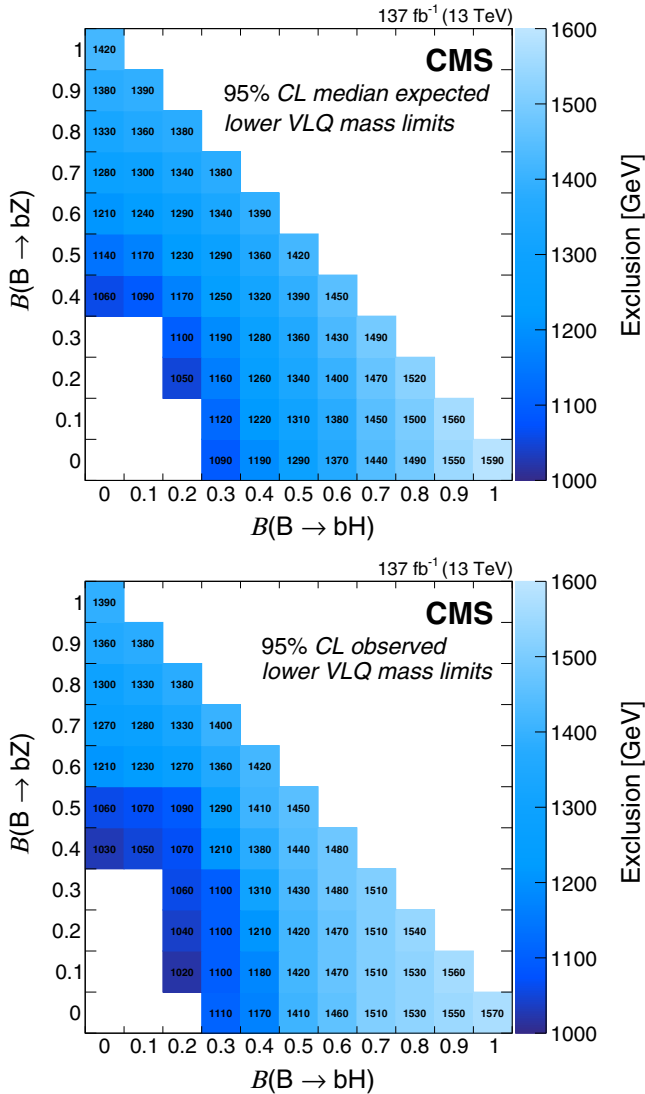


FIG. 10. Expected (upper) and observed (lower) limits on the VLQ mass at 95% C.L. as a function of the branching fractions $\mathcal{B}(B \rightarrow bH)$ and $\mathcal{B}(B \rightarrow bZ)$.

VLQ pair production cross section. This uncertainty depends only weakly on VLQ mass and an average value of 6% is used for all masses [34].

X. RESULTS

Figure 9 shows the distribution of the reconstructed VLQ mass, after the optimized selections described in Sec. VII have been applied, for data, the expected background, and for simulated signal events with a VLQ mass of 1200, 1400, 1600, and 1800 GeV and $\mathcal{B}(B \rightarrow bH) = 100\%$. The signal distributions are normalized to the expected number of events as determined by the VLQ production cross section. No statistically significant excess of data over the background expectation is observed; the largest difference across all nine mass points and branching fraction scenarios is slightly less than 2σ .

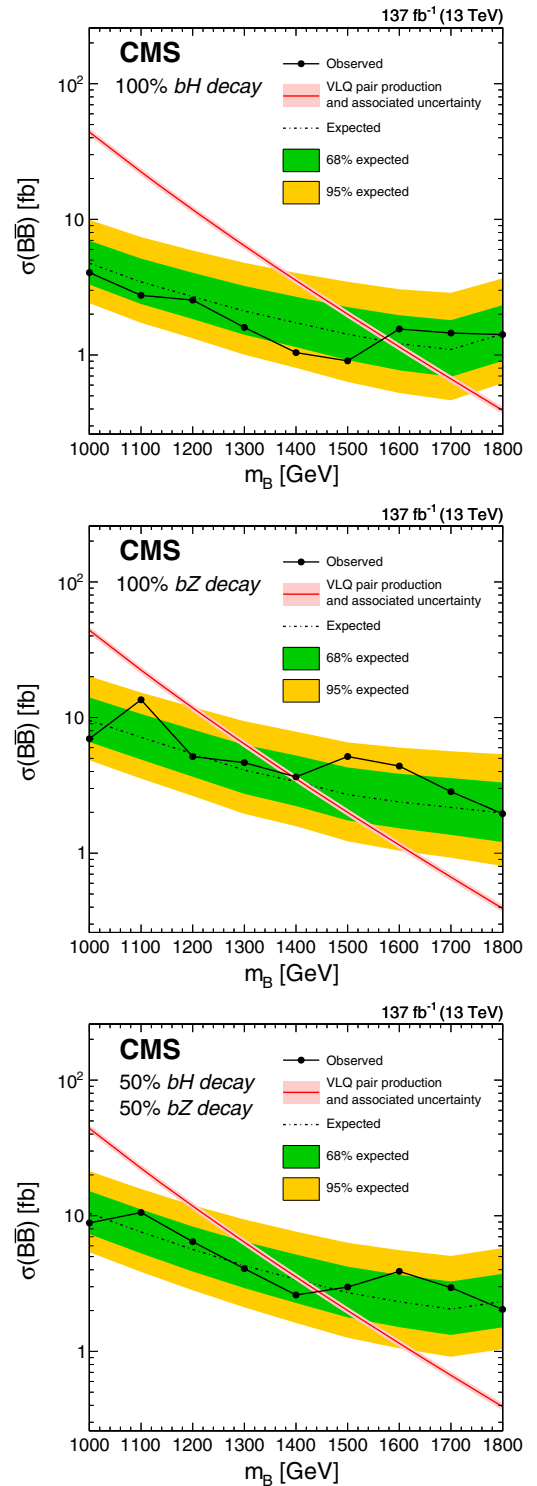


FIG. 11. The 95% confidence limit on the cross section for VLQ pair production as a function of VLQ mass for three branching fraction hypotheses: $\mathcal{B}(B \rightarrow bH) = 100\%$ (upper left), $\mathcal{B}(B \rightarrow bZ) = 100\%$ (middle), and $\mathcal{B}(B \rightarrow bH) = \mathcal{B}(B \rightarrow bZ) = 50\%$ (lower). The solid black line indicates the observed limit and the dashed line indicates the expected limit with 1 sigma (green band) and 2 sigma (yellow band) uncertainties. The theoretical cross section and its uncertainty are shown as the red line and pale red band; the band is only slightly visible outside the line.

We proceed to set exclusion limits on the VLQ mass as a function of the branching fractions. The signal extraction procedure is based on a binned maximum likelihood fit. All systematic uncertainties are incorporated into the fit as nuisance parameters, where the effect of each systematic uncertainty is included as a log normal probability distribution per bin. A limit at 95% C.L. is calculated using the CL_s method [52,53] using the profile likelihood test statistic [54] with the asymptotic limit approximation. Figure 10 shows the final expected and observed limits on the VLQ mass as a function of $\mathcal{B}(B \rightarrow bH)$ and $\mathcal{B}(B \rightarrow bZ)$, after all of the individual jet multiplicities and event modes have been combined. Points for which the exclusion limit is less than 1000 GeV are not shown.

Figure 11 shows the expected limits at 95% C.L. on the cross section of VLQ pair production as a function of VLQ mass assuming three different branching fraction combinations: $\mathcal{B}(B \rightarrow bH) = 100\%$, $\mathcal{B}(B \rightarrow bZ) = 100\%$, and $\mathcal{B}(B \rightarrow bH) = \mathcal{B}(B \rightarrow bZ) = 50\%$. The observed limits at 95% C.L. are 1570 GeV in the 100% bH case, 1390 GeV in the 100% bZ case, and 1450 GeV in the 50% bH plus 50% bZ case. In the fully $B \rightarrow bH$ and $B \rightarrow bZ$ modes, as well as the mixed $bHbZ$ mode, where this analysis is most sensitive, these limits represent significant improvements over previously published VLQ limits (1010, 1070, and 1025 GeV respectively), extending the existing limits by several hundred GeV. These improvements can be attributed to the use of the $\chi^2_{\text{mod}}/\text{ndf}$ method, which allows the hadronic final state to be fully reconstructed, as well as to the increased size of the data sample.

XI. SUMMARY

This paper describes a search for bottom-type, vectorlike quark (VLQ) pair production in data collected by the CMS detector in 2016–2018 at $\sqrt{s} = 13$ TeV, where the VLQ B decays into a b or \bar{b} quark and either a Higgs boson H or a Z boson. The analysis targets the fully hadronic $B \rightarrow bH$ and $B \rightarrow bZ$ decays by tagging jets and using a modified χ^2 metric to reconstruct the event. Different jet multiplicity categories were used to account for the fact that Higgs or Z boson decays can produce either two distinct jets or, if highly Lorentz boosted, a single merged jet. Backgrounds were estimated from a region of low VLQ mass and extrapolated into the signal region using a modified χ^2 control region. Limits were set on the VLQ mass at 95% confidence level as a function of the branching fractions for $B \rightarrow bH$ and $B \rightarrow bZ$. Compared to previous measurements [17,18], limits on the B VLQ mass have been increased from 1010 to 1570 GeV in the $\mathcal{B}(B \rightarrow bH) = 100\%$ case, from 1070 to 1390 GeV in the $\mathcal{B}(B \rightarrow bZ) = 100\%$ case, and from 1025 to 1450 GeV in the $\mathcal{B}(B \rightarrow bH) = \mathcal{B}(B \rightarrow bZ) = 50\%$ case.

ACKNOWLEDGMENTS

We congratulate our colleagues in the CERN accelerator departments for the excellent performance of the LHC and thank the technical and administrative staffs at CERN and at other CMS institutes for their contributions to the success of the CMS effort. In addition, we gratefully acknowledge the computing centers and personnel of the Worldwide LHC Computing Grid for delivering so effectively the computing infrastructure essential to our analyses. Finally, we acknowledge the enduring support for the construction and operation of the LHC and the CMS detector provided by the following funding agencies: BMBWF and FWF (Austria); FNRS and FWO (Belgium); CNPq, CAPES, FAPERJ, FAPERGS, and FAPESP (Brazil); MES (Bulgaria); CERN; CAS, MoST, and NSFC (China); COLCIENCIAS (Colombia); MSES and CSF (Croatia); RIF (Cyprus); SENESCYT (Ecuador); MoER, ERC IUT, PUT and ERDF (Estonia); Academy of Finland, MEC, and HIP (Finland); CEA and CNRS/IN2P3 (France); BMBF, DFG, and HGF (Germany); GSRT (Greece); NKFI (Hungary); DAE and DST (India); IPM (Iran); SFI (Ireland); INFN (Italy); MSIP and NRF (Republic of Korea); MES (Latvia); LAS (Lithuania); MOE and UM (Malaysia); BUAP, CINVESTAV, CONACYT, LNS, SEP, and UASLP-FAI (Mexico); MOS (Montenegro); MBIE (New Zealand); PAEC (Pakistan); MSHE and NSC (Poland); FCT (Portugal); JINR (Dubna); MON, RosAtom, RAS, RFBR, and NRC KI (Russia); MESTD (Serbia); SEIDI, CPAN, PCTI, and FEDER (Spain); MOSTR (Sri Lanka); Swiss Funding Agencies (Switzerland); MST (Taipei); ThEPCenter, IPST, STAR, and NSTDA (Thailand); TUBITAK and TAEK (Turkey); NASU (Ukraine); STFC (United Kingdom); DOE and NSF (USA). Individuals have received support from the Marie-Curie program and the European Research Council and Horizon 2020 Grant, contracts No. 675440, No. 752730, and No. 765710 (European Union); the Leventis Foundation; the A. P. Sloan Foundation; the Alexander von Humboldt Foundation; the Belgian Federal Science Policy Office; the Fonds pour la Formation à la Recherche dans l'Industrie et dans l'Agriculture (FRIA-Belgium); the Agentschap voor Innovatie door Wetenschap en Technologie (IWT-Belgium); the F. R. S.-FNRS and FWO (Belgium) under the “Excellence of Science—EOS”—be.h project n. 30820817; the Beijing Municipal Science & Technology Commission, No. Z191100007219010; the Ministry of Education, Youth and Sports (MEYS) of the Czech Republic; the Deutsche Forschungsgemeinschaft (DFG) under Germany’s Excellence Strategy—EXC 2121 “Quantum Universe”—390833306; the Lendület (“Momentum”) Program and the János Bolyai Research Scholarship of the Hungarian Academy of Sciences, the New National Excellence Program ÚNKP, the NKFI research grants No. 123842, No. 123959, No. 124845, No. 124850,

No. 125105, No. 128713, No. 128786, and No. 129058 (Hungary); the Council of Science and Industrial Research, India; the HOMING PLUS program of the Foundation for Polish Science, cofinanced from European Union, Regional Development Fund, the Mobility Plus program of the Ministry of Science and Higher Education, the National Science Center (Poland), contracts Harmonia 2014/14/M/ST2/00428, Opus 2014/13/B/ST2/02543, 2014/15/B/ST2/03998, and 2015/19/B/ST2/02861, Sonata-bis 2012/07/E/ST2/01406; the National Priorities Research Program by Qatar National Research Fund; the Ministry of Science and Higher Education, project no. 02.a03.21.0005 (Russia); the

Programa Estatal de Fomento de la Investigación Científica y Técnica de Excelencia María de Maeztu, grant MDM-2015-0509 and the Programa Severo Ochoa del Principado de Asturias; the Thalís and Aristeia programs cofinanced by EU-ESF and the Greek NSRF; the Rachadapisek Sompot Fund for Postdoctoral Fellowship, Chulalongkorn University and the Chulalongkorn Academic into Its 2nd Century Project Advancement Project (Thailand); the Kavli Foundation; the Nvidia Corporation; the SuperMicro Corporation; the Welch Foundation, contract C-1845; and the Weston Havens Foundation (USA).

-
- [1] G. 't Hooft, Naturalness, chiral symmetry, and spontaneous chiral symmetry breaking, *NATO Sci. Ser. B* **59**, 135 (1980).
- [2] J. Wess and B. Zumino, A Lagrangian model invariant under supergauge transformations, *Phys. Lett.* **49B**, 52 (1974).
- [3] P. Fayet and S. Ferrara, Supersymmetry, *Phys. Rep.* **32**, 249 (1977).
- [4] H. Georgi and A. Pais, Calculability and naturalness in gauge theories, *Phys. Rev. D* **10**, 539 (1974).
- [5] D. B. Kaplan, H. Georgi, and S. Dimopoulos, Composite Higgs scalars, *Phys. Lett.* **136B**, 187 (1984).
- [6] K. Agashe, R. Contino, and A. Pomarol, The minimal composite Higgs model, *Nucl. Phys.* **B719**, 165 (2005).
- [7] N. Arkani-Hamed, A. G. Cohen, and H. Georgi, Electroweak symmetry breaking from dimensional deconstruction, *Phys. Lett. B* **513**, 232 (2001).
- [8] N. Arkani-Hamed, A. G. Cohen, E. Katz, and A. E. Nelson, The littlest Higgs, *J. High Energy Phys.* **07** (2002) 034.
- [9] F. del Aguila and M. J. Bowick, The possibility of new fermions with $\Delta I = 0$ mass, *Nucl. Phys.* **B224**, 107 (1983).
- [10] ATLAS Collaboration, Combined measurements of Higgs boson production and decay using up to 80 fb⁻¹ of proton-proton collision data at $\sqrt{s} = 13$ TeV collected with the ATLAS experiment, *Phys. Rev. D* **101**, 012002 (2020).
- [11] CMS Collaboration, Measurement and interpretation of differential cross sections for Higgs boson production at $\sqrt{s} = 13$ TeV, *Phys. Lett. B* **792**, 369 (2019).
- [12] J. A. Aguilar-Saavedra, R. Benbrik, S. Heinemeyer, and M. Pérez-Victoria, Handbook of vectorlike quarks: Mixing and single production, *Phys. Rev. D* **88**, 094010 (2013).
- [13] F. del Aguila, M. Pérez-Victoria, and J. Santiago, Observable contributions of new exotic quarks to quark mixing, *J. High Energy Phys.* **09** (2000) 011.
- [14] J. A. Aguilar-Saavedra, Mixing with vector-like quarks: Constraints and expectations, *EPJ Web Conf.* **60**, 16012 (2013).
- [15] A. Atre, M. Carena, T. Han, and J. Santiago, Heavy quarks above the top at the Tevatron, *Phys. Rev. D* **79**, 054018 (2009).
- [16] A. Atre, G. Azuelos, M. Carena, T. Han, E. Ozcan, J. Santiago, and G. Unel, Model-independent searches for new quarks at the LHC, *J. High Energy Phys.* **08** (2011) 080.
- [17] ATLAS Collaboration, Search for pair production of heavy vector-like quarks decaying into hadronic final states in pp collisions at $\sqrt{s} = 13$ TeV with the ATLAS detector, *Phys. Rev. D* **98**, 092005 (2018).
- [18] CMS Collaboration, Search for pair production of vectorlike quarks in the fully hadronic final state, *Phys. Rev. D* **100**, 072001 (2019).
- [19] ATLAS Collaboration, Combination of the Searches for Pair-Produced Vector-Like Partners of the Third-Generation Quarks at $\sqrt{s} = 13$ TeV with the ATLAS Detector, *Phys. Rev. Lett.* **121**, 211801 (2018).
- [20] The ATLAS and CMS Collaborations, The LHC Higgs Combination Group, Procedure for the LHC Higgs boson search combination in Summer 2011, Technical Report Nos. CMS-NOTE-2011-005, ATL-PHYS-PUB-2011-11, 2011, <https://cds.cern.ch/record/1379837>.
- [21] CMS Collaboration, Jet energy scale and resolution in the CMS experiment in pp collisions at 8 TeV, *J. Instrum.* **12**, P02014 (2017).
- [22] CMS Collaboration, The CMS trigger system, *J. Instrum.* **12**, P01020 (2017).
- [23] CMS Collaboration, The CMS experiment at the CERN LHC, *J. Instrum.* **3**, S08004 (2008).
- [24] CMS Collaboration, CMS Luminosity Measurement for the 2016 data taking period, CMS Physics Analysis Summary CMS-PAS-LUM-17-001 (2017), <https://cds.cern.ch/record/2257069>.
- [25] CMS Collaboration, CMS luminosity measurement for the 2017 data-taking period at $\sqrt{s} = 13$ TeV, CMS Physics Analysis Summary CMS-PAS-LUM-17-004 (2018), <https://cds.cern.ch/record/2621960>.
- [26] CMS Collaboration, CMS luminosity measurement for the 2018 data-taking period at $\sqrt{s} = 13$ TeV, CMS Physics Analysis Summary CMS-PAS-LUM-18-002 (2019), <https://cds.cern.ch/record/2676164>.
- [27] J. Alwall, R. Frederix, S. Frixione, V. Hirschi, F. Maltoni, O. Mattelaer, H. S. Shao, T. Stelzer, P. Torrielli, and M. Zaro, The automated computation of tree-level and next-to-leading order differential cross sections, and their matching to parton shower simulations, *J. High Energy Phys.* **07** (2014) 079.

- [28] R. D. Ball *et al.* (NNPDF Collaboration), Parton distributions for the LHC Run II, *J. High Energy Phys.* **04** (2015) 040.
- [29] T. Sjöstrand, S. Ask, J. R. Christiansen, R. Corke, N. Desai, P. Ilten, S. Mrenna, S. Prestel, C. O. Rasmussen, and P. Z. Skands, An introduction to PYTHIA 8.2, *Comput. Phys. Commun.* **191**, 159 (2015).
- [30] CMS Collaboration, Event generator tunes obtained from underlying event and multiparton scattering measurements, *Eur. Phys. J. C* **76**, 155 (2016).
- [31] CMS Collaboration, Extraction and validation of a new set of CMS PYTHIA8 tunes from underlying-event measurements, *Eur. Phys. J. C* **80**, 4 (2020).
- [32] M. Czakon, P. Fiedler, and A. Mitov, Total Top-Quark Pair-Production Cross Section at Hadron Colliders through $O(\alpha_s^4)$, *Phys. Rev. Lett.* **110**, 252004 (2013).
- [33] M. R. Whalley, D. Bourilkov, and R. C. Group, The Les Houches accord PDFs (LHAPDF) and LHAGLUE, in *HERA and the LHC: A workshop on the implications of HERA for LHC physics. Proceedings, Part B* (2005), p. 575, <https://doi.org/10.5170/CERN-2005-014.575>.
- [34] CMS Collaboration, Search for vector-like T and B quark pairs in final states with leptons at $\sqrt{s} = 13$ TeV, *J. High Energy Phys.* **08** (2018) 177.
- [35] LHCb Collaboration, Measurement of the inelastic pp cross-section at a centre-of-mass energy of 13 TeV, *J. High Energy Phys.* **06** (2018) 100.
- [36] S. Agostinelli *et al.* (GEANT4 Collaboration), GEANT4—A simulation toolkit, *Nucl. Instrum. Methods Phys. Res., Sect. A* **506**, 250 (2003).
- [37] J. Allison *et al.*, GEANT4 developments and applications, *IEEE Trans. Nucl. Sci.* **53**, 270 (2006).
- [38] CMS Collaboration, Performance of the DeepJet b tagging algorithm using 41.9/fb of data from proton-proton collisions at 13 TeV with Phase 1 CMS detector, CMS Detector Performance Summary CMS-DP-2018-058 (2018), <http://cds.cern.ch/record/2646773>.
- [39] CMS Collaboration, Identification of heavy-flavour jets with the CMS detector in pp collisions at 13 TeV, *J. Instrum.* **13**, P05011 (2018).
- [40] CMS Collaboration, Particle-flow reconstruction and global event description with the CMS detector, *J. Instrum.* **12**, P10003 (2017).
- [41] M. Cacciari, G. P. Salam, and G. Soyez, The anti- k_T jet clustering algorithm, *J. High Energy Phys.* **04** (2008) 063.
- [42] M. Cacciari, G. P. Salam, and G. Soyez, FastJet user manual, *Eur. Phys. J. C* **72**, 1896 (2012).
- [43] D. Bertolini, P. Harris, M. Low, and N. Tran, Pileup per particle identification, *J. High Energy Phys.* **10** (2014) 059.
- [44] CMS Collaboration, Jet algorithms performance in 13 TeV data, CMS Physics Analysis Summary CMS-PAS-JME-16-003 (2017), <https://cds.cern.ch/record/2256875>.
- [45] Y. L. Dokshitzer, G. D. Leder, S. Moretti, and B. R. Webber, Better jet clustering algorithms, *J. High Energy Phys.* **08** (1997) 001.
- [46] M. Wobisch and T. Wengler, Hadronization corrections to jet cross-sections in deep inelastic scattering, in *Proceedings of the Workshop on Monte Carlo Generators for HERA Physics, Hamburg, Germany* (1998), p. 270.
- [47] M. Dasgupta, A. Fregoso, S. Marzani, and G. P. Salam, Towards an understanding of jet substructure, *J. High Energy Phys.* **09** (2013) 029.
- [48] J. M. Butterworth, A. R. Davison, M. Rubin, and G. P. Salam, Jet Substructure as a New Higgs Search Channel at the LHC, *Phys. Rev. Lett.* **100**, 242001 (2008).
- [49] A. J. Larkoski, S. Marzani, G. Soyez, and J. Thaler, Soft drop, *J. High Energy Phys.* **05** (2014) 146.
- [50] F. M. Fisher, Tests of equality between sets of coefficients in two linear regressions: An expository note, *Econometrica* **38**, 361 (1970).
- [51] J. Butterworth *et al.*, PDF4LHC recommendations for LHC Run II, *J. Phys. G* **43**, 023001 (2016).
- [52] T. Junk, Confidence level computation for combining searches with small statistics, *Nucl. Instrum. Methods Phys. Res., Sect. A* **434**, 435 (1999).
- [53] A. L. Read, Presentation of search results: The CL_s technique, *J. Phys. G* **28**, 2693 (2002).
- [54] G. Cowan, K. Cranmer, E. Gross, and O. Vitells, Asymptotic formulae for likelihood-based tests of new physics, *Eur. Phys. J. C* **71**, 1554 (2011); Erratum, *Eur. Phys. J. C* **73**, 2501 (2013).

A. M. Sirunyan,^{1,a} A. Tumasyan,¹ W. Adam,² T. Bergauer,² M. Dragicevic,² J. Erö,² A. Escalante Del Valle,² R. Frühwirth,^{2,b} M. Jeitler,^{2,b} N. Krammer,² L. Lechner,² D. Liko,² T. Madlener,² I. Mikulec,² F. M. Pitters,² N. Rad,² J. Schieck,^{2,b} R. Schöfbeck,² M. Spanring,² S. Templ,² W. Waltenberger,² C.-E. Wulz,^{2,b} M. Zarucki,² V. Chekhovsky,³ A. Litomin,³ V. Makarenko,³ J. Suarez Gonzalez,³ M. R. Darwish,^{4,c} E. A. De Wolf,⁴ D. Di Croce,⁴ X. Janssen,⁴ T. Kello,^{4,d} A. Lelek,⁴ M. Pieters,⁴ H. Rejeb Sfar,⁴ H. Van Haeve,maet,⁴ P. Van Mechelen,⁴ S. Van Putte,⁴ N. Van Remortel,⁴ F. Blekman,⁵ E. S. Bols,⁵ S. S. Chhibra,⁵ J. D'Hondt,⁵ J. De Clercq,⁵ D. Lontkovskiy,⁵ S. Lowette,⁵ I. Marchesini,⁵ S. Moortgat,⁵ A. Morton,⁵ Q. Python,⁵ S. Tavernier,⁵ W. Van Doninck,⁵ P. Van Mulders,⁵ D. Beghin,⁶ B. Bilin,⁶ B. Clerbaux,⁶ G. De Lentdecker,⁶ B. Dorney,⁶ L. Favart,⁶ A. Grebenyuk,⁶ A. K. Kalsi,⁶ I. Makarenko,⁶ L. Moureaux,⁶ L. Pétré,⁶ A. Popov,⁶ N. Postiau,⁶ E. Starling,⁶ L. Thomas,⁶ C. Vander Velde,⁶ P. Vanlaer,⁶ D. Vannerom,⁶ L. Wezenbeek,⁶ T. Cornelis,⁷ D. Dobur,⁷ M. Gruchala,⁷ I. Khvastunov,^{7,e} M. Niedziela,⁷ C. Roskas,⁷ K. Skovpen,⁷ M. Tytgat,⁷ W. Verbeke,⁷ B. Vermassen,⁷ M. Vit,⁷ G. Bruno,⁸ F. Bury,⁸ C. Caputo,⁸ P. David,⁸ C. Delaere,⁸ M. Delcourt,⁸ I. S. Donertas,⁸ A. Giammanco,⁸ V. Lemaître,⁸ K. Mondal,⁸ J. Prisciandaro,⁸ A. Talierecio,⁸ M. Teklishyn,⁸ P. Vischia,⁸ S. Wertz,⁸

S. Wuyckens,⁸ G. A. Alves,⁹ C. Hensel,⁹ A. Moraes,⁹ W. L. Aldá Júnior,¹⁰ E. Belchior Batista Das Chagas,¹⁰ H. Brandao Malbouisson,¹⁰ W. Carvalho,¹⁰ J. Chinellato,^{10,f} E. Coelho,¹⁰ E. M. Da Costa,¹⁰ G. G. Da Silveira,^{10,g} D. De Jesus Damiao,¹⁰ S. Fonseca De Souza,¹⁰ J. Martins,^{10,h} D. Matos Figueiredo,¹⁰ M. Medina Jaime,^{10,i} C. Mora Herrera,¹⁰ L. Mundim,¹⁰ H. Nogima,¹⁰ P. Rebello Teles,¹⁰ L. J. Sanchez Rosas,¹⁰ A. Santoro,¹⁰ S. M. Silva Do Amaral,¹⁰ A. Sznajder,¹⁰ M. Thiel,¹⁰ F. Torres Da Silva De Araujo,¹⁰ A. Vilela Pereira,¹⁰ C. A. Bernardes,^{11a} L. Calligaris,^{11a} T. R. Fernandez Perez Tomei,^{11a} E. M. Gregores,^{11a,11b} D. S. Lemos,^{11a} P. G. Mercadante,^{11a,11b} S. F. Novaes,^{11a} Sandra S. Padula,^{11a} A. Aleksandrov,¹² G. Antchev,¹² I. Atanasov,¹² R. Hadjiiska,¹² P. Iaydjiev,¹² M. Misheva,¹² M. Rodozov,¹² M. Shopova,¹² G. Sultanov,¹² M. Bonchev,¹³ A. Dimitrov,¹³ T. Ivanov,¹³ L. Litov,¹³ B. Pavlov,¹³ P. Petkov,¹³ A. Petrov,¹³ W. Fang,^{14,d} Q. Guo,¹⁴ H. Wang,¹⁴ L. Yuan,¹⁴ M. Ahmad,¹⁵ Z. Hu,¹⁵ Y. Wang,¹⁵ E. Chapon,¹⁶ G. M. Chen,^{16,j} H. S. Chen,^{16,j} M. Chen,¹⁶ T. Javaid,^{16,j} A. Kapoor,¹⁶ D. Leggat,¹⁶ H. Liao,¹⁶ Z. Liu,¹⁶ R. Sharma,¹⁶ A. Spiezia,¹⁶ J. Tao,¹⁶ J. Thomas-wilsker,¹⁶ J. Wang,¹⁶ H. Zhang,¹⁶ S. Zhang,^{16,j} J. Zhao,¹⁶ A. Agapitos,¹⁷ Y. Ban,¹⁷ C. Chen,¹⁷ Q. Huang,¹⁷ A. Levin,¹⁷ Q. Li,¹⁷ M. Lu,¹⁷ X. Lyu,¹⁷ Y. Mao,¹⁷ S. J. Qian,¹⁷ D. Wang,¹⁷ Q. Wang,¹⁷ J. Xiao,¹⁷ Z. You,¹⁸ X. Gao,^{19,d} M. Xiao,²⁰ C. Avila,²¹ A. Cabrera,²¹ C. Florez,²¹ J. Fraga,²¹ A. Sarkar,²¹ M. A. Segura Delgado,²¹ J. Jaramillo,²² J. Mejia Guisao,²² F. Ramirez,²² J. D. Ruiz Alvarez,²² C. A. Salazar González,²² N. Vanegas Arbelaez,²² D. Giljanovic,²³ N. Godinovic,²³ D. Lelas,²³ I. Puljak,²³ Z. Antunovic,²⁴ M. Kovac,²⁴ T. Sculac,²⁴ V. Brigljevic,²⁵ D. Ferencek,²⁵ D. Majumder,²⁵ M. Roguljic,²⁵ A. Starodumov,^{25,k} T. Susa,²⁵ M. W. Ather,²⁶ A. Attikis,²⁶ E. Erodoutou,²⁶ A. Ioannou,²⁶ G. Kole,²⁶ M. Kolosova,²⁶ S. Konstantinou,²⁶ J. Mousa,²⁶ C. Nicolaou,²⁶ F. Ptochos,²⁶ P. A. Razis,²⁶ H. Rykaczewski,²⁶ H. Saka,²⁶ D. Tsiakkouri,²⁶ M. Finger,^{27,l} M. Finger Jr.,^{27,l} A. Kveton,²⁷ J. Tomsa,²⁷ E. Ayala,²⁸ E. Carrera Jarrin,²⁹ S. Abu Zeid,^{30,m} S. Khalil,^{30,n} E. Salama,^{30,m,o} M. A. Mahmoud,³¹ Y. Mohammed,^{31,p} S. Bhowmik,³² A. Carvalho Antunes De Oliveira,³² R. K. Dewanjee,³² K. Ehataht,³² M. Kadastik,³² M. Raidal,³² C. Veelken,³² P. Eerola,³³ L. Forthomme,³³ H. Kirschenmann,³³ K. Osterberg,³³ M. Voutilainen,³³ E. Brücken,³⁴ F. Garcia,³⁴ J. Havukainen,³⁴ V. Karimäki,³⁴ M. S. Kim,³⁴ R. Kinnunen,³⁴ T. Lampén,³⁴ K. Lassila-Perini,³⁴ S. Lehti,³⁴ T. Lindén,³⁴ H. Siikonen,³⁴ E. Tuominen,³⁴ J. Tuominiemi,³⁴ P. Luukka,³⁵ T. Tuuva,³⁵ C. Amendola,³⁶ M. Besancon,³⁶ F. Couderc,³⁶ M. Dejardin,³⁶ D. Denegri,³⁶ J. L. Faure,³⁶ F. Ferri,³⁶ S. Ganjour,³⁶ A. Givernaud,³⁶ P. Gras,³⁶ G. Hamel de Monchenault,³⁶ P. Jarry,³⁶ B. Lenzi,³⁶ E. Locci,³⁶ J. Malcles,³⁶ J. Rander,³⁶ A. Rosowsky,³⁶ M. Ö. Sahin,³⁶ A. Savoy-Navarro,^{36,q} M. Titov,³⁶ G. B. Yu,³⁶ S. Ahuja,³⁷ F. Beaudette,³⁷ M. Bonanomi,³⁷ A. Buchot Perraguin,³⁷ P. Busson,³⁷ C. Charlot,³⁷ O. Davignon,³⁷ B. Diab,³⁷ G. Falmagne,³⁷ R. Granier de Cassagnac,³⁷ A. Hakimi,³⁷ I. Kucher,³⁷ A. Lobanov,³⁷ C. Martin Perez,³⁷ M. Nguyen,³⁷ C. Ochando,³⁷ P. Paganini,³⁷ J. Rembser,³⁷ R. Salerno,³⁷ J. B. Sauvan,³⁷ Y. Sirois,³⁷ A. Zabi,³⁷ A. Zghiche,³⁷ J.-L. Agram,^{38,r} J. Andrea,³⁸ D. Bloch,³⁸ G. Bourgatte,³⁸ J.-M. Brom,³⁸ E. C. Chabert,³⁸ C. Collard,³⁸ J.-C. Fontaine,^{38,r} D. Gelé,³⁸ U. Goerlach,³⁸ C. Grimault,³⁸ A.-C. Le Bihan,³⁸ P. Van Hove,³⁸ E. Asilar,³⁹ S. Beauceron,³⁹ C. Bernet,³⁹ G. Boudoul,³⁹ C. Camen,³⁹ A. Carle,³⁹ N. Chanon,³⁹ D. Contardo,³⁹ P. Depasse,³⁹ H. El Mamouni,³⁹ J. Fay,³⁹ S. Gascon,³⁹ M. Gouzevitch,³⁹ B. Ille,³⁹ Sa. Jain,³⁹ I. B. Laktineh,³⁹ H. Lattaud,³⁹ A. Lesauvage,³⁹ M. Lethuillier,³⁹ L. Mirabito,³⁹ L. Torterotot,³⁹ G. Touquet,³⁹ M. Vander Donckt,³⁹ S. Viret,³⁹ A. Khvedelidze,^{40,l} Z. Tsamalaidze,^{40,l} L. Feld,⁴¹ K. Klein,⁴¹ M. Lipinski,⁴¹ D. Meuser,⁴¹ A. Pauls,⁴¹ M. Preuten,⁴¹ M. P. Rauch,⁴¹ J. Schulz,⁴¹ M. Teroerde,⁴¹ D. Eliseev,⁴² M. Erdmann,⁴² P. Fackeldey,⁴² B. Fischer,⁴² S. Ghosh,⁴² T. Hebbeker,⁴² K. Hoepfner,⁴² H. Keller,⁴² L. Mastrolorenzo,⁴² M. Merschmeyer,⁴² A. Meyer,⁴² G. Mocellin,⁴² S. Mondal,⁴² S. Mukherjee,⁴² D. Noll,⁴² A. Novak,⁴² T. Pook,⁴² A. Pozdnyakov,⁴² Y. Rath,⁴² H. Reithler,⁴² J. Roemer,⁴² A. Schmidt,⁴² S. C. Schuler,⁴² A. Sharma,⁴² S. Wiedenbeck,⁴² S. Zaleski,⁴² C. Dziwok,⁴³ G. Flügge,⁴³ W. Haj Ahmad,^{43,s} O. Hlushchenko,⁴³ T. Kress,⁴³ A. Nowack,⁴³ C. Pistone,⁴³ O. Pooth,⁴³ D. Roy,⁴³ H. Sert,⁴³ A. Stahl,^{43,t} T. Ziemons,⁴³ H. Aarup Petersen,⁴⁴ M. Aldaya Martin,⁴⁴ P. Asmuss,⁴⁴ I. Babounikau,⁴⁴ S. Baxter,⁴⁴ O. Behnke,⁴⁴ A. Bermúdez Martínez,⁴⁴ A. A. Bin Anuar,⁴⁴ K. Borras,^{44,u} V. Botta,⁴⁴ D. Brunner,⁴⁴ A. Campbell,⁴⁴ A. Cardini,⁴⁴ P. Connor,⁴⁴ S. Consuegra Rodríguez,⁴⁴ V. Danilov,⁴⁴ A. De Wit,⁴⁴ M. M. Defranichis,⁴⁴ L. Didikh,⁴⁴ D. Domínguez Damiani,⁴⁴ G. Eckerlin,⁴⁴ D. Eckstein,⁴⁴ T. Eichhorn,⁴⁴ L. I. Estevez Banos,⁴⁴ E. Gallo,^{44,v} A. Geiser,⁴⁴ A. Giralddi,⁴⁴ A. Grohsjean,⁴⁴ M. Guthoff,⁴⁴ A. Harb,⁴⁴ A. Jafari,^{44,w} N. Z. Jomhari,⁴⁴ H. Jung,⁴⁴ A. Kasem,^{44,u} M. Kasemann,⁴⁴ H. Kaveh,⁴⁴ C. Kleinwort,⁴⁴ J. Knolle,⁴⁴ D. Krücker,⁴⁴ W. Lange,⁴⁴ T. Lenz,⁴⁴ J. Lidrych,⁴⁴ K. Lipka,⁴⁴ W. Lohmann,^{44,x} R. Mankel,⁴⁴ I.-A. Melzer-Pellmann,⁴⁴ J. Metwally,⁴⁴ A. B. Meyer,⁴⁴ M. Meyer,⁴⁴ M. Missiroli,⁴⁴ J. Mnich,⁴⁴ A. Mussgiller,⁴⁴ V. Myronenko,⁴⁴ Y. Otari,⁴⁴ D. Pérez Adán,⁴⁴ S. K. Pflitsch,⁴⁴ D. Pitzl,⁴⁴ A. Raspereza,⁴⁴ A. Saggio,⁴⁴ A. Saibel,⁴⁴ M. Savitskiy,⁴⁴ V. Scheurer,⁴⁴ C. Schwanenberger,⁴⁴ A. Singh,⁴⁴ R. E. Sosa Ricardo,⁴⁴ N. Tonon,⁴⁴ O. Turkot,⁴⁴ A. Vagnerini,⁴⁴ M. Van De Klundert,⁴⁴ R. Walsh,⁴⁴ D. Walter,⁴⁴ Y. Wen,⁴⁴ K. Wichmann,⁴⁴ C. Wissing,⁴⁴ S. Wuchterl,⁴⁴ O. Zenaiev,⁴⁴ R. Zlebick,⁴⁴ R. Aggleton,⁴⁵ S. Bein,⁴⁵ L. Benato,⁴⁵ A. Benecke,⁴⁵ K. De Leo,⁴⁵ T. Dreyer,⁴⁵

A. Ebrahimi,⁴⁵ M. Eich,⁴⁵ F. Feindt,⁴⁵ A. Fröhlich,⁴⁵ C. Garbers,⁴⁵ E. Garutti,⁴⁵ P. Gunnellini,⁴⁵ J. Haller,⁴⁵ A. Hinzmann,⁴⁵ A. Karavdina,⁴⁵ G. Kasieczka,⁴⁵ R. Klanner,⁴⁵ R. Kogler,⁴⁵ V. Kutzner,⁴⁵ J. Lange,⁴⁵ T. Lange,⁴⁵ A. Malara,⁴⁵ C. E. N. Niemeyer,⁴⁵ A. Nigamova,⁴⁵ K. J. Pena Rodriguez,⁴⁵ O. Rieger,⁴⁵ P. Schlexer,⁴⁵ S. Schumann,⁴⁵ J. Schwandt,⁴⁵ D. Schwarz,⁴⁵ J. Sonneveld,⁴⁵ H. Stadie,⁴⁵ G. Steinbrück,⁴⁵ B. Vormwald,⁴⁵ I. Zoi,⁴⁵ J. Bechtel,⁴⁶ T. Berger,⁴⁶ E. Butz,⁴⁶ R. Caspart,⁴⁶ T. Chwalek,⁴⁶ W. De Boer,⁴⁶ A. Dierlamm,⁴⁶ A. Droll,⁴⁶ K. El Morabit,⁴⁶ N. Faltermann,⁴⁶ K. Flöh,⁴⁶ M. Giffels,⁴⁶ A. Gottmann,⁴⁶ F. Hartmann,^{46,t} C. Heidecker,⁴⁶ U. Husemann,⁴⁶ M. A. Iqbal,⁴⁶ I. Katkov,^{46,y} P. Keicher,⁴⁶ R. Koppenhöfer,⁴⁶ S. Maier,⁴⁶ M. Metzler,⁴⁶ S. Mitra,⁴⁶ D. Müller,⁴⁶ Th. Müller,⁴⁶ M. Musich,⁴⁶ G. Quast,⁴⁶ K. Rabbertz,⁴⁶ J. Rauser,⁴⁶ D. Savoie,⁴⁶ D. Schäfer,⁴⁶ M. Schnepf,⁴⁶ M. Schröder,⁴⁶ D. Seith,⁴⁶ I. Shvetsov,⁴⁶ H. J. Simonis,⁴⁶ R. Ulrich,⁴⁶ M. Wassmer,⁴⁶ M. Weber,⁴⁶ R. Wolf,⁴⁶ S. Wozniowski,⁴⁶ G. Anagnostou,⁴⁷ P. Asenov,⁴⁷ G. Daskalakis,⁴⁷ T. Gerasis,⁴⁷ A. Kyriakis,⁴⁷ D. Loukas,⁴⁷ G. Paspalaki,⁴⁷ A. Stakia,⁴⁷ M. Diamantopoulou,⁴⁸ D. Karasavvas,⁴⁸ G. Karathanasis,⁴⁸ P. Kontaxakis,⁴⁸ C. K. Koraka,⁴⁸ A. Manousakis-katsikakis,⁴⁸ A. Panagiotou,⁴⁸ I. Papavergou,⁴⁸ N. Saoulidou,⁴⁸ K. Theofilatos,⁴⁸ K. Vellidis,⁴⁸ E. Vourliotis,⁴⁸ G. Bakas,⁴⁹ K. Kousouris,⁴⁹ I. Papakrivopoulos,⁴⁹ G. Tsiapolitis,⁴⁹ A. Zacharopoulou,⁴⁹ I. Evangelou,⁵⁰ C. Foudas,⁵⁰ P. Gianneios,⁵⁰ P. Katsoulis,⁵⁰ P. Kokkas,⁵⁰ K. Manitaras,⁵⁰ N. Manthos,⁵⁰ I. Papadopoulos,⁵⁰ J. Strogas,⁵⁰ M. Bartók,^{51,z} M. Csanad,⁵¹ M. M. A. Gadallah,^{51,aa} S. Lökös,^{51,bb} P. Major,⁵¹ K. Mandal,⁵¹ A. Mehta,⁵¹ G. Pasztor,⁵¹ O. Surányi,⁵¹ G. I. Veres,⁵¹ G. Bencze,⁵² C. Hajdu,⁵² D. Horvath,^{52,cc} F. Sikler,⁵² V. Veszpremi,⁵² G. Vesztergombi,^{52,ab} S. Czellar,⁵³ J. Karancsi,^{53,z} J. Molnar,⁵³ Z. Szillasi,⁵³ D. Teyssier,⁵³ P. Raics,⁵⁴ Z. L. Trocsanyi,⁵⁴ B. Ujvari,⁵⁴ T. Csorgo,⁵⁵ F. Nemes,⁵⁵ T. Novak,⁵⁵ S. Choudhury,⁵⁶ J. R. Komaragiri,⁵⁶ D. Kumar,⁵⁶ L. Panwar,⁵⁶ P. C. Tiwari,⁵⁶ S. Bahinipati,^{57,dd} D. Dash,⁵⁷ C. Kar,⁵⁷ P. Mal,⁵⁷ T. Mishra,⁵⁷ V. K. Muraleedharan Nair Bindhu,⁵⁷ A. Nayak,^{57,ee} D. K. Sahoo,^{57,dd} N. Sur,⁵⁷ S. K. Swain,⁵⁷ S. Bansal,⁵⁸ S. B. Beri,⁵⁸ V. Bhatnagar,⁵⁸ G. Chaudhary,⁵⁸ S. Chauhan,⁵⁸ N. Dhingra,^{58,ff} R. Gupta,⁵⁸ A. Kaur,⁵⁸ S. Kaur,⁵⁸ P. Kumari,⁵⁸ M. Meena,⁵⁸ K. Sandeep,⁵⁸ S. Sharma,⁵⁸ J. B. Singh,⁵⁸ A. K. Viridi,⁵⁸ A. Ahmed,⁵⁹ A. Bhardwaj,⁵⁹ B. C. Choudhary,⁵⁹ R. B. Garg,⁵⁹ M. Gola,⁵⁹ S. Keshri,⁵⁹ A. Kumar,⁵⁹ M. Naimuddin,⁵⁹ P. Priyanka,⁵⁹ K. Ranjan,⁵⁹ A. Shah,⁵⁹ M. Bharti,^{60,gg} R. Bhattacharya,⁶⁰ S. Bhattacharya,⁶⁰ D. Bhowmik,⁶⁰ S. Dutta,⁶⁰ S. Ghosh,⁶⁰ B. Gomber,^{60,hh} M. Maity,^{60,ii} S. Nandan,⁶⁰ P. Palit,⁶⁰ P. K. Rout,⁶⁰ G. Saha,⁶⁰ B. Sahu,⁶⁰ S. Sarkar,⁶⁰ M. Sharan,⁶⁰ B. Singh,^{60,gg} S. Thakur,^{60,gg} P. K. Behera,⁶¹ S. C. Behera,⁶¹ P. Kalbhor,⁶¹ A. Muhammad,⁶¹ R. Pradhan,⁶¹ P. R. Pujahari,⁶¹ A. Sharma,⁶¹ A. K. Sikdar,⁶¹ D. Dutta,⁶² V. Kumar,⁶² K. Naskar,^{62,jj} P. K. Netrakanti,⁶² L. M. Pant,⁶² P. Shukla,⁶² T. Aziz,⁶³ M. A. Bhat,⁶³ S. Dugad,⁶³ R. Kumar Verma,⁶³ G. B. Mohanty,⁶³ U. Sarkar,⁶³ S. Banerjee,⁶⁴ S. Bhattacharya,⁶⁴ S. Chatterjee,⁶⁴ R. Chudasama,⁶⁴ M. Guchait,⁶⁴ S. Karmakar,⁶⁴ S. Kumar,⁶⁴ G. Majumder,⁶⁴ K. Mazumdar,⁶⁴ S. Mukherjee,⁶⁴ D. Roy,⁶⁴ S. Dube,⁶⁵ B. Kansal,⁶⁵ S. Pandey,⁶⁵ A. Rane,⁶⁵ A. Rastogi,⁶⁵ S. Sharma,⁶⁵ H. Bakhshiansohi,^{66,kk} M. Zeinali,^{66,ll} S. Chenarani,^{67,mm} S. M. Etesami,⁶⁷ M. Khakzad,⁶⁷ M. Mohammadi Najafabadi,⁶⁷ M. Felcini,⁶⁸ M. Grunewald,⁶⁸ M. Abbrescia,^{69a,69b} R. Aly,^{69a,69b,nn} C. Aruta,^{69a,69b} A. Colaleo,^{69a} D. Creanza,^{69a,69c} N. De Filippis,^{69a,69c} M. De Palma,^{69a,69b} A. Di Florio,^{69a,69b} A. Di Pilato,^{69a,69b} W. Elmetenawee,^{69a,69b} L. Fiore,^{69a} A. Gelmi,^{69a,69b} M. Gul,^{69a} G. Iaselli,^{69a,69c} M. Ince,^{69a,69b} S. Lezki,^{69a,69b} G. Maggi,^{69a,69c} M. Maggi,^{69a} I. Margjeka,^{69a,69b} V. Mastrapasqua,^{69a,69b} J. A. Merlin,^{69a} S. My,^{69a,69b} S. Nuzzo,^{69a,69b} A. Pompili,^{69a,69b} G. Pugliese,^{69a,69c} A. Ranieri,^{69a} G. Selvaggi,^{69a,69b} L. Silvestris,^{69a} F. M. Simone,^{69a,69b} R. Venditti,^{69a} P. Verwilligen,^{69a} G. Abbiendi,^{70a} C. Battilana,^{70a,70b} D. Bonacorsi,^{70a,70b} L. Borgonovi,^{70a} S. Braibant-Giacomelli,^{70a,70b} R. Campanini,^{70a,70b} P. Capiluppi,^{70a,70b} A. Castro,^{70a,70b} F. R. Cavallo,^{70a} C. Ciocca,^{70a} M. Cuffiani,^{70a,70b} G. M. Dallavalle,^{70a} T. Diotallevi,^{70a,70b} F. Fabbri,^{70a} A. Fanfani,^{70a,70b} E. Fontanesi,^{70a,70b} P. Giacomelli,^{70a} C. Grandi,^{70a} L. Guiducci,^{70a,70b} F. Iemmi,^{70a,70b} S. Lo Meo,^{70a,oo} S. Marcellini,^{70a} G. Masetti,^{70a} F. L. Navarria,^{70a,70b} A. Perrotta,^{70a} F. Primavera,^{70a,70b} A. M. Rossi,^{70a,70b} T. Rovelli,^{70a,70b} G. P. Siroli,^{70a,70b} N. Tosi,^{70a} S. Albergo,^{71a,71b,pp} S. Costa,^{71a,71b} A. Di Mattia,^{71a} R. Potenza,^{71a,71b} A. Tricoli,^{71a,71b,pp} C. Tuve,^{71a,71b} G. Barbagli,^{72a} A. Cassese,^{72a} R. Ceccarelli,^{72a,72b} V. Ciulli,^{72a,72b} C. Civinini,^{72a} R. D'Alessandro,^{72a,72b} F. Fiori,^{72a} E. Focardi,^{72a,72b} G. Latino,^{72a,72b} P. Lenzi,^{72a,72b} M. Lizzo,^{72a,72b} M. Meschini,^{72a} S. Paoletti,^{72a} R. Seidita,^{72a,72b} G. Sguazzoni,^{72a} L. Viliani,^{72a} L. Benussi,⁷³ S. Bianco,⁷³ D. Piccolo,⁷³ M. Bozzo,^{74a,74b} F. Ferro,^{74a} R. Mulargia,^{74a,74b} E. Robutti,^{74a} S. Tosi,^{74a,74b} A. Benaglia,^{75a} A. Beschi,^{75a,75b} F. Brivio,^{75a,75b} F. Cetorelli,^{75a,75b} V. Ciriolo,^{75a,75b,t} F. De Guio,^{75a,75b} M. E. Dinardo,^{75a,75b} P. Dini,^{75a} S. Gennai,^{75a} A. Ghezzi,^{75a,75b} P. Govoni,^{75a,75b} L. Guzzi,^{75a,75b} M. Malberti,^{75a} S. Malvezzi,^{75a} D. Menasce,^{75a} F. Monti,^{75a,75b} L. Moroni,^{75a} M. Paganoni,^{75a,75b} D. Pedrini,^{75a} S. Ragazzi,^{75a,75b} T. Tabarelli de Fatis,^{75a,75b} D. Valsecchi,^{75a,75b,t} D. Zuolo,^{75a,75b} S. Buontempo,^{76a} N. Cavallo,^{76a,76c} A. De Iorio,^{76a,76b} F. Fabozzi,^{76a,76c} F. Fienga,^{76a} A. O. M. Iorio,^{76a,76b} L. Lista,^{76a,76b} S. Meola,^{76a,76d,t} P. Paolucci,^{76a,t} B. Rossi,^{76a} C. Sciacca,^{76a,76b} E. Voevodina,^{76a,76b} P. Azzi,^{77a} N. Bacchetta,^{77a} D. Bisello,^{77a,77b} P. Bortignon,^{77a} A. Bragagnolo,^{77a,77b} R. Carlin,^{77a,77b} P. Checchia,^{77a}

P. De Castro Manzano,^{77a} T. Dorigo,^{77a} F. Gasparini,^{77a,77b} U. Gasparini,^{77a,77b} S. Y. Hoh,^{77a,77b} L. Layer,^{77a,qq}
 M. Margoni,^{77a,77b} A. T. Meneguzzo,^{77a,77b} M. Presilla,^{77a,77b} P. Ronchese,^{77a,77b} R. Rossin,^{77a,77b} F. Simonetto,^{77a,77b}
 G. Strong,^{77a} M. Tosi,^{77a,77b} H. Yarar,^{77a,77b} M. Zanetti,^{77a,77b} P. Zotto,^{77a,77b} A. Zucchetta,^{77a,77b} G. Zumerle,^{77a,77b}
 C. Aime,^{78a,78b} A. Braghieri,^{78a} S. Calzaferri,^{78a,78b} D. Fiorina,^{78a,78b} P. Montagna,^{78a,78b} S. P. Ratti,^{78a,78b} V. Re,^{78a}
 M. Ressegotti,^{78a,78b} C. Riccardi,^{78a,78b} P. Salvini,^{78a} I. Vai,^{78a} P. Vitulo,^{78a,78b} M. Biasini,^{79a,79b} G. M. Bilei,^{79a}
 D. Ciangottini,^{79a,79b} L. Fanò,^{79a,79b} P. Lariccia,^{79a,79b} G. Mantovani,^{79a,79b} V. Mariani,^{79a,79b} M. Menichelli,^{79a}
 F. Moscatelli,^{79a} A. Piccinelli,^{79a,79b} A. Rossi,^{79a,79b} A. Santocchia,^{79a,79b} D. Spiga,^{79a} T. Tedeschi,^{79a,79b} K. Androsof,^{80a}
 P. Azzurri,^{80a} G. Bagliesi,^{80a} V. Bertacchi,^{80a,80c} L. Bianchini,^{80a} T. Boccali,^{80a} R. Castaldi,^{80a} M. A. Ciocci,^{80a,80b}
 R. Dell'Orso,^{80a} M. R. Di Domenico,^{80a,80b} S. Donato,^{80a} L. Giannini,^{80a,80c} A. Giassi,^{80a} M. T. Grippo,^{80a} F. Ligabue,^{80a,80c}
 E. Manca,^{80a,80c} G. Mandorli,^{80a,80c} A. Messineo,^{80a,80b} F. Palla,^{80a} G. Ramirez-Sanchez,^{80a,80c} A. Rizzi,^{80a,80b}
 G. Rolandi,^{80a,80c} S. Roy Chowdhury,^{80a,80c} A. Scribano,^{80a} N. Shafiei,^{80a,80b} P. Spagnolo,^{80a} R. Tenchini,^{80a} G. Tonelli,^{80a,80b}
 N. Turini,^{80a} A. Venturi,^{80a} P. G. Verdini,^{80a} F. Cavallari,^{81a} M. Cipriani,^{81a,81b} D. Del Re,^{81a,81b} E. Di Marco,^{81a}
 M. Diemoz,^{81a} E. Longo,^{81a,81b} P. Meridiani,^{81a} G. Organtini,^{81a,81b} F. Pandolfi,^{81a} R. Paramatti,^{81a,81b} C. Quaranta,^{81a,81b}
 S. Rahatlou,^{81a,81b} C. Rovelli,^{81a} F. Santanastasio,^{81a,81b} L. Soffi,^{81a,81b} R. Tramontano,^{81a,81b} N. Amapane,^{82a,82b}
 R. Arcidiacono,^{82a,82c} S. Argiro,^{82a,82b} M. Arneodo,^{82a,82c} N. Bartosik,^{82a} R. Bellan,^{82a,82b} A. Bellora,^{82a,82b} C. Biino,^{82a}
 A. Cappati,^{82a,82b} N. Cartiglia,^{82a} S. Cometti,^{82a} M. Costa,^{82a,82b} R. Covarelli,^{82a,82b} N. Demaria,^{82a} B. Kiani,^{82a,82b}
 F. Legger,^{82a} C. Mariotti,^{82a} S. Maselli,^{82a} E. Migliore,^{82a,82b} V. Monaco,^{82a,82b} E. Monteil,^{82a,82b} M. Monteno,^{82a}
 M. M. Obertino,^{82a,82b} G. Ortona,^{82a} L. Pacher,^{82a,82b} N. Pastrone,^{82a} M. Pelliccioni,^{82a} G. L. Pinna Angioni,^{82a,82b}
 M. Ruspa,^{82a,82c} R. Salvatico,^{82a,82b} F. Siviero,^{82a,82b} V. Sola,^{82a} A. Solano,^{82a,82b} D. Soldi,^{82a,82b} A. Staiano,^{82a}
 D. Trocino,^{82a,82b} S. Belforte,^{83a} V. Candelise,^{83a,83b} M. Casarsa,^{83a} F. Cossutti,^{83a} A. Da Rold,^{83a,83b} G. Della Ricca,^{83a,83b}
 F. Vazzoler,^{83a,83b} S. Dogra,⁸⁴ C. Huh,⁸⁴ B. Kim,⁸⁴ D. H. Kim,⁸⁴ G. N. Kim,⁸⁴ J. Lee,⁸⁴ S. W. Lee,⁸⁴ C. S. Moon,⁸⁴ Y. D. Oh,⁸⁴
 S. I. Pak,⁸⁴ B. C. Radburn-Smith,⁸⁴ S. Sekmen,⁸⁴ Y. C. Yang,⁸⁴ H. Kim,⁸⁵ D. H. Moon,⁸⁵ B. Francois,⁸⁶ T. J. Kim,⁸⁶ J. Park,⁸⁶
 S. Cho,⁸⁷ S. Choi,⁸⁷ Y. Go,⁸⁷ S. Ha,⁸⁷ B. Hong,⁸⁷ K. Lee,⁸⁷ K. S. Lee,⁸⁷ J. Lim,⁸⁷ J. Park,⁸⁷ S. K. Park,⁸⁷ J. Yoo,⁸⁷ J. Goh,⁸⁸
 A. Gurtu,⁸⁸ H. S. Kim,⁸⁹ Y. Kim,⁸⁹ J. Almond,⁹⁰ J. H. Bhyun,⁹⁰ J. Choi,⁹⁰ S. Jeon,⁹⁰ J. Kim,⁹⁰ J. S. Kim,⁹⁰ S. Ko,⁹⁰
 H. Kwon,⁹⁰ H. Lee,⁹⁰ K. Lee,⁹⁰ S. Lee,⁹⁰ K. Nam,⁹⁰ B. H. Oh,⁹⁰ M. Oh,⁹⁰ S. B. Oh,⁹⁰ H. Seo,⁹⁰ U. K. Yang,⁹⁰ I. Yoon,⁹⁰
 D. Jeon,⁹¹ J. H. Kim,⁹¹ B. Ko,⁹¹ J. S. H. Lee,⁹¹ I. C. Park,⁹¹ Y. Roh,⁹¹ D. Song,⁹¹ I. J. Watson,⁹¹ H. D. Yoo,⁹² Y. Choi,⁹³
 C. Hwang,⁹³ Y. Jeong,⁹³ H. Lee,⁹³ Y. Lee,⁹³ I. Yu,⁹³ Y. Maghrbi,⁹⁴ V. Veckalns,^{95,rr} A. Juodagalvis,⁹⁶ A. Rinkevicius,⁹⁶
 G. Tamulaitis,⁹⁶ W. A. T. Wan Abdullah,⁹⁷ M. N. Yusli,⁹⁷ Z. Zolkapli,⁹⁷ J. F. Benitez,⁹⁸ A. Castaneda Hernandez,⁹⁸
 J. A. Murillo Quijada,⁹⁸ L. Valencia Palomo,⁹⁸ G. Ayala,⁹⁹ H. Castilla-Valdez,⁹⁹ E. De La Cruz-Burelo,⁹⁹
 I. Heredia-De La Cruz,^{99,ss} R. Lopez-Fernandez,⁹⁹ C. A. Mondragon Herrera,⁹⁹ D. A. Perez Navarro,⁹⁹
 A. Sanchez-Hernandez,⁹⁹ S. Carrillo Moreno,¹⁰⁰ C. Oropeza Barrera,¹⁰⁰ M. Ramirez-Garcia,¹⁰⁰ F. Vazquez Valencia,¹⁰⁰
 J. Eysermans,¹⁰¹ I. Pedraza,¹⁰¹ H. A. Salazar Ibarquen,¹⁰¹ C. Uribe Estrada,¹⁰¹ A. Morelos Pineda,¹⁰² J. Mijuskovic,^{103,e}
 N. Raicevic,¹⁰³ D. Krofcheck,¹⁰⁴ S. Bheesette,¹⁰⁵ P. H. Butler,¹⁰⁵ P. Lujan,¹⁰⁵ A. Ahmad,¹⁰⁶ M. I. Asghar,¹⁰⁶ A. Awais,¹⁰⁶
 M. I. M. Awan,¹⁰⁶ H. R. Hoorani,¹⁰⁶ W. A. Khan,¹⁰⁶ M. A. Shah,¹⁰⁶ M. Shoaib,¹⁰⁶ M. Waqas,¹⁰⁶ V. Avati,¹⁰⁷ L. Grzanka,¹⁰⁷
 M. Malawski,¹⁰⁷ H. Bialkowska,¹⁰⁸ M. Bluj,¹⁰⁸ B. Boimska,¹⁰⁸ T. Frueboes,¹⁰⁸ M. Górski,¹⁰⁸ M. Kazana,¹⁰⁸ M. Szeleper,¹⁰⁸
 P. Traczyk,¹⁰⁸ P. Zalewski,¹⁰⁸ K. Bunkowski,¹⁰⁹ A. Byszuk,^{109,tt} K. Doroba,¹⁰⁹ A. Kalinowski,¹⁰⁹ M. Konecki,¹⁰⁹
 J. Krolikowski,¹⁰⁹ M. Olszewski,¹⁰⁹ M. Walczak,¹⁰⁹ M. Araujo,¹¹⁰ P. Bargassa,¹¹⁰ D. Bastos,¹¹⁰ A. Boletti,¹¹⁰ P. Faccioli,¹¹⁰
 M. Gallinaro,¹¹⁰ J. Hollar,¹¹⁰ N. Leonardo,¹¹⁰ T. Niknejad,¹¹⁰ J. Seixas,¹¹⁰ K. Shchelina,¹¹⁰ O. Toldaiev,¹¹⁰ J. Varela,¹¹⁰
 S. Afanasiev,¹¹¹ P. Bunin,¹¹¹ M. Gavrilenko,¹¹¹ I. Golutvin,¹¹¹ I. Gorbunov,¹¹¹ A. Kamenev,¹¹¹ V. Karjavine,¹¹¹ A. Lanev,¹¹¹
 A. Malakhov,¹¹¹ V. Matveev,^{111,uu,vv} V. Palichik,¹¹¹ V. Perelygin,¹¹¹ M. Savina,¹¹¹ D. Seitova,¹¹¹ V. Shalaev,¹¹¹
 S. Shmatov,¹¹¹ S. Shulha,¹¹¹ V. Smirnov,¹¹¹ O. Teryaev,¹¹¹ N. Voytishin,¹¹¹ A. Zarubin,¹¹¹ I. Zhizhin,¹¹¹ G. Gavrilo,¹¹²
 V. Golovtsov,¹¹² Y. Ivanov,¹¹² V. Kim,^{112,ww} E. Kuznetsova,^{112,xx} V. Murzin,¹¹² V. Oreshkin,¹¹² I. Smirnov,¹¹² D. Sosnov,¹¹²
 V. Sulimov,¹¹² L. Uvarov,¹¹² S. Volkov,¹¹² A. Vorobyev,¹¹² Yu. Andreev,¹¹³ A. Dermenev,¹¹³ S. Gninenko,¹¹³ N. Golubev,¹¹³
 A. Karneyeu,¹¹³ M. Kirsanov,¹¹³ N. Krasnikov,¹¹³ A. Pashenkov,¹¹³ G. Pivovarov,¹¹³ D. Tlisov,^{113,a} A. Toropin,¹¹³
 V. Epshteyn,¹¹⁴ V. Gavrilov,¹¹⁴ N. Lychkovskaya,¹¹⁴ A. Nikitenko,^{114,yy} V. Popov,¹¹⁴ G. Safronov,¹¹⁴ A. Spiridonov,¹¹⁴
 A. Stepennov,¹¹⁴ M. Toms,¹¹⁴ E. Vlasov,¹¹⁴ A. Zhokin,¹¹⁴ T. Aushev,¹¹⁵ O. Bychkova,¹¹⁶ M. Chadeeva,^{116,zz} D. Philippov,¹¹⁶
 E. Popova,¹¹⁶ V. Rusinov,¹¹⁶ V. Andreev,¹¹⁷ M. Azarkin,¹¹⁷ I. Dremin,¹¹⁷ M. Kirakosyan,¹¹⁷ A. Terkulov,¹¹⁷ A. Belyaev,¹¹⁸
 E. Boos,¹¹⁸ V. Bunichev,¹¹⁸ M. Dubinin,^{118,aaa} L. Dudko,¹¹⁸ A. Ershov,¹¹⁸ A. Gribushin,¹¹⁸ V. Klyukhin,¹¹⁸ O. Kodolova,¹¹⁸
 I. Lokhtin,¹¹⁸ S. Obraztsov,¹¹⁸ M. Perfilov,¹¹⁸ V. Savrin,¹¹⁸ V. Blinov,^{119,bbb} T. Dimova,^{119,bbb} L. Kardapolitsev,^{119,bbb}

I. Ovtin,^{119,bbb} Y. Skovpen,^{119,bbb} I. Azhgirey,¹²⁰ I. Bayshev,¹²⁰ V. Kachanov,¹²⁰ A. Kalinin,¹²⁰ D. Konstantinov,¹²⁰
 V. Petrov,¹²⁰ R. Ryutin,¹²⁰ A. Sobol,¹²⁰ S. Troshin,¹²⁰ N. Tyurin,¹²⁰ A. Uzunian,¹²⁰ A. Volkov,¹²⁰ A. Babaev,¹²¹
 A. Iuzhakov,¹²¹ V. Okhotnikov,¹²¹ L. Sukhikh,¹²¹ V. Borchsh,¹²² V. Ivanchenko,¹²² E. Tcherniaev,¹²² P. Adzic,^{123,ccc}
 P. Cirkovic,¹²³ M. Dordevic,¹²³ P. Milenovic,¹²³ J. Milosevic,¹²³ M. Aguilar-Benitez,¹²⁴ J. Alcaraz Maestre,¹²⁴
 A. Álvarez Fernández,¹²⁴ I. Bachiller,¹²⁴ M. Barrio Luna,¹²⁴ Cristina F. Bedoya,¹²⁴ J. A. Brochero Cifuentes,¹²⁴
 C. A. Carrillo Montoya,¹²⁴ M. Cepeda,¹²⁴ M. Cerrada,¹²⁴ N. Colino,¹²⁴ B. De La Cruz,¹²⁴ A. Delgado Peris,¹²⁴
 J. P. Fernández Ramos,¹²⁴ J. Flix,¹²⁴ M. C. Fouz,¹²⁴ A. García Alonso,¹²⁴ O. Gonzalez Lopez,¹²⁴ S. Goy Lopez,¹²⁴
 J. M. Hernandez,¹²⁴ M. I. Josa,¹²⁴ J. León Holgado,¹²⁴ D. Moran,¹²⁴ Á. Navarro Tobar,¹²⁴ A. Pérez-Calero Yzquierdo,¹²⁴
 J. Puerta Pelayo,¹²⁴ I. Redondo,¹²⁴ L. Romero,¹²⁴ S. Sánchez Navas,¹²⁴ M. S. Soares,¹²⁴ A. Triossi,¹²⁴ L. Urda Gómez,¹²⁴
 C. Willmott,¹²⁴ C. Albajar,¹²⁵ J. F. de Trocóniz,¹²⁵ R. Reyes-Almanza,¹²⁵ B. Alvarez Gonzalez,¹²⁶ J. Cuevas,¹²⁶ C. Erice,¹²⁶
 J. Fernandez Menendez,¹²⁶ S. Folgueras,¹²⁶ I. Gonzalez Caballero,¹²⁶ E. Palencia Cortezon,¹²⁶ C. Ramón Álvarez,¹²⁶
 J. Ripoll Sau,¹²⁶ V. Rodríguez Bouza,¹²⁶ S. Sanchez Cruz,¹²⁶ A. Trapote,¹²⁶ I. J. Cabrillo,¹²⁷ A. Calderon,¹²⁷
 B. Chazin Quero,¹²⁷ J. Duarte Campderros,¹²⁷ M. Fernandez,¹²⁷ P. J. Fernández Manteca,¹²⁷ G. Gomez,¹²⁷
 C. Martinez Rivero,¹²⁷ P. Martinez Ruiz del Arbol,¹²⁷ F. Matorras,¹²⁷ J. Piedra Gomez,¹²⁷ C. Prieels,¹²⁷ F. Ricci-Tam,¹²⁷
 T. Rodrigo,¹²⁷ A. Ruiz-Jimeno,¹²⁷ L. Scodellaro,¹²⁷ I. Vila,¹²⁷ J. M. Vizan Garcia,¹²⁷ MK Jayananda,¹²⁸
 B. Kailasapathy,^{128,ddd} D. U. J. Sonnadara,¹²⁸ DDC Wickramaratna,¹²⁸ W. G. D. Dharmaratna,¹²⁹ K. Liyanage,¹²⁹
 N. Perera,¹²⁹ N. Wickramage,¹²⁹ T. K. Aarrestad,¹³⁰ D. Abbaneo,¹³⁰ B. Akgun,¹³⁰ E. Auffray,¹³⁰ G. Auzinger,¹³⁰
 J. Baechler,¹³⁰ P. Baillon,¹³⁰ A. H. Ball,¹³⁰ D. Barney,¹³⁰ J. Bendavid,¹³⁰ N. Beni,¹³⁰ M. Bianco,¹³⁰ A. Bocci,¹³⁰ E. Bossini,¹³⁰
 E. Brondolin,¹³⁰ T. Camporesi,¹³⁰ G. Cerminara,¹³⁰ L. Cristella,¹³⁰ D. d'Enterria,¹³⁰ A. Dabrowski,¹³⁰ N. Daci,¹³⁰
 V. Daponte,¹³⁰ A. David,¹³⁰ A. De Roeck,¹³⁰ M. Deile,¹³⁰ R. Di Maria,¹³⁰ M. Dobson,¹³⁰ M. Dünser,¹³⁰ N. Dupont,¹³⁰
 A. Elliott-Peisert,¹³⁰ N. Emrskova,¹³⁰ F. Fallavollita,^{130,eee} D. Fasanella,¹³⁰ S. Fiorendi,¹³⁰ A. Florent,¹³⁰ G. Franzoni,¹³⁰
 J. Fulcher,¹³⁰ W. Funk,¹³⁰ S. Giani,¹³⁰ D. Gigi,¹³⁰ K. Gill,¹³⁰ F. Glege,¹³⁰ L. Gouskos,¹³⁰ M. Guilbaud,¹³⁰ D. Gulhan,¹³⁰
 M. Haranko,¹³⁰ J. Hegeman,¹³⁰ Y. Iiyama,¹³⁰ V. Innocente,¹³⁰ T. James,¹³⁰ P. Janot,¹³⁰ J. Kaspar,¹³⁰ J. Kieseler,¹³⁰
 M. Komm,¹³⁰ N. Kratochwil,¹³⁰ C. Lange,¹³⁰ S. Laurila,¹³⁰ P. Lecoq,¹³⁰ K. Long,¹³⁰ C. Lourenço,¹³⁰ L. Malgeri,¹³⁰
 S. Mallios,¹³⁰ M. Mannelli,¹³⁰ A. Massironi,¹³⁰ F. Meijers,¹³⁰ S. Mersi,¹³⁰ E. Meschi,¹³⁰ F. Moortgat,¹³⁰ M. Mulders,¹³⁰
 J. Niedziela,¹³⁰ S. Orfanelli,¹³⁰ L. Orsini,¹³⁰ F. Pantaleo,^{130,t} L. Pape,¹³⁰ E. Perez,¹³⁰ M. Peruzzi,¹³⁰ A. Petrilli,¹³⁰
 G. Petrucciani,¹³⁰ A. Pfeiffer,¹³⁰ M. Pierini,¹³⁰ T. Quast,¹³⁰ D. Rabady,¹³⁰ A. Racz,¹³⁰ M. Rieger,¹³⁰ M. Rovere,¹³⁰
 H. Sakulin,¹³⁰ J. Salfeld-Nebgen,¹³⁰ S. Scarfi,¹³⁰ C. Schäfer,¹³⁰ C. Schwick,¹³⁰ M. Selvaggi,¹³⁰ A. Sharma,¹³⁰ P. Silva,¹³⁰
 W. Snoeys,¹³⁰ P. Sphicas,^{130,fff} S. Summers,¹³⁰ V. R. Tavolaro,¹³⁰ D. Treille,¹³⁰ A. Tsirou,¹³⁰ G. P. Van Onsem,¹³⁰
 A. Vartak,¹³⁰ M. Verzetti,¹³⁰ K. A. Wozniak,¹³⁰ W. D. Zeuner,¹³⁰ L. Caminada,^{131,ggg} W. Erdmann,¹³¹ R. Horisberger,¹³¹
 Q. Ingram,¹³¹ H. C. Kaestli,¹³¹ D. Kotlinski,¹³¹ U. Langenegger,¹³¹ T. Rohe,¹³¹ M. Backhaus,¹³² P. Berger,¹³² A. Calandri,¹³²
 N. Chernyavskaya,¹³² A. De Cosa,¹³² G. Dissertori,¹³² M. Dittmar,¹³² M. Donegà,¹³² C. Dorfer,¹³² T. Gadek,¹³²
 T. A. Gómez Espinosa,¹³² C. Grab,¹³² D. Hits,¹³² W. Lustermann,¹³² A.-M. Lyon,¹³² R. A. Manzoni,¹³² M. T. Meinhard,¹³²
 F. Micheli,¹³² F. Nessi-Tedaldi,¹³² F. Pauss,¹³² V. Perovic,¹³² G. Perrin,¹³² S. Pigazzini,¹³² M. G. Ratti,¹³² M. Reichmann,¹³²
 C. Reissel,¹³² T. Reitenspiess,¹³² B. Ristic,¹³² D. Ruini,¹³² D. A. Sanz Becerra,¹³² M. Schönenberger,¹³² V. Stampf,¹³²
 M. L. Vesterbacka Olsson,¹³² R. Wallny,¹³² D. H. Zhu,¹³² C. Amsler,^{133,hhh} C. Botta,¹³³ D. Brzhechko,¹³³ M. F. Canelli,¹³³
 R. Del Burgo,¹³³ J. K. Heikkilä,¹³³ M. Huwiler,¹³³ A. Jofrehei,¹³³ B. Kilminster,¹³³ S. Leontsinis,¹³³ A. Macchiolo,¹³³
 P. Meiring,¹³³ V. M. Mikuni,¹³³ U. Molinatti,¹³³ I. Neutelings,¹³³ G. Rauco,¹³³ A. Reimers,¹³³ P. Robmann,¹³³
 K. Schweiger,¹³³ Y. Takahashi,¹³³ C. Adloff,^{134,iii} C. M. Kuo,¹³⁴ W. Lin,¹³⁴ A. Roy,¹³⁴ T. Sarkar,^{134,ii} S. S. Yu,¹³⁴ L. Ceard,¹³⁵
 P. Chang,¹³⁵ Y. Chao,¹³⁵ K. F. Chen,¹³⁵ P. H. Chen,¹³⁵ W.-S. Hou,¹³⁵ Y. y. Li,¹³⁵ R.-S. Lu,¹³⁵ E. Paganis,¹³⁵ A. Psallidas,¹³⁵
 A. Steen,¹³⁵ E. Yazgan,¹³⁵ B. Asavapibhop,¹³⁶ C. Asawatangtrakuldee,¹³⁶ N. Srimanobhas,¹³⁶ F. Boran,¹³⁷
 S. Damarseekin,^{137,jjj} Z. S. Demiroglu,¹³⁷ F. Dolek,¹³⁷ C. Dozen,^{137,kkk} I. Dumanoglu,^{137,lli} E. Eskut,¹³⁷ G. Gokbulut,¹³⁷
 Y. Guler,¹³⁷ E. Gurpinar Guler,^{137,mmm} I. Hos,^{137,nnn} C. Isik,¹³⁷ E. E. Kangal,^{137,ooo} O. Kara,¹³⁷ A. Kayis Topaksu,¹³⁷
 U. Kiminsu,¹³⁷ G. Onengut,¹³⁷ K. Ozdemir,^{137,ppp} A. Polatoz,¹³⁷ A. E. Simsek,¹³⁷ B. Tali,^{137,qqq} U. G. Tok,¹³⁷
 S. Turcpar,¹³⁷ I. S. Zorbakir,¹³⁷ C. Zorbilmez,¹³⁷ B. Isildak,^{138,rrr} G. Karapinar,^{138,sss} K. Ocalan,^{138,ttt} M. Yalvac,^{138,uuu}
 I. O. Atakisi,¹³⁹ E. Gülmez,¹³⁹ M. Kaya,^{139,vvv} O. Kaya,^{139,www} Ö. Özçelik,¹³⁹ S. Tekten,^{139,xxx} E. A. Yetkin,^{139,yyy}
 A. Cakir,¹⁴⁰ K. Cankocak,^{140,lll} Y. Komurcu,¹⁴⁰ S. Sen,^{140,zzz} F. Aydogmus Sen,¹⁴¹ S. Cerci,^{141,qqq} B. Kaynak,¹⁴¹
 S. Ozkorucuklu,¹⁴¹ D. Sunar Cerci,^{141,qqq} B. Grynyov,¹⁴² L. Levchuk,¹⁴³ E. Bhal,¹⁴⁴ S. Bologna,¹⁴⁴ J. J. Brooke,¹⁴⁴
 E. Clement,¹⁴⁴ D. Cussans,¹⁴⁴ H. Flacher,¹⁴⁴ J. Goldstein,¹⁴⁴ G. P. Heath,¹⁴⁴ H. F. Heath,¹⁴⁴ L. Kreczko,¹⁴⁴ B. Krikler,¹⁴⁴

S. Paramesvaran,¹⁴⁴ T. Sakuma,¹⁴⁴ S. Seif El Nasr-Storey,¹⁴⁴ V. J. Smith,¹⁴⁴ J. Taylor,¹⁴⁴ A. Titterton,¹⁴⁴ K. W. Bell,¹⁴⁵
 A. Belyaev,^{145,aaaa} C. Brew,¹⁴⁵ R. M. Brown,¹⁴⁵ D. J. A. Cockerill,¹⁴⁵ K. V. Ellis,¹⁴⁵ K. Harder,¹⁴⁵ S. Harper,¹⁴⁵ J. Linacre,¹⁴⁵
 K. Manolopoulos,¹⁴⁵ D. M. Newbold,¹⁴⁵ E. Olaiya,¹⁴⁵ D. Petyt,¹⁴⁵ T. Reis,¹⁴⁵ T. Schuh,¹⁴⁵
 C. H. Shepherd-Themistocleous,¹⁴⁵ A. Thea,¹⁴⁵ I. R. Tomalin,¹⁴⁵ T. Williams,¹⁴⁵ R. Bainbridge,¹⁴⁶ P. Bloch,¹⁴⁶
 S. Bonomally,¹⁴⁶ J. Borg,¹⁴⁶ S. Breeze,¹⁴⁶ O. Buchmuller,¹⁴⁶ A. Bundock,¹⁴⁶ V. Cepaitis,¹⁴⁶ G. S. Chahal,^{146,bbbb}
 D. Colling,¹⁴⁶ P. Dauncey,¹⁴⁶ G. Davies,¹⁴⁶ M. Della Negra,¹⁴⁶ G. Fedi,¹⁴⁶ G. Hall,¹⁴⁶ G. Iles,¹⁴⁶ J. Langford,¹⁴⁶ L. Lyons,¹⁴⁶
 A.-M. Magnan,¹⁴⁶ S. Malik,¹⁴⁶ A. Martelli,¹⁴⁶ V. Milosevic,¹⁴⁶ J. Nash,^{146,cccc} V. Palladino,¹⁴⁶ M. Pesaresi,¹⁴⁶
 D. M. Raymond,¹⁴⁶ A. Richards,¹⁴⁶ A. Rose,¹⁴⁶ E. Scott,¹⁴⁶ C. Seez,¹⁴⁶ A. Shtipliyski,¹⁴⁶ M. Stoye,¹⁴⁶ A. Tapper,¹⁴⁶
 K. Uchida,¹⁴⁶ T. Virdee,^{146,t} N. Wardle,¹⁴⁶ S. N. Webb,¹⁴⁶ D. Winterbottom,¹⁴⁶ A. G. Zecchinelli,¹⁴⁶ J. E. Cole,¹⁴⁷
 P. R. Hobson,¹⁴⁷ A. Khan,¹⁴⁷ P. Kyberd,¹⁴⁷ C. K. Mackay,¹⁴⁷ I. D. Reid,¹⁴⁷ L. Teodorescu,¹⁴⁷ S. Zahid,¹⁴⁷ S. Abdullin,¹⁴⁸
 A. Brinkerhoff,¹⁴⁸ K. Call,¹⁴⁸ B. Caraway,¹⁴⁸ J. Dittmann,¹⁴⁸ K. Hatakeyama,¹⁴⁸ A. R. Kanuganti,¹⁴⁸ C. Madrid,¹⁴⁸
 B. McMaster,¹⁴⁸ N. Pastika,¹⁴⁸ S. Sawant,¹⁴⁸ C. Smith,¹⁴⁸ J. Wilson,¹⁴⁸ S. Johnson,¹⁴⁹ R. Bartek,¹⁵⁰ A. Dominguez,¹⁵⁰
 R. Uniyal,¹⁵⁰ A. M. Vargas Hernandez,¹⁵⁰ A. Buccilli,¹⁵¹ O. Charaf,¹⁵¹ S. I. Cooper,¹⁵¹ S. V. Gleyzer,¹⁵¹ C. Henderson,¹⁵¹
 P. Rumerio,¹⁵¹ C. West,¹⁵¹ A. Akpınar,¹⁵² A. Albert,¹⁵² D. Arcaro,¹⁵² C. Cosby,¹⁵² Z. Demiragli,¹⁵² D. Gastler,¹⁵² J. Rohlf,¹⁵²
 K. Salyer,¹⁵² D. Sperka,¹⁵² D. Spitzbart,¹⁵² I. Suarez,¹⁵² S. Yuan,¹⁵² D. Zou,¹⁵² G. Benelli,¹⁵³ B. Burkle,¹⁵³ X. Coubez,^{153,u}
 D. Cutts,¹⁵³ Y. t. Duh,¹⁵³ M. Hadley,¹⁵³ U. Heintz,¹⁵³ J. M. Hogan,^{153,dddd} K. H. M. Kwok,¹⁵³ E. Laird,¹⁵³ G. Landsberg,¹⁵³
 K. T. Lau,¹⁵³ J. Lee,¹⁵³ M. Narain,¹⁵³ S. Sagir,^{153,eeee} R. Syarif,¹⁵³ E. Usai,¹⁵³ W. Y. Wong,¹⁵³ D. Yu,¹⁵³ W. Zhang,¹⁵³
 R. Band,¹⁵⁴ C. Brainerd,¹⁵⁴ R. Breedon,¹⁵⁴ M. Calderon De La Barca Sanchez,¹⁵⁴ M. Chertok,¹⁵⁴ J. Conway,¹⁵⁴
 R. Conway,¹⁵⁴ P. T. Cox,¹⁵⁴ R. Erbacher,¹⁵⁴ C. Flores,¹⁵⁴ G. Funk,¹⁵⁴ F. Jensen,¹⁵⁴ W. Ko,^{154,a} O. Kukral,¹⁵⁴ R. Lander,¹⁵⁴
 M. Mulhearn,¹⁵⁴ D. Pellett,¹⁵⁴ J. Pilot,¹⁵⁴ M. Shi,¹⁵⁴ D. Taylor,¹⁵⁴ K. Tos,¹⁵⁴ M. Tripathi,¹⁵⁴ Y. Yao,¹⁵⁴ F. Zhang,¹⁵⁴
 M. Bachtis,¹⁵⁵ R. Cousins,¹⁵⁵ A. Dasgupta,¹⁵⁵ D. Hamilton,¹⁵⁵ J. Hauser,¹⁵⁵ M. Ignatenko,¹⁵⁵ T. Lam,¹⁵⁵ N. Mccoll,¹⁵⁵
 W. A. Nash,¹⁵⁵ S. Regnard,¹⁵⁵ D. Saltzberg,¹⁵⁵ C. Schnaible,¹⁵⁵ B. Stone,¹⁵⁵ V. Valuev,¹⁵⁵ K. Burt,¹⁵⁶ Y. Chen,¹⁵⁶ R. Clare,¹⁵⁶
 J. W. Gary,¹⁵⁶ G. Hanson,¹⁵⁶ G. Karapostoli,¹⁵⁶ O. R. Long,¹⁵⁶ N. Manganelli,¹⁵⁶ M. Olmedo Negrete,¹⁵⁶ M. I. Paneva,¹⁵⁶
 W. Si,¹⁵⁶ S. Wimpenny,¹⁵⁶ Y. Zhang,¹⁵⁶ J. G. Branson,¹⁵⁷ P. Chang,¹⁵⁷ S. Cittolin,¹⁵⁷ S. Cooperstein,¹⁵⁷ N. Deelen,¹⁵⁷
 J. Duarte,¹⁵⁷ R. Gerosa,¹⁵⁷ D. Gilbert,¹⁵⁷ V. Krutelyov,¹⁵⁷ J. Letts,¹⁵⁷ M. Masciovecchio,¹⁵⁷ S. May,¹⁵⁷ S. Padhi,¹⁵⁷
 M. Pieri,¹⁵⁷ V. Sharma,¹⁵⁷ M. Tadel,¹⁵⁷ F. Würthwein,¹⁵⁷ A. Yagil,¹⁵⁷ N. Amin,¹⁵⁸ C. Campagnari,¹⁵⁸ M. Citron,¹⁵⁸
 A. Dorsett,¹⁵⁸ V. Dutta,¹⁵⁸ J. Incandela,¹⁵⁸ B. Marsh,¹⁵⁸ H. Mei,¹⁵⁸ A. Ovcharova,¹⁵⁸ H. Qu,¹⁵⁸ M. Quinlan,¹⁵⁸ J. Richman,¹⁵⁸
 U. Sarica,¹⁵⁸ D. Stuart,¹⁵⁸ S. Wang,¹⁵⁸ A. Bornheim,¹⁵⁹ O. Cerri,¹⁵⁹ I. Dutta,¹⁵⁹ J. M. Lawhorn,¹⁵⁹ N. Lu,¹⁵⁹ J. Mao,¹⁵⁹
 H. B. Newman,¹⁵⁹ J. Ngadiuba,¹⁵⁹ T. Q. Nguyen,¹⁵⁹ J. Pata,¹⁵⁹ M. Spiropulu,¹⁵⁹ J. R. Vlimant,¹⁵⁹ C. Wang,¹⁵⁹ S. Xie,¹⁵⁹
 Z. Zhang,¹⁵⁹ R. Y. Zhu,¹⁵⁹ J. Alison,¹⁶⁰ M. B. Andrews,¹⁶⁰ T. Ferguson,¹⁶⁰ T. Mudholkar,¹⁶⁰ M. Paulini,¹⁶⁰ M. Sun,¹⁶⁰
 I. Vorobiev,¹⁶⁰ J. P. Cumalat,¹⁶¹ W. T. Ford,¹⁶¹ E. MacDonald,¹⁶¹ T. Mulholland,¹⁶¹ R. Patel,¹⁶¹ A. Perloff,¹⁶¹ K. Stenson,¹⁶¹
 K. A. Ulmer,¹⁶¹ S. R. Wagner,¹⁶¹ J. Alexander,¹⁶² Y. Cheng,¹⁶² J. Chu,¹⁶² D. J. Cranshaw,¹⁶² A. Datta,¹⁶² A. Frankenthal,¹⁶²
 K. Mcdermott,¹⁶² J. Monroy,¹⁶² J. R. Patterson,¹⁶² D. Quach,¹⁶² A. Ryd,¹⁶² W. Sun,¹⁶² S. M. Tan,¹⁶² Z. Tao,¹⁶² J. Thom,¹⁶²
 P. Wittich,¹⁶² M. Zientek,¹⁶² M. Albrow,¹⁶³ M. Alyari,¹⁶³ G. Apollinari,¹⁶³ A. Apresyan,¹⁶³ A. Apyan,¹⁶³ S. Banerjee,¹⁶³
 L. A. T. Bauerdick,¹⁶³ A. Beretvas,¹⁶³ D. Berry,¹⁶³ J. Berryhill,¹⁶³ P. C. Bhat,¹⁶³ K. Burkett,¹⁶³ J. N. Butler,¹⁶³ A. Canepa,¹⁶³
 G. B. Cerati,¹⁶³ H. W. K. Cheung,¹⁶³ F. Chlebana,¹⁶³ M. Cremonesi,¹⁶³ V. D. Elvira,¹⁶³ J. Freeman,¹⁶³ Z. Gece,¹⁶³
 E. Gottschalk,¹⁶³ L. Gray,¹⁶³ D. Green,¹⁶³ S. Grünendahl,¹⁶³ O. Gutsche,¹⁶³ R. M. Harris,¹⁶³ S. Hasegawa,¹⁶³ R. Heller,¹⁶³
 T. C. Herwig,¹⁶³ J. Hirschauer,¹⁶³ B. Jayatilaka,¹⁶³ S. Jindariani,¹⁶³ M. Johnson,¹⁶³ U. Joshi,¹⁶³ P. Klabbers,¹⁶³
 T. Klijnsma,¹⁶³ B. Klima,¹⁶³ M. J. Kortelainen,¹⁶³ S. Lammel,¹⁶³ D. Lincoln,¹⁶³ R. Lipton,¹⁶³ M. Liu,¹⁶³ T. Liu,¹⁶³
 J. Lykken,¹⁶³ K. Maeshima,¹⁶³ D. Mason,¹⁶³ P. McBride,¹⁶³ P. Merkel,¹⁶³ S. Mrenna,¹⁶³ S. Nahn,¹⁶³ V. O'Dell,¹⁶³
 V. Papadimitriou,¹⁶³ K. Pedro,¹⁶³ C. Pena,^{163,aaa} O. Prokofyev,¹⁶³ F. Ravera,¹⁶³ A. Reinsvold Hall,¹⁶³ L. Ristori,¹⁶³
 B. Schneider,¹⁶³ E. Sexton-Kennedy,¹⁶³ N. Smith,¹⁶³ A. Soha,¹⁶³ W. J. Spalding,¹⁶³ L. Spiegel,¹⁶³ S. Stoynev,¹⁶³ J. Strait,¹⁶³
 L. Taylor,¹⁶³ S. Tkaczyk,¹⁶³ N. V. Tran,¹⁶³ L. Uplegger,¹⁶³ E. W. Vaandering,¹⁶³ H. A. Weber,¹⁶³ A. Woodard,¹⁶³
 D. Acosta,¹⁶⁴ P. Avery,¹⁶⁴ D. Bourilkov,¹⁶⁴ L. Cadamuro,¹⁶⁴ V. Cherepanov,¹⁶⁴ F. Errico,¹⁶⁴ R. D. Field,¹⁶⁴ D. Guerrero,¹⁶⁴
 B. M. Joshi,¹⁶⁴ M. Kim,¹⁶⁴ J. Konigsberg,¹⁶⁴ A. Korytov,¹⁶⁴ K. H. Lo,¹⁶⁴ K. Matchev,¹⁶⁴ N. Menendez,¹⁶⁴
 G. Mitselmakher,¹⁶⁴ D. Rosenzweig,¹⁶⁴ K. Shi,¹⁶⁴ J. Sturdy,¹⁶⁴ J. Wang,¹⁶⁴ S. Wang,¹⁶⁴ X. Zuo,¹⁶⁴ T. Adams,¹⁶⁵ A. Askew,¹⁶⁵
 D. Diaz,¹⁶⁵ R. Habibullah,¹⁶⁵ S. Hagopian,¹⁶⁵ V. Hagopian,¹⁶⁵ K. F. Johnson,¹⁶⁵ R. Khurana,¹⁶⁵ T. Kolberg,¹⁶⁵
 G. Martinez,¹⁶⁵ H. Prosper,¹⁶⁵ C. Schiber,¹⁶⁵ R. Yohay,¹⁶⁵ J. Zhang,¹⁶⁵ M. M. Baarmand,¹⁶⁶ S. Butalla,¹⁶⁶ T. Elkafrawy,^{166,m}
 M. Hohmann,¹⁶⁶ D. Noonan,¹⁶⁶ M. Rahmani,¹⁶⁶ M. Saunders,¹⁶⁶ F. Yumiceva,¹⁶⁶ M. R. Adams,¹⁶⁷ L. Apanasevich,¹⁶⁷

H. Becerril Gonzalez,¹⁶⁷ R. Cavanaugh,¹⁶⁷ X. Chen,¹⁶⁷ S. Dittmer,¹⁶⁷ O. Evdokimov,¹⁶⁷ C. E. Gerber,¹⁶⁷ D. A. Hangal,¹⁶⁷ D. J. Hofman,¹⁶⁷ C. Mills,¹⁶⁷ G. Oh,¹⁶⁷ T. Roy,¹⁶⁷ M. B. Tonjes,¹⁶⁷ N. Varelas,¹⁶⁷ J. Viinikainen,¹⁶⁷ X. Wang,¹⁶⁷ Z. Wu,¹⁶⁷ M. Alhusseini,¹⁶⁸ K. Dilsiz,^{168,ffff} S. Durgut,¹⁶⁸ R. P. Gandrajula,¹⁶⁸ M. Haytmyradov,¹⁶⁸ V. Khristenko,¹⁶⁸ O. K. Köseyan,¹⁶⁸ J.-P. Merlo,¹⁶⁸ A. Mestvirishvili,^{168,gggg} A. Moeller,¹⁶⁸ J. Nachtman,¹⁶⁸ H. Ogul,^{168,hhhh} Y. Onel,¹⁶⁸ F. Ozok,^{168,iiii} A. Penzo,¹⁶⁸ C. Snyder,¹⁶⁸ E. Tiras,¹⁶⁸ J. Wetzel,¹⁶⁸ K. Yi,^{168,jjjj} O. Amram,¹⁶⁹ B. Blumenfeld,¹⁶⁹ L. Corcodilos,¹⁶⁹ M. Eminizer,¹⁶⁹ A. V. Gritsan,¹⁶⁹ S. Kyriacou,¹⁶⁹ P. Maksimovic,¹⁶⁹ C. Mantilla,¹⁶⁹ J. Roskes,¹⁶⁹ M. Swartz,¹⁶⁹ T. Á. Vámi,¹⁶⁹ C. Baldenegro Barrera,¹⁷⁰ P. Baringer,¹⁷⁰ A. Bean,¹⁷⁰ A. Bylinkin,¹⁷⁰ T. Isidori,¹⁷⁰ S. Khalil,¹⁷⁰ J. King,¹⁷⁰ G. Krintiras,¹⁷⁰ A. Kropivnitskaya,¹⁷⁰ C. Lindsey,¹⁷⁰ N. Minafra,¹⁷⁰ M. Murray,¹⁷⁰ C. Rogan,¹⁷⁰ C. Royon,¹⁷⁰ S. Sanders,¹⁷⁰ E. Schmitz,¹⁷⁰ J. D. Tapia Takaki,¹⁷⁰ Q. Wang,¹⁷⁰ J. Williams,¹⁷⁰ G. Wilson,¹⁷⁰ S. Duric,¹⁷¹ A. Ivanov,¹⁷¹ K. Kaadze,¹⁷¹ D. Kim,¹⁷¹ Y. Maravin,¹⁷¹ T. Mitchell,¹⁷¹ A. Modak,¹⁷¹ A. Mohammadi,¹⁷¹ F. Rebassoo,¹⁷² D. Wright,¹⁷² E. Adams,¹⁷³ A. Baden,¹⁷³ O. Baron,¹⁷³ A. Belloni,¹⁷³ S. C. Eno,¹⁷³ Y. Feng,¹⁷³ N. J. Hadley,¹⁷³ S. Jabeen,¹⁷³ G. Y. Jeng,¹⁷³ R. G. Kellogg,¹⁷³ T. Koeth,¹⁷³ A. C. Mignerey,¹⁷³ S. Nabili,¹⁷³ M. Seidel,¹⁷³ A. Skuja,¹⁷³ S. C. Tonwar,¹⁷³ L. Wang,¹⁷³ K. Wong,¹⁷³ D. Abercrombie,¹⁷⁴ B. Allen,¹⁷⁴ R. Bi,¹⁷⁴ S. Brandt,¹⁷⁴ W. Busza,¹⁷⁴ I. A. Cali,¹⁷⁴ Y. Chen,¹⁷⁴ M. D'Alfonso,¹⁷⁴ G. Gomez Ceballos,¹⁷⁴ M. Goncharov,¹⁷⁴ P. Harris,¹⁷⁴ D. Hsu,¹⁷⁴ M. Hu,¹⁷⁴ M. Klute,¹⁷⁴ D. Kovalskyi,¹⁷⁴ J. Krupa,¹⁷⁴ Y.-J. Lee,¹⁷⁴ P. D. Luckey,¹⁷⁴ B. Maier,¹⁷⁴ A. C. Marini,¹⁷⁴ C. McGinn,¹⁷⁴ C. Mironov,¹⁷⁴ S. Narayanan,¹⁷⁴ X. Niu,¹⁷⁴ C. Paus,¹⁷⁴ D. Rankin,¹⁷⁴ C. Roland,¹⁷⁴ G. Roland,¹⁷⁴ Z. Shi,¹⁷⁴ G. S. F. Stephans,¹⁷⁴ K. Sumorok,¹⁷⁴ K. Tatar,¹⁷⁴ D. Velicanu,¹⁷⁴ J. Wang,¹⁷⁴ T. W. Wang,¹⁷⁴ Z. Wang,¹⁷⁴ B. Wyslouch,¹⁷⁴ R. M. Chatterjee,¹⁷⁵ A. Evans,¹⁷⁵ P. Hansen,¹⁷⁵ J. Hiltbrand,¹⁷⁵ Sh. Jain,¹⁷⁵ M. Krohn,¹⁷⁵ Y. Kubota,¹⁷⁵ Z. Lesko,¹⁷⁵ J. Mans,¹⁷⁵ M. Revering,¹⁷⁵ R. Rusack,¹⁷⁵ R. Saradhy,¹⁷⁵ N. Schroeder,¹⁷⁵ N. Strobe,¹⁷⁵ M. A. Wadud,¹⁷⁵ J. G. Acosta,¹⁷⁶ S. Oliveros,¹⁷⁶ K. Bloom,¹⁷⁷ S. Chauhan,¹⁷⁷ D. R. Claes,¹⁷⁷ C. Fangmeier,¹⁷⁷ L. Finco,¹⁷⁷ F. Golf,¹⁷⁷ J. R. González Fernández,¹⁷⁷ I. Kravchenko,¹⁷⁷ J. E. Siado,¹⁷⁷ G. R. Snow,^{177,a} W. Tabb,¹⁷⁷ F. Yan,¹⁷⁷ G. Agarwal,¹⁷⁸ H. Bandyopadhyay,¹⁷⁸ C. Harrington,¹⁷⁸ L. Hay,¹⁷⁸ I. Iashvili,¹⁷⁸ A. Kharchilava,¹⁷⁸ C. McLean,¹⁷⁸ D. Nguyen,¹⁷⁸ J. Pekkanen,¹⁷⁸ S. Rappoccio,¹⁷⁸ B. Roozbahani,¹⁷⁸ G. Alverson,¹⁷⁹ E. Barberis,¹⁷⁹ C. Freer,¹⁷⁹ Y. Haddad,¹⁷⁹ A. Hortiangtham,¹⁷⁹ J. Li,¹⁷⁹ G. Madigan,¹⁷⁹ B. Marzocchi,¹⁷⁹ D. M. Morse,¹⁷⁹ V. Nguyen,¹⁷⁹ T. Orimoto,¹⁷⁹ A. Parker,¹⁷⁹ L. Skinnari,¹⁷⁹ A. Tishelman-Charny,¹⁷⁹ T. Wamorkar,¹⁷⁹ B. Wang,¹⁷⁹ A. Wisecarver,¹⁷⁹ D. Wood,¹⁷⁹ S. Bhattacharya,¹⁸⁰ J. Bueghly,¹⁸⁰ Z. Chen,¹⁸⁰ A. Gilbert,¹⁸⁰ T. Gunter,¹⁸⁰ K. A. Hahn,¹⁸⁰ N. Odell,¹⁸⁰ M. H. Schmitt,¹⁸⁰ K. Sung,¹⁸⁰ M. Velasco,¹⁸⁰ R. Bucci,¹⁸¹ N. Dev,¹⁸¹ R. Goldouzian,¹⁸¹ M. Hildreth,¹⁸¹ K. Hurtado Anampa,¹⁸¹ C. Jessop,¹⁸¹ D. J. Karmgard,¹⁸¹ K. Lannon,¹⁸¹ N. Loukas,¹⁸¹ N. Marinelli,¹⁸¹ I. Mcalister,¹⁸¹ F. Meng,¹⁸¹ K. Mohrman,¹⁸¹ Y. Musienko,^{181,uu} R. Ruchti,¹⁸¹ P. Siddireddy,¹⁸¹ S. Taroni,¹⁸¹ M. Wayne,¹⁸¹ A. Wightman,¹⁸¹ M. Wolf,¹⁸¹ L. Zygala,¹⁸¹ J. Alimena,¹⁸² B. Bylsma,¹⁸² B. Cardwell,¹⁸² L. S. Durkin,¹⁸² B. Francis,¹⁸² C. Hill,¹⁸² A. Lefeld,¹⁸² B. L. Winer,¹⁸² B. R. Yates,¹⁸² P. Das,¹⁸³ G. Dezoort,¹⁸³ P. Elmer,¹⁸³ B. Greenberg,¹⁸³ N. Haubrich,¹⁸³ S. Higginbotham,¹⁸³ A. Kalogeropoulos,¹⁸³ G. Kopp,¹⁸³ S. Kwan,¹⁸³ D. Lange,¹⁸³ M. T. Lucchini,¹⁸³ J. Luo,¹⁸³ D. Marlow,¹⁸³ K. Mei,¹⁸³ I. Ojalvo,¹⁸³ J. Olsen,¹⁸³ C. Palmer,¹⁸³ P. Piroué,¹⁸³ D. Stickland,¹⁸³ C. Tully,¹⁸³ S. Malik,¹⁸⁴ S. Norberg,¹⁸⁴ V. E. Barnes,¹⁸⁵ R. Chawla,¹⁸⁵ S. Das,¹⁸⁵ L. Gutay,¹⁸⁵ M. Jones,¹⁸⁵ A. W. Jung,¹⁸⁵ G. Negro,¹⁸⁵ N. Neumeister,¹⁸⁵ C. C. Peng,¹⁸⁵ S. Piperov,¹⁸⁵ A. Purohit,¹⁸⁵ H. Qiu,¹⁸⁵ J. F. Schulte,¹⁸⁵ M. Stojanovic,^{185,q} N. Trevisani,¹⁸⁵ F. Wang,¹⁸⁵ A. Wildridge,¹⁸⁵ R. Xiao,¹⁸⁵ W. Xie,¹⁸⁵ T. Cheng,¹⁸⁶ J. Dolen,¹⁸⁶ N. Parashar,¹⁸⁶ A. Baty,¹⁸⁷ S. Dildick,¹⁸⁷ K. M. Ecklund,¹⁸⁷ S. Freed,¹⁸⁷ F. J. M. Geurts,¹⁸⁷ M. Kilpatrick,¹⁸⁷ A. Kumar,¹⁸⁷ W. Li,¹⁸⁷ B. P. Padley,¹⁸⁷ R. Redjimi,¹⁸⁷ J. Roberts,^{187,a} J. Rorie,¹⁸⁷ W. Shi,¹⁸⁷ A. G. Stahl Leiton,¹⁸⁷ A. Bodek,¹⁸⁸ P. de Barbaro,¹⁸⁸ R. Demina,¹⁸⁸ J. L. Dulemba,¹⁸⁸ C. Fallon,¹⁸⁸ T. Ferbel,¹⁸⁸ M. Galanti,¹⁸⁸ A. Garcia-Bellido,¹⁸⁸ O. Hindrichs,¹⁸⁸ A. Khukhunaishvili,¹⁸⁸ E. Ranken,¹⁸⁸ R. Taus,¹⁸⁸ B. Chiarito,¹⁸⁹ J. P. Chou,¹⁸⁹ R. Gambhir,¹⁸⁹ A. Gandrakota,¹⁸⁹ Y. Gershtein,¹⁸⁹ E. Halkiadakis,¹⁸⁹ A. Hart,¹⁸⁹ M. Heindl,¹⁸⁹ E. Hughes,¹⁸⁹ S. Kaplan,¹⁸⁹ O. Karacheban,^{189,x} I. Laflotte,¹⁸⁹ A. Lath,¹⁸⁹ R. Montalvo,¹⁸⁹ K. Nash,¹⁸⁹ M. Osherson,¹⁸⁹ P. Pajarillo,¹⁸⁹ N. Paladino,¹⁸⁹ S. Salur,¹⁸⁹ S. Schnetzer,¹⁸⁹ S. Somalwar,¹⁸⁹ R. Stone,¹⁸⁹ S. A. Thayil,¹⁸⁹ S. Thomas,¹⁸⁹ A. Venugopal,¹⁸⁹ H. Wang,¹⁸⁹ H. Acharya,¹⁹⁰ A. G. Delannoy,¹⁹⁰ S. Spanier,¹⁹⁰ O. Bouhali,^{191,kkkk} M. Dalchenko,¹⁹¹ A. Delgado,¹⁹¹ R. Eusebi,¹⁹¹ J. Gilmore,¹⁹¹ T. Huang,¹⁹¹ T. Kamon,^{191,llll} H. Kim,¹⁹¹ S. Luo,¹⁹¹ S. Malhotra,¹⁹¹ R. Mueller,¹⁹¹ D. Overton,¹⁹¹ L. Perniè,¹⁹¹ D. Rathjens,¹⁹¹ A. Safonov,¹⁹¹ N. Akchurin,¹⁹² J. Damgov,¹⁹² V. Hegde,¹⁹² S. Kunori,¹⁹² K. Lamichhane,¹⁹² S. W. Lee,¹⁹² T. Mengke,¹⁹² S. Muthumuni,¹⁹² T. Peltola,¹⁹² S. Undleeb,¹⁹² I. Volobouev,¹⁹² Z. Wang,¹⁹² A. Whitbeck,¹⁹² E. Appelt,¹⁹³ S. Greene,¹⁹³ A. Gurrola,¹⁹³ R. Janjam,¹⁹³ W. Johns,¹⁹³ C. Maguire,¹⁹³ A. Melo,¹⁹³ H. Ni,¹⁹³ K. Padeken,¹⁹³ F. Romeo,¹⁹³ P. Sheldon,¹⁹³ S. Tuo,¹⁹³ J. Velkovska,¹⁹³ M. W. Arenton,¹⁹⁴ B. Cox,¹⁹⁴ G. Cummings,¹⁹⁴ J. Hakala,¹⁹⁴ R. Hirosky,¹⁹⁴ M. Joyce,¹⁹⁴ A. Ledovskoy,¹⁹⁴ A. Li,¹⁹⁴ C. Neu,¹⁹⁴ B. Tannenwald,¹⁹⁴ Y. Wang,¹⁹⁴ E. Wolfe,¹⁹⁴ F. Xia,¹⁹⁴ P. E. Karchin,¹⁹⁵ N. Poudyal,¹⁹⁵ P. Thapa,¹⁹⁵ K. Black,¹⁹⁶ T. Bose,¹⁹⁶ J. Buchanan,¹⁹⁶ C. Caillol,¹⁹⁶ S. Dasu,¹⁹⁶

I. De Bruyn,¹⁹⁶ P. Everaerts,¹⁹⁶ C. Galloni,¹⁹⁶ H. He,¹⁹⁶ M. Herndon,¹⁹⁶ A. Hervé,¹⁹⁶ U. Hussain,¹⁹⁶ A. Lanaro,¹⁹⁶
 A. Loeliger,¹⁹⁶ R. Loveless,¹⁹⁶ J. Madhusudanan Sreekala,¹⁹⁶ A. Mallampalli,¹⁹⁶ D. Pinna,¹⁹⁶ A. Savin,¹⁹⁶ V. Shang,¹⁹⁶
 V. Sharma,¹⁹⁶ W. H. Smith,¹⁹⁶ J. Steggemann,¹⁹⁶ D. Teague,¹⁹⁶ S. Trembath-reichert,¹⁹⁶ and W. Vetens¹⁹⁶

(CMS Collaboration)

- ¹*Yerevan Physics Institute, Yerevan, Armenia*
²*Institut für Hochenergiephysik, Wien, Austria*
³*Institute for Nuclear Problems, Minsk, Belarus*
⁴*Universiteit Antwerpen, Antwerpen, Belgium*
⁵*Vrije Universiteit Brussel, Brussel, Belgium*
⁶*Université Libre de Bruxelles, Bruxelles, Belgium*
⁷*Ghent University, Ghent, Belgium*
⁸*Université Catholique de Louvain, Louvain-la-Neuve, Belgium*
⁹*Centro Brasileiro de Pesquisas Físicas, Rio de Janeiro, Brazil*
¹⁰*Universidade do Estado do Rio de Janeiro, Rio de Janeiro, Brazil*
^{11a}*Universidade Estadual Paulista, São Paulo, Brazil*
^{11b}*Universidade Federal do ABC, São Paulo, Brazil*
¹²*Institute for Nuclear Research and Nuclear Energy, Bulgarian Academy of Sciences, Sofia, Bulgaria*
¹³*University of Sofia, Sofia, Bulgaria*
¹⁴*Beihang University, Beijing, China*
¹⁵*Department of Physics, Tsinghua University, Beijing, China*
¹⁶*Institute of High Energy Physics, Beijing, China*
¹⁷*State Key Laboratory of Nuclear Physics and Technology, Peking University, Beijing, China*
¹⁸*Sun Yat-Sen University, Guangzhou, China*
¹⁹*Institute of Modern Physics and Key Laboratory of Nuclear Physics and Ion-beam Application (MOE)—
 Fudan University, Shanghai, China*
²⁰*Zhejiang University, Hangzhou, China*
²¹*Universidad de Los Andes, Bogota, Colombia*
²²*Universidad de Antioquia, Medellin, Colombia*
²³*University of Split, Faculty of Electrical Engineering, Mechanical Engineering and Naval Architecture,
 Split, Croatia*
²⁴*University of Split, Faculty of Science, Split, Croatia*
²⁵*Institute Rudjer Boskovic, Zagreb, Croatia*
²⁶*University of Cyprus, Nicosia, Cyprus*
²⁷*Charles University, Prague, Czech Republic*
²⁸*Escuela Politécnica Nacional, Quito, Ecuador*
²⁹*Universidad San Francisco de Quito, Quito, Ecuador*
³⁰*Academy of Scientific Research and Technology of the Arab Republic of Egypt,
 Egyptian Network of High Energy Physics, Cairo, Egypt*
³¹*Center for High Energy Physics (CHEP-FU), Fayoum University, El-Fayoum, Egypt*
³²*National Institute of Chemical Physics and Biophysics, Tallinn, Estonia*
³³*Department of Physics, University of Helsinki, Helsinki, Finland*
³⁴*Helsinki Institute of Physics, Helsinki, Finland*
³⁵*Lappeenranta University of Technology, Lappeenranta, Finland*
³⁶*IRFU, CEA, Université Paris-Saclay, Gif-sur-Yvette, France*
³⁷*Laboratoire Leprince-Ringuet, CNRS/IN2P3, Ecole Polytechnique, Institut Polytechnique de Paris,
 Paris, France*
³⁸*Université de Strasbourg, CNRS, IPHC UMR 7178, Strasbourg, France*
³⁹*Université de Lyon, Université Claude Bernard Lyon 1, CNRS-IN2P3, Institut de Physique Nucléaire de
 Lyon, Villeurbanne, France*
⁴⁰*Georgian Technical University, Tbilisi, Georgia*
⁴¹*RWTH Aachen University, I. Physikalisches Institut, Aachen, Germany*
⁴²*RWTH Aachen University, III. Physikalisches Institut A, Aachen, Germany*
⁴³*RWTH Aachen University, III. Physikalisches Institut B, Aachen, Germany*
⁴⁴*Deutsches Elektronen-Synchrotron, Hamburg, Germany*
⁴⁵*University of Hamburg, Hamburg, Germany*
⁴⁶*Karlsruher Institut fuer Technologie, Karlsruhe, Germany*
⁴⁷*Institute of Nuclear and Particle Physics (INPP), NCSR Demokritos, Aghia Paraskevi, Greece*

- ⁴⁸*National and Kapodistrian University of Athens, Athens, Greece*
⁴⁹*National Technical University of Athens, Athens, Greece*
⁵⁰*University of Ioánnina, Ioánnina, Greece*
⁵¹*MTA-ELTE Lendület CMS Particle and Nuclear Physics Group, Eötvös Loránd University, Budapest, Hungary*
⁵²*Wigner Research Centre for Physics, Budapest, Hungary*
⁵³*Institute of Nuclear Research ATOMKI, Debrecen, Hungary*
⁵⁴*Institute of Physics, University of Debrecen, Debrecen, Hungary*
⁵⁵*Eszterhazy Karoly University, Karoly Robert Campus, Gyongyos, Hungary*
⁵⁶*Indian Institute of Science (IISc), Bangalore, India*
⁵⁷*National Institute of Science Education and Research, HBNI, Bhubaneswar, India*
⁵⁸*Panjab University, Chandigarh, India*
⁵⁹*University of Delhi, Delhi, India*
⁶⁰*Saha Institute of Nuclear Physics, HBNI, Kolkata, India*
⁶¹*Indian Institute of Technology Madras, Madras, India*
⁶²*Bhabha Atomic Research Centre, Mumbai, India*
⁶³*Tata Institute of Fundamental Research-A, Mumbai, India*
⁶⁴*Tata Institute of Fundamental Research-B, Mumbai, India*
⁶⁵*Indian Institute of Science Education and Research (IISER), Pune, India*
⁶⁶*Department of Physics, Isfahan University of Technology, Isfahan, Iran*
⁶⁷*Institute for Research in Fundamental Sciences (IPM), Tehran, Iran*
⁶⁸*University College Dublin, Dublin, Ireland*
^{69a}*INFN Sezione di Bari*
^{69b}*Università di Bari*
^{69c}*Politecnico di Bari*
^{70a}*INFN Sezione di Bologna, Bologna, Italy*
^{70b}*Università di Bologna, Bologna, Italy*
^{71a}*INFN Sezione di Catania, Catania, Italy*
^{71b}*Università di Catania, Catania, Italy*
^{72a}*INFN Sezione di Firenze, Firenze, Italy*
^{72b}*Università di Firenze, Firenze, Italy*
⁷³*INFN Laboratori Nazionali di Frascati, Frascati, Italy*
^{74a}*INFN Sezione di Genova, Genova, Italy*
^{74b}*Università di Genova, Genova, Italy*
^{75a}*INFN Sezione di Milano-Bicocca, Milano, Italy*
^{75b}*Università di Milano-Bicocca, Milano, Italy*
^{76a}*INFN Sezione di Napoli, Napoli, Italy*
^{76b}*Università di Napoli 'Federico II', Napoli, Italy*
^{76c}*Università della Basilicata, Potenza, Italy*
^{76d}*Università G. Marconi, Napoli, Italy*
^{77a}*INFN Sezione di Padova, Padova, Italy*
^{77b}*Università di Padova, Padova, Italy*
^{77c}*Università di Trento, Trento, Italy*
^{78a}*INFN Sezione di Pavia*
^{78b}*Università di Pavia*
^{79a}*INFN Sezione di Perugia, Perugia, Italy*
^{79b}*Università di Perugia, Perugia, Italy*
^{80a}*INFN Sezione di Pisa, Pisa, Italy*
^{80b}*Università di Pisa, Pisa, Italy*
^{80c}*Scuola Normale Superiore di Pisa, Pisa, Italy*
^{81a}*INFN Sezione di Roma, Rome, Italy*
^{81b}*Sapienza Università di Roma, Rome, Italy*
^{82a}*INFN Sezione di Torino, Torino, Italy*
^{82b}*Università di Torino, Torino, Italy*
^{82c}*Università del Piemonte Orientale, Novara, Italy*
^{83a}*INFN Sezione di Trieste, Trieste, Italy*
^{83b}*Università di Trieste, Trieste, Italy*
⁸⁴*Kyungpook National University, Daegu, Korea*
⁸⁵*Chonnam National University, Institute for Universe and Elementary Particles, Kwangju, Korea*
⁸⁶*Hanyang University, Seoul, Korea*

- ⁸⁷*Korea University, Seoul, Korea*
- ⁸⁸*Kyung Hee University, Department of Physics, Seoul, Republic of Korea*
- ⁸⁹*Sejong University, Seoul, Korea*
- ⁹⁰*Seoul National University, Seoul, Korea*
- ⁹¹*University of Seoul, Seoul, Korea*
- ⁹²*Yonsei University, Department of Physics, Seoul, Korea*
- ⁹³*Sungkyunkwan University, Suwon, Korea*
- ⁹⁴*American University of the Middle East (AUM), Dasman, Kuwait*
- ⁹⁵*Riga Technical University, Riga, Latvia*
- ⁹⁶*Vilnius University, Vilnius, Lithuania*
- ⁹⁷*National Centre for Particle Physics, Universiti Malaya, Kuala Lumpur, Malaysia*
- ⁹⁸*Universidad de Sonora (UNISON), Hermosillo, Mexico*
- ⁹⁹*Centro de Investigacion y de Estudios Avanzados del IPN, Mexico City, Mexico*
- ¹⁰⁰*Universidad Iberoamericana, Mexico City, Mexico*
- ¹⁰¹*Benemerita Universidad Autonoma de Puebla, Puebla, Mexico*
- ¹⁰²*Universidad Autónoma de San Luis Potosí, San Luis Potosí, Mexico*
- ¹⁰³*University of Montenegro, Podgorica, Montenegro*
- ¹⁰⁴*University of Auckland, Auckland, New Zealand*
- ¹⁰⁵*University of Canterbury, Christchurch, New Zealand*
- ¹⁰⁶*National Centre for Physics, Quaid-I-Azam University, Islamabad, Pakistan*
- ¹⁰⁷*AGH University of Science and Technology Faculty of Computer Science, Electronics and Telecommunications, Krakow, Poland*
- ¹⁰⁸*National Centre for Nuclear Research, Swierk, Poland*
- ¹⁰⁹*Institute of Experimental Physics, Faculty of Physics, University of Warsaw, Warsaw, Poland*
- ¹¹⁰*Laboratório de Instrumentação e Física Experimental de Partículas, Lisboa, Portugal*
- ¹¹¹*Joint Institute for Nuclear Research, Dubna, Russia*
- ¹¹²*Petersburg Nuclear Physics Institute, Gatchina (St. Petersburg), Russia*
- ¹¹³*Institute for Nuclear Research, Moscow, Russia*
- ¹¹⁴*Institute for Theoretical and Experimental Physics named by A.I. Alikhanov of NRC ‘Kurchatov Institute’, Moscow, Russia*
- ¹¹⁵*Moscow Institute of Physics and Technology, Moscow, Russia*
- ¹¹⁶*National Research Nuclear University ‘Moscow Engineering Physics Institute’ (MEPhI), Moscow, Russia*
- ¹¹⁷*P.N. Lebedev Physical Institute, Moscow, Russia*
- ¹¹⁸*Skobeltsyn Institute of Nuclear Physics, Lomonosov Moscow State University, Moscow, Russia*
- ¹¹⁹*Novosibirsk State University (NSU), Novosibirsk, Russia*
- ¹²⁰*Institute for High Energy Physics of National Research Centre ‘Kurchatov Institute’, Protvino, Russia*
- ¹²¹*National Research Tomsk Polytechnic University, Tomsk, Russia*
- ¹²²*Tomsk State University, Tomsk, Russia*
- ¹²³*University of Belgrade: Faculty of Physics and VINCA Institute of Nuclear Sciences, Belgrade, Serbia*
- ¹²⁴*Centro de Investigaciones Energéticas Medioambientales y Tecnológicas (CIEMAT), Madrid, Spain*
- ¹²⁵*Universidad Autónoma de Madrid, Madrid, Spain*
- ¹²⁶*Universidad de Oviedo, Instituto Universitario de Ciencias y Tecnologías Espaciales de Asturias (ICTEA), Oviedo, Spain*
- ¹²⁷*Instituto de Física de Cantabria (IFCA), CSIC-Universidad de Cantabria, Santander, Spain*
- ¹²⁸*University of Colombo, Colombo, Sri Lanka*
- ¹²⁹*University of Ruhuna, Department of Physics, Matara, Sri Lanka*
- ¹³⁰*CERN, European Organization for Nuclear Research, Geneva, Switzerland*
- ¹³¹*Paul Scherrer Institut, Villigen, Switzerland*
- ¹³²*ETH Zurich—Institute for Particle Physics and Astrophysics (IPA), Zurich, Switzerland*
- ¹³³*Universität Zürich, Zurich, Switzerland*
- ¹³⁴*National Central University, Chung-Li, Taiwan*
- ¹³⁵*National Taiwan University (NTU), Taipei, Taiwan*
- ¹³⁶*Chulalongkorn University, Faculty of Science, Department of Physics, Bangkok, Thailand*
- ¹³⁷*Çukurova University, Physics Department, Science and Art Faculty, Adana, Turkey*
- ¹³⁸*Middle East Technical University, Physics Department, Ankara, Turkey*
- ¹³⁹*Bogazici University, Istanbul, Turkey*
- ¹⁴⁰*Istanbul Technical University, Istanbul, Turkey*
- ¹⁴¹*Istanbul University, Istanbul, Turkey*
- ¹⁴²*Institute for Scintillation Materials of National Academy of Science of Ukraine, Kharkov, Ukraine*

- ¹⁴³*National Scientific Center, Kharkov Institute of Physics and Technology, Kharkov, Ukraine*
- ¹⁴⁴*University of Bristol, Bristol, United Kingdom*
- ¹⁴⁵*Rutherford Appleton Laboratory, Didcot, United Kingdom*
- ¹⁴⁶*Imperial College, London, United Kingdom*
- ¹⁴⁷*Brunel University, Uxbridge, United Kingdom*
- ¹⁴⁸*Baylor University, Waco, Texas, USA*
- ¹⁴⁹*Bethel University, St. Paul, Minneapolis, USA*
- ¹⁵⁰*Catholic University of America, Washington, DC, USA*
- ¹⁵¹*The University of Alabama, Tuscaloosa, Alabama, USA*
- ¹⁵²*Boston University, Boston, Massachusetts, USA*
- ¹⁵³*Brown University, Providence, Rhode Island, USA*
- ¹⁵⁴*University of California, Davis, Davis, California, USA*
- ¹⁵⁵*University of California, Los Angeles, California, USA*
- ¹⁵⁶*University of California, Riverside, Riverside, California, USA*
- ¹⁵⁷*University of California, San Diego, La Jolla, California, USA*
- ¹⁵⁸*University of California, Santa Barbara—Department of Physics, Santa Barbara, California, USA*
- ¹⁵⁹*California Institute of Technology, Pasadena, California, USA*
- ¹⁶⁰*Carnegie Mellon University, Pittsburgh, Pennsylvania, USA*
- ¹⁶¹*University of Colorado Boulder, Boulder, Colorado, USA*
- ¹⁶²*Cornell University, Ithaca, New York, USA*
- ¹⁶³*Fermi National Accelerator Laboratory, Batavia, Illinois, USA*
- ¹⁶⁴*University of Florida, Gainesville, Florida, USA*
- ¹⁶⁵*Florida State University, Tallahassee, Florida, USA*
- ¹⁶⁶*Florida Institute of Technology, Melbourne, Florida, USA*
- ¹⁶⁷*University of Illinois at Chicago (UIC), Chicago, Illinois, USA*
- ¹⁶⁸*The University of Iowa, Iowa City, Iowa, USA*
- ¹⁶⁹*Johns Hopkins University, Baltimore, Maryland, USA*
- ¹⁷⁰*The University of Kansas, Lawrence, Kansas, USA*
- ¹⁷¹*Kansas State University, Manhattan, Kansas, USA*
- ¹⁷²*Lawrence Livermore National Laboratory, Livermore, California, USA*
- ¹⁷³*University of Maryland, College Park, Maryland, USA*
- ¹⁷⁴*Massachusetts Institute of Technology, Cambridge, Massachusetts, USA*
- ¹⁷⁵*University of Minnesota, Minneapolis, Minnesota, USA*
- ¹⁷⁶*University of Mississippi, Oxford, Mississippi, USA*
- ¹⁷⁷*University of Nebraska-Lincoln, Lincoln, Nebraska, USA*
- ¹⁷⁸*State University of New York at Buffalo, Buffalo, New York, USA*
- ¹⁷⁹*Northeastern University, Boston, Massachusetts, USA*
- ¹⁸⁰*Northwestern University, Evanston, Illinois, USA*
- ¹⁸¹*University of Notre Dame, Notre Dame, Indiana, USA*
- ¹⁸²*The Ohio State University, Columbus, Ohio, USA*
- ¹⁸³*Princeton University, Princeton, New Jersey, USA*
- ¹⁸⁴*University of Puerto Rico, Mayaguez, Puerto Rico, USA*
- ¹⁸⁵*Purdue University, West Lafayette, Indiana, USA*
- ¹⁸⁶*Purdue University Northwest, Hammond, Indiana, USA*
- ¹⁸⁷*Rice University, Houston, Texas, USA*
- ¹⁸⁸*University of Rochester, Rochester, New York, USA*
- ¹⁸⁹*Rutgers, The State University of New Jersey, Piscataway, New Jersey, USA*
- ¹⁹⁰*University of Tennessee, Knoxville, Tennessee, USA*
- ¹⁹¹*Texas A&M University, College Station, Texas, USA*
- ¹⁹²*Texas Tech University, Lubbock, Texas, USA*
- ¹⁹³*Vanderbilt University, Nashville, Tennessee, USA*
- ¹⁹⁴*University of Virginia, Charlottesville, Virginia, USA*
- ¹⁹⁵*Wayne State University, Detroit, Michigan, USA*
- ¹⁹⁶*University of Wisconsin—Madison, Madison, Wisconsin, USA*

^aDeceased.^bAlso at Vienna University of Technology, Vienna, Austria.^cAlso at Institute of Basic and Applied Sciences, Faculty of Engineering, Arab Academy for Science, Technology and Maritime Transport, Alexandria, Egypt.^dAlso at Université Libre de Bruxelles, Bruxelles, Belgium.

- ^e Also at IRFU, CEA, Université Paris-Saclay, Gif-sur-Yvette, France.
- ^f Also at Universidade Estadual de Campinas, Campinas, Brazil.
- ^g Also at Federal University of Rio Grande do Sul, Porto Alegre, Brazil.
- ^h Federal University of Mato Grosso do Sul (UFMS), Campo Grande, Mato Grosso do Sul, Brazil.
- ⁱ Also at Universidade Federal de Pelotas, Pelotas, Brazil.
- ^j Also at University of Chinese Academy of Sciences, Beijing, China.
- ^k Also at Institute for Theoretical and Experimental Physics named by A.I. Alikhanov of NRC ‘Kurchatov Institute’, Moscow, Russia.
- ^l Also at Joint Institute for Nuclear Research, Dubna, Russia.
- ^m Also at Ain Shams University, Cairo, Egypt.
- ⁿ Also at Zewail City of Science and Technology, Zewail, Egypt.
- ^o Also at British University in Egypt, Cairo, Egypt.
- ^p Also at Fayoum University, El-Fayoum, Egypt.
- ^q Also at Purdue University, West Lafayette, Indiana, USA.
- ^r Also at Université de Haute Alsace, Mulhouse, France.
- ^s Also at Erzincan Binali Yildirim University, Erzincan, Turkey.
- ^t Also at CERN, European Organization for Nuclear Research, Geneva, Switzerland.
- ^u Also at RWTH Aachen University, III. Physikalisches Institut A, Aachen, Germany.
- ^v Also at University of Hamburg, Hamburg, Germany.
- ^w Also at Department of Physics, Isfahan University of Technology, Isfahan, Iran.
- ^x Also at Brandenburg University of Technology, Cottbus, Germany.
- ^y Also at Skobeltsyn Institute of Nuclear Physics, Lomonosov Moscow State University, Moscow, Russia.
- ^z Also at Institute of Physics, University of Debrecen, Debrecen, Hungary.
- ^{aa} Also at Physics Department, Faculty of Science, Assiut University.
- ^{bb} Also at MTA-ELTE Lendület CMS Particle and Nuclear Physics Group, Eötvös Loránd University, Budapest, Hungary.
- ^{cc} Also at Institute of Nuclear Research ATOMKI, Debrecen, Hungary.
- ^{dd} Also at IIT Bhubaneswar, Bhubaneswar, India.
- ^{ee} Also at Institute of Physics, Bhubaneswar, India.
- ^{ff} Also at G.H.G. Khalsa College, Punjab, India.
- ^{gg} Also at Shoolini University, Solan, India.
- ^{hh} Also at University of Hyderabad, Hyderabad, India.
- ⁱⁱ Also at University of Visva-Bharati, Santiniketan, India.
- ^{ji} Also at Indian Institute of Technology (IIT), Mumbai, India.
- ^{kk} Also at Deutsches Elektronen-Synchrotron, Hamburg, Germany.
- ^{ll} Also at Sharif University of Technology, Tehran, Iran.
- ^{mm} Also at Department of Physics, University of Science and Technology of Mazandaran, Behshahr, Iran.
- ⁿⁿ Also at INFN Sezione di Bari, Università di Bari, Politecnico di Bari, Bari, Italy.
- ^{oo} Also at Italian National Agency for New Technologies, Energy and Sustainable Economic Development, Rome, Italy.
- ^{pp} Also at Centro Siciliano di Fisica Nucleare e di Struttura Della Materia, Catania, Italy.
- ^{qq} Also at Università di Napoli ‘Federico II’, Naples, Italy.
- ^{rr} Also at Riga Technical University, Riga, Latvia.
- ^{ss} Also at Consejo Nacional de Ciencia y Tecnología, Mexico City, Mexico.
- ^{tt} Also at Warsaw University of Technology, Institute of Electronic Systems, Warsaw, Poland.
- ^{uu} Also at Institute for Nuclear Research, Moscow, Russia.
- ^{vv} Also at National Research Nuclear University ‘Moscow Engineering Physics Institute’ (MEPhI), Moscow, Russia.
- ^{ww} Also at St. Petersburg State Polytechnical University, St. Petersburg, Russia.
- ^{xx} Also at University of Florida, Gainesville, Florida, USA.
- ^{yy} Also at Imperial College, London, United Kingdom.
- ^{zz} Also at P.N. Lebedev Physical Institute, Moscow, Russia.
- ^{aaa} Also at California Institute of Technology, Pasadena, California, USA.
- ^{bbb} Also at Budker Institute of Nuclear Physics, Novosibirsk, Russia.
- ^{ccc} Also at Faculty of Physics, University of Belgrade, Belgrade, Serbia.
- ^{ddd} Also at Trincomalee Campus, Eastern University, Sri Lanka.
- ^{eee} Also at INFN Sezione di Pavia, Università di Pavia, Pavia, Italy.
- ^{fff} Also at National and Kapodistrian University of Athens, Athens, Greece.
- ^{ggg} Also at Universität Zürich, Zurich, Switzerland.
- ^{hhh} Also at Stefan Meyer Institute for Subatomic Physics, Vienna, Austria.
- ⁱⁱⁱ Also at Laboratoire d’Annecy-le-Vieux de Physique des Particules, IN2P3-CNRS, Annecy-le-Vieux, France.
- ^{jjj} Also at Şırnak University, Şırnak, Turkey.
- ^{kkk} Also at Department of Physics, Tsinghua University, Beijing, China.
- ^{lll} Also at Near East University, Research Center of Experimental Health Science, Nicosia, Turkey.

- ^{mmm} Also at Beykent University, Istanbul, Turkey.
- ⁿⁿⁿ Also at Istanbul Aydin University, Application and Research Center for Advanced Studies (App. & Res. Cent. for Advanced Studies), Istanbul, Turkey.
- ^{ooo} Also at Mersin University, Mersin, Turkey.
- ^{ppp} Also at Piri Reis University, Istanbul, Turkey.
- ^{qqq} Also at Adiyaman University, Adiyaman, Turkey.
- ^{rrr} Also at Ozyegin University, Istanbul, Turkey.
- ^{sss} Also at Izmir Institute of Technology, Izmir, Turkey.
- ^{ttt} Also at Necmettin Erbakan University, Konya, Turkey.
- ^{uuu} Also at Bozok Universitetesi Rektörlüğü, Yozgat, Turkey.
- ^{vvv} Also at Marmara University, Istanbul, Turkey.
- ^{www} Also at Milli Savunma University, Istanbul, Turkey.
- ^{xxx} Also at Kafkas University, Kars, Turkey.
- ^{yyy} Also at Istanbul Bilgi University, Istanbul, Turkey.
- ^{zzz} Also at Hacettepe University, Ankara, Turkey.
- ^{aaa} Also at School of Physics and Astronomy, University of Southampton, Southampton, United Kingdom.
- ^{bbb} Also at IPPP Durham University, Durham, UK.
- ^{ccc} Also at Monash University, Faculty of Science, Clayton, Australia.
- ^{ddd} Also at Bethel University, St. Paul, Minneapolis, USA.
- ^{eee} Also at Karamanoğlu Mehmetbey University, Karaman, Turkey.
- ^{fff} Also at Bingol University, Bingol, Turkey.
- ^{ggg} Also at Georgian Technical University, Tbilisi, Georgia.
- ^{hhh} Also at Sinop University, Sinop, Turkey.
- ⁱⁱⁱ Also at Mimar Sinan University, Istanbul, Istanbul, Turkey.
- ^{jjj} Also at Nanjing Normal University Department of Physics.
- ^{kkk} Also at Texas A&M University at Qatar, Doha, Qatar.
- ^{lll} Also at Kyungpook National University, Daegu, Korea.